การตั้งสูตรตำรับของนาโนอิมัลชันที่มีเอลลาจิกแอซิดจากสารสกัดเปลือกทับทิม เพื่อการนำส่งทางผิวหนัง

นางสาวณัฐวีร์ อินตะนัย

วิทยานิพนธ์นี้เป็นส่วนหนึ่งของการศึกษาตามหลักสูตรปริญญาเภสัชศาสตรมหาบัณฑิต
สาขาวิชาเภสัชกรรม ภาควิชาวิทยาการเภสัชกรรมและเภสัชอุตสาหกรรม
คณะเภสัชศาสตร์ จุฬาลงกรณ์มหาวิทยาลัย
ปีการศึกษา 2554

FORMULATION OF NANOEMULSION CONTAINING ELLAGIC ACID FROM POMEGRANATE RIND EXTRACT FOR SKIN DELIVERY

Miss Nattawee Intanai

A Thesis Submitted in Partial Fulfillment of the Requirements

for the Degree of Master of Science in Pharmacy Program in Pharmaceutics

Department of Pharmaceutics and Industrial Pharmacy

Faculty of Pharmaceutical Sciences

Chulalongkorn University

Academic Year 2011

Thesis Title	FORMULATION OF NANOEMULSION CONTAINING ELLAGIC ACID FROM POMEGRANATE RIND EXTRACT FOR SKIN DELIVERY
By	Miss Nattawee Intanai
Field of Study	Pharmaceutics
Thesis Advisor	Prapasri Sinswat, Ph.D.
Thesis Co-advisor	Associate Professor Waraporn Suwakul, Ph.D.

Accepted by the Faculty of Pharmaceutical Sciences, Chulalongkorn University in Partial Fulfillment of the Requirements for the Master's Degree

……. Dean of the Faculty of Pharmaceutical Sciences

(Associate Professor Pintip Pongpech, Ph.D.)

THESIS COMMITTEE

…….Chairman

(Associate Professor Uthai Suvanakoot, Ph.D.)

…….Thesis Advisor

(Prapasri Sinswat, Ph.D.)

…….Thesis Co-advisor

(Associate Professor Waraporn Suwakul, Ph.D.)

……..Examiner

(Anyarporn Tansirikongkol, Ph.D.)

……..External Examiner

(Assistant Professor Toemsak Srikhirin, Ph.D)

ณัฐวีร์ อินตะนัย : การตั้งสูตรตำรับของนาโนอิมัลชันที่มีเอลลาจิกแอซิดจากสารสกัดเปลือกทับทิมเพื่อการนำส่งทางผิวหนัง. (FORMULATION OF NANOEMULSION CONTAINING ELLAGIC ACID FROM POMEGRANATE RIND EXTRACT FOR SKIN DELIVERY) อ.ที่ปรึกษาวิทยานิพนธ์หลัก: อ. ดร.ประภาศรี สินสวัสดิ์, อ.ที่ปรึกษาวิทยานิพนธ์ร่วม: รศ. ดร.วราภรณ์ สุวกูล, 123 หน้า.

วัตถุประสงค์การศึกษานี้เพื่อพัฒนาตำรับนาโนอิมัลชันที่บรรจุเอลลาจิกแอซิดที่สกัดจากเปลือกทับทิมเพื่อนำส่งทางผิวหนัง เปรียบเทียบวิธีการสกัดสองวิธีเพื่อคัดเลือกวิธีที่เหมาะสม ระหว่างวิธีไฮโดรลิซิสและวิธีไฮโดรลิซิสร่วมกับวิธีการเกิดผลึกใหม่ ศึกษาผลของชนิดและปริมาณของน้ำมันและสารลดแรงตึงผิวรวมทั้งสารสกัดเอลลาจิกต่อการเกิดนาโนอิมัลชันที่เตรียมโดยวิธีการใช้พลังงานต่ำ ศึกษาความคงตัวทางกายภาพของตำรับเอลลาจิกแอซิดนาโนอิมัลชันในสภาวะเร่ง ประกอบด้วยการปั่นเหวี่ยงและเก็บที่อุณหภูมิ 45 องศาเซลเซียสเป็นเวลา 3 เดือน และศึกษาการปลดปล่อยและการซึมผ่านของสารสกัดเอลลาจิกแอซิดจากตำรับนาโนอิมัลชัน จากการศึกษานี้พบว่า วิธีการสกัดที่ใช้ไฮโดรไลซิสร่วมกับวิธีการเกิดผลึกใหม่เป็นวิธีการสกัดที่เหมาะสมเนื่องจากให้สารเอลลาจิกแอซิดที่มีความบริสุทธิ์สูงกว่าวิธีวิธีไฮโดรลิซิสอย่างเดียว ตำรับที่ประกอบด้วยน้ำมันรำข้าวไม่สามารถเกิดนาโนอิมัลชันได้ในขณะที่น้ำมันหอมระเหยส้มสามารถเกิดนาโนอิมัลชันได้ง่ายกว่ากรดโอเลอิก สารลดแรงตึงผิวคู่ที่มีโครงสร้างต่างกันเกิดนาโนอิมัลชันได้ง่ายกว่าคู่ที่มีโครงสร้างเหมือนกัน อัตราส่วนระหว่างน้ำมันและสารลดแรงตึงผิวที่เหมาะสมที่ทำให้เกิดนาโนอิมัลชันคือ ไม่มากกว่า 2:1 ขึ้นกับชนิดของสารลดแรงตึงผิว นอกจากนี้สารสกัดเอลลาจิกแอซิดไม่มีผลต่อการเกิดนาโนอิมัลชัน จากการศึกษาความคงตัวทางกายภาพในสภาวะเร่งพบว่า ทุกสูตรตำรับมีความคงตัวดีเมื่อปั่นเหวี่ยงแต่ตำรับที่มีความคงตัวที่ 45 องศาเซลเซียส เมื่อเก็บไว้นาน 17 วัน คือตำรับที่ประกอบด้วย น้ำมันหอมระเหยส้ม (10%) และ ทวีน 20 กับบริจ 97 (10%) ซึ่งมีลักษณะการปลดปล่อยอย่างช้าเมื่อเทียบกับสารละลายและไม่พบการซึมผ่านผิวหนังหน้าท้องลูกสุกรแรกเกิดของเอลลาจิกแอซิด อย่างไรก็ตาม ตำรับที่พัฒนาขึ้นในการศึกษานี้อาจจะเป็นประโยชน์ในการพัฒนานาโนอิมัลชันที่บรรจุด้วยสารประกอบอื่นๆ ที่มีคุณสมบัติคล้ายกับเอลลาจิกแอซิด

ภาควิชา วิทยาการเภสัชกรรมและเภสัชอุตสาหกรรม ลายมือชื่อนิสิต.....

สาขาวิชา เภสัชกรรม ลายมือชื่อ อ.ที่ปรึกษาวิทยานิพนธ์หลัก.....

ปีการศึกษา 2554 ลายมือชื่อ อ.ที่ปรึกษาวิทยานิพนธ์ร่วม.....

5176562433: MAJOR PHARMACEUTICS

KEYWORDS: ELLAGIG ACID / NANOEMULSION / SKIN DELIVERY

NATTAWEE INTANAI: FORMULATION OF NANOEMULSION CONTAINING ELLAGIC ACID FROM POMEGRANATE RIND EXTRACT FOR SKIN DELIVERY. ADVISOR: PRAPASRI SINSWAT, Ph.D., CO-ADVISOR: ASSOC. PROF. WARAPORN SUWAKUL, Ph.D., 123 pp.

The objective of this study was to develop nanoemulsions containing ellagic acid extracted from pomegranate rind for the skin delivery. The two extraction methods were compared to select the suitable method between the hydrolysis and the hydrolysis followed by the recrystallization. The effect of the types and amounts of oils and surfactants including ellagic acid extract to the formation of nanoemulsions, which were prepared by low energy emulsification method, was studied. The physical stability of ellagic acid loaded nanoemulsion under accelerated conditions, including the centrifugation and the storage at 45 ^{o}C for 3 months, was investigated. The studies of release and permeation of ellagic acid-loaded nanoemulsion were carried out. This study found that the extraction method with the hydrolysis followed by the recrystallization was the suitable method because it gave the high purity of ellagic acid more than the hydrolysis only. Formulation which composed of rice bran oil could not form nanoemulsion, while sweet orange oil could form nanoemulsion easier than oleic acid. The different structures of surfactants formed nanoemulsion easier than the same structure. The optimal oil to surfactant ratios which could form nanoemulsions were not more than 2:1 depending on the types of surfactants. Moreover, ellagic acid loading did not affect the formation of nanoemulsion. The study of physical stability under the accelerated conditions found that all formulations were stable after centrifugation. In contrast, the stable formulation which was kept at 45 ^{o}C for 17 days was the formulation composed of sweet orange oil (10%) and Tween®20:Brij®97 (10%). This ellagic acid loaded nanoemulsion had a slow release profile compared to the solution, and ellagic acid did not permeated through new born pig skin. The developed nanoemulsions from this study would be of benefit for developing nanoemulsions containing other compounds that possess similar property of ellagic acid.

Department: Pharmaceutics and Industrial Pharmacy Student's Signature.....

Field of Study: Pharmaceutics Advisor's Signature…….

Academic Year: 2011 Co-advisor's Signature……

ACKNOWLEDGEMENTS

I would like to express my sincere gratitude to my advisor, Dr. Prapasri Sinswat, for the continue support of my Master study and research, for her patience, motivation, enthusiasm and immense knowledge. Her guidance helped me in all the time of research and writing of this thesis. Besides my advisor, I would also like to thank my co-advisor, Associate Professor Dr. Waraporn Suwakul, for her patience, guidance and invaluable suggestions concerning all aspects of this research project. In addition, I would also like to thank the other member of my thesis committee, Associate Professor Dr. Uthai Suvanakoot, Assistant Professor Dr. Toemsak Srikhirin and Dr. Anyarporn Tansirikongkol, for their invaluable advice and time. It was a privilege to have them on my Master committee.

I would like to thank THE 90th ANNIVERSARY OF CHULALONGKORN UNIVERSITY FUND (Ratchadaphiseksomphot Endownment Fund) for partially financial support to my thesis work. I especially wish to acknowledge thanks to Croda Co., Ltd. for contribution of surfactants, and Soonthorn farm for giving the dead newborn pigs.

I wish to express my gratitude to all friends for the stimulating discussions, for the sleepless nights we were working together, and for all the fun we have had in the last four years. Also I thank staff members of Department of Pharmaceutics and Industrial Pharmacy for their kindness. And most of all, I would like to thank my mother for guiding me throughout my life with her endless love and unconditional support.

CONTENTS

PAGE

ABSTRACT (THAI)…….. iv

ABSTRACT (ENGLISH)…….. v

ACKNOWLEDGEMENTS……... vi

CONTENTS…….. vii

LIST OF TABLES……. x

LIST OF FIGURES…… xi

LIST OF EQUATIONS……. xiii

LIST OF ABBREVIATIONS…… xiv

CHAPTER

I INTRODUCTION…….. 1

II LITERATURE REVIEW…… 5

Ellagic acid…….. 5

Activities and sources of ellagic acid…… 5

Extraction method of ellagic acid…….. 5

Formulation of ellagic acid…… 6

Nanoemulsion……. 7

Nanoemulsion formation…… 7

Nanoemulsion preparation……. 8

High energy emulsification……... 8

Low energy emulsification…….. 9

Factors affecting emulsion formation…… 12

Factors of composition…… 12

Factors of preparation method…… 15

Nanoemulsion stability……. 17

Nanoemulsion as a drug delivery system for the skin…….. 18

III MATERIALS AND METHODS……. 20

Materials…… 20

Equipments…… 21

CHAPTER PAGE

Methods…….. 22
Extraction of ellagic acid in dried pomegranate rind…….. 22
Sample preparation……. 22
Extraction methods……. 22
Method A…… 22
Method B…… 24
Comparison of the two extraction methods…… 24
Total yield of dried extract…… 24
Thin Layer Chromatography (TLC)……. 25
Ultraviolet (UV) spectroscopic method…… 25
Identification by UV-spectrum…… 25
Percentage purity……. 26
High Performance Liquid Chromatographic (HPLC) method…… 26
Saturated solubility study of ellagic acid in various oils and surfactants…….. 28
Saturated solubility study in different oils……. 28
Saturated solubility study in different surfactants……. 29
Formation of o/w nanoemulsion by low energy emulsification method…… 29
Determination of HLB values of oils……. 30
Effect of types and amounts of oils and surfactants on nanoemulsion formation 30
Physical stability of formulations in accelerated conditions…….. 32
Investigation of ellagic acid loaded nanoemulsion…… 32
Effect of ellagic acid loading on nanoemulsion formation……. 32
Effect of ellagic acid loading on physical stability……. 33
In vitro release study…… 34
In vitro permeation study…….. 35
Preparation of new born pig skin membrane…… 35
Permeation study…… 35
Skin retention of ellagic acid…… 35
Statistical analysis……. 36

CHAPTER PAGE

IV RESULTS AND DISCUSSION…….. 37
Extraction of ellagic acid in dried pomegranate rind…… 37
Saturated solubility study of ellagic acid in various oils and surfactants……. 39
Saturated solubility study in different oils…… 39
Saturated solubility study in different surfactants……..…….. 41
Formation of nanoemulsion by low energy emulsification method…… 42
Determination of HLB values of oils……. 42
Effect of types and amounts of oils and surfactants on nanoemulsion formation 44
Effect of oil types…… 45
Effect of surfactant types…… 51
Effect of amounts of oils and surfactants…….. 52
Physical stability of nanoemulsions in accelerated conditions…… 55
Investigation of ellagic acid loaded nanoemulsion…….. 65
Effect of ellagic acid loading on nanoemulsion formation……. 65
Effect of ellagic acid loading on physical stability……. 67
In vitro release study…… 70
In vitro permeation study……. 71
V CONCLUSIONS…….. 76
REFERENCES…… 78
APPENDICES……..... 92
APPENDIX A…… 93
APPENDIX B…….. 102
APPENDIX C……. 116
VITA……. 123

LIST OF TABLES

TABLE		PAGE
1	Percentage of yields and purity of ellagic acid from each extraction method…….	39
2	Saturated solubility of dried extract in different oils…….	40
3	Saturated solubility of dried extract in different surfactants……	42
4	Coupling of matching surfactants with the same and different structures……	45
5	Formation of nanoemulsions of rice bran oil with various surfactant types……..	46
6	Formation of nanoemulsions of oleic acid with various surfactant types……..	47
7	Formation of nanoemulsion of sweet orange oil with various surfactant types…….	48
8	Formation of nanoemulsions of rice bran oil with different surfactant types and o/s ratios……	53
9	Formation of nanoemulsions of oleic acid with different surfactant types and o/s ratios……	53
10	Formation of nanoemulsions of sweet orange oil with different surfactant types and o/s ratios……	53
11	List of abbreviations……	54
12	All thirteen nanoemulsion formulations……..	55
13	Particle sizes and physical stability of nanoemulsion after passing through 6…….. heating-cooling cycles…….	57
14	Particle sizes and physical stability of nanoemulsion with 0.5% w/w xanthan gum after passing through 6 heating-cooling cycles……	64
15	Content of ellagic acid in formulations and %label amount……..	66
16	Particle sizes of blank formulation, ellagic acid-loaded formulations before and after centrifugation……...	66
17	Ellagic acid content at donor, skin, and receiver component of Franz-diffusion cell at 24 hours…….	72

LIST OF FIGURES

FIGURE		PAGE
1	Structure of ellagic acid……	2
2	Turbulent flow in the high pressure homogenizer……	8
3	Emulsion droplets collision in the microfluidizer chamber…….	9
4	Spontaneous surfactant curvature changes……..	10
5	Schematic diagram of extraction method A and B…….	23
6	Thin-layer chromatogram of dried extract obtained from pomegranate rind…….	37
7	Ultraviolet spectra of dried extract from method A and B…….	38
8	Structures of triglyceride and mineral oil…….	41
9	Emulsion at various HLB_{mix} values……..	43
10	The turbidity of the gel phase of rice bran oil, oleic acid and sweet orange oil……	49
11	The size profile of rice bran oil, oleic acid and sweet orange oil……..	50
12	Nanoemulsion formulation of S10T2S205 before and after centrifugation……..	56
13	Particle size of formulations before and after centrifugation……	57
14	The physical appearance and particle size distribution of S10T2B9710 at various cycles…….	58
15	Appearance and average particle size (nm) of O20T2C4010 after freeze thaw 3 cycles……	60
16	The particle size distribution of S10T2B9310……	61
17	The particle size distribution of S10T2S210…….	62
18	Appearance of S10T2S210X, S10T2S810X and S10T2B9310X before and after centrifugation……	63
19	Size distributions of S10T2S210X before and after adding 0.5% w/w xanthan gum	63
20	Size distribution of S10T2B9310X at 3 freeze thaw cycles…….	65
21	Average droplet size of blank and ellagic acid-loaded in formulation as a function of time…….	68

FIGURE **PAGE**

22 The physical appearance of O20T2C4010EA and S10T2B9310XEA …….. 69

23 Gel formation of S10T2B9710EA and S10T2B9710 after storage for 7 days…… 70

24 The release profiles of ellagic acid from nanoemulsion and saturated solution … 71

25 Chromatogram of standard of ellagic acid solution at LOQ (0.2 µg/mL)…….
in phosphate buffer solution. …….. 72

26 Chromatogram of standard of ellagic acid solution at LOQ (0.2 µg/mL)……
spiked in blank receiver medium…….. 73

27 UV-spectrum of spiked standard solution into…….
blank receiver medium…… 73

28 UV-spectrum of the peak of spiked standard solution……..
into phosphate buffer solution pH 7.4……... 74

29 Chromatogram of ellagic standard solution (4µg/mL) spiked in receiver medium 74

30 Chromatogram of ellagic standard solution (4µg/mL) spiked in phosphate buffer 75

LIST OF EQUATIONS

EQUATION		PAGE
1	Gibbs free energy	7
2	Percentage of total yield	24
3	Percentage of purity	27
4	The solubility of dried extract	28
5	HLB_{mix}	30

LIST OF ABBREVIATIONS

ANOVA	=	analysis of variance
T2	=	Tween®20
T8	=	Tween®80
S2	=	Span®20
S8	=	Span®80
B93	=	Brij®93
B97	=	Brij®97
C40	=	Cremophor RH®40
^{o}C	=	degree Celsius
mL	=	milliliters
min	=	minute
o/w	=	oil in water
rpm	=	round per minute
SD	=	standard deviation
µg	=	microgram
w/w	=	weight by weight
X	=	xanthan gum
S	=	sweet orange oil
O	=	oleic acid
R	=	rice bran oil
EA	=	ellagic acid
10	=	10% oil or total 10% surfactant
5	=	total 5% surfactant
20	=	20% oil
30	=	30% oil
15	=	total 15% surfactant

CHAPTER I

INTRODUCTION

Ellagic acid is a phenolic compound which can be found in nature. Ellagic acid is presented in free form or bound form, or so called Ellagitannins. Pomegranate (*Punica granatum* L.) is a fruit that its rind contains a high percentage of ellagitannins (90% w/w) (Seeram et al., 2006). Therefore, such a high percentage of ellagitannins interests many researchers to extract ellagic acid from the fruits. Moreover, this also increases a value of a waste product produced from the juice industry. Nowadays, the extraction methods of ellagic acid involve with extraction of free ellagic acid (Panichayupakaranant, Itsuriya, and Sirikatitham, 2010; Zhang et al., 2010; Amakura et al., 2000; Srivastava, Jagan Mohan Rao, and Shivanandappa, 2007). However, free ellagic acid is naturally presented in low amount and gives low ellagic acid content. Therefore, the extraction method for producing high ellagic acid content is required. From high amount of ellagitannins containing in pomegranate rind, Lu and Yuan (2008) developed the extraction method for producing high percentage purity of ellagic acid from that fruit. This method involved with two steps. Hydrolysis reaction of ellagitannins was carried out and then recrystallization by methanol was produced. This method could give 90% purity of ellagic acid. Yoshimura et al. (2005) also obtained 90% purity of ellagic acid by the same method without further recrystallization step. In this study, the extraction methods from Lu and Yuan (2008) and Yoshimura et al. (2005) were compared for selecting one extraction method which has no complexity, less organic solvent use and still gives high percentage yield and purity of ellagic acid.

At the present time, ellagic acid is more important in the cosmetic field because manufacturers increasingly use ellagic acid as a raw material (Guglielmini, 2008). Ellagic acid has various advantages in cosmetic purposes. Ellagic acid has been reported as whitening agent by inhibiting tyrosinase enzyme (Shimogaki et al., 2000; Yoshimura et al., 2005) and photoprotective agent by protecting collagen breakdown from UVB-radiation (Bae et al., 2010). Moreover, ellagic acid can increases elasticity of skin tissue by protecting skin fiber from proteolytic enzyme in dermal fibroblast cultures (Jimenez et al., 2006). Although ellagic acid is a potent substance as described above, there is a limitation of using in skin formulation. Ellagic acid is a poorly water soluble substance (97 μg/ml) because of its lipophilicity from four rings in

the structure (Figure 1) (Delaney, 2004). This may be responsible for a low efficiency of skin permeation.

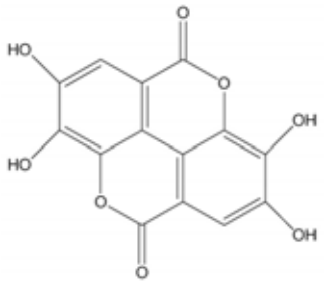

Figure 1 Structure of ellagic acid (Bala et al., 2006)

Nanoemulsion delivery system has been used for increasing the solubility of a poorly water soluble drug (Shakeel et al., 2008; Li et al., 2012; Shakeel and Faisal, 2010; Sakeena et al., 2010) because oil and surfactant in the formulation can increase drug solubility. Shakeel and Faisal (2010) found that the solubility of celecoxib is significantly increased by incorporating the drug in nanoemulsion. This solubilizing power of nanoemulsion is also performed with aceclofenac (Shakeel, Ramadan, and Shafiq, 2009), benzyl isothiocyanate (Qhattal et al., 2011), flutamide (Jeevana and Sreelakshmi, 2011), and atorvastatin (Chouksey et al., 2011). Besides the ability of improving drug solubilization, nanoemulsion has been also used for increasing skin permeability. Shakeel et al. (2008) studied skin permeability of celecoxib through rat skin and found that nanoemulsion can increases skin penetration through lipid bilayer and enhances skin permeability. Azeem et al. (2009a) also found that skin permeation of ropinirole contained in nanoemulsion was enhanced significantly. Similar to Mou et al. (2008), they revealed that nanoemulsion containing camphor, menthol and methyl salicylate could increase skin permeation of such substances. In addition, blank nanoemulsion has high rate of skin penetration more than conventional emulsion and increases the power of skin hydration (Sonneville-Aubrun et al., 2004). From the ability of increasing drug solubility and skin permeability, this study aims to increase the solubility and permeability of ellagic acid by incorporating in nanoemulsion.

Low energy emulsification has been increasingly interesting by industries because of low energy usage, low cost production, no complexicity of emulsification process, and ability of scale up in industries (Solè et al., 2010). However, low energy emulsification employs the properties

of compositions in formulation to attain small droplet size in nanometer ranges. The mechanism of emulsification is the change of surfactant curvature. When water is added to an oil phase, negative curvature of surfactant will be formed resulting in water in oil microemulsion at the initial stage. With further increased volume fraction of water, hydration forces between polyoxyethylene groups of surfactants and OH groups of water progressively increase. These make spontaneous changes of surfactant curvature from a negative curvature to a zero curvature. When further increased water component is added until it reaches the transition point, the zero curvature of surfactant is changed to the positive direction to form oil in water droplets (Solans et al., 2009). Therefore, all compositions in the formulation are involved in generating nano-droplet. Such compositions include oil types (Forgiarini et al., 2006), surfactant types (Dai, Li, and Hou, 1997) and the amount of oil and surfactant (Fernandez et al., 2004; Liu et al., 2006; Sadurní et al., 2005). In addition, nanoemulsion can be formed easily and gives high stability when HLB of surfactant mixture closes to the HLB of oil (Liu et al., 2006)

Therefore, the aim of this study was to formulate nanoemulsion containing ellagic acid extracted from pomegranate rind for skin delivery. The two eallgic acid extraction methods were compared (Lu and Yuan, 2008; Yoshimura et al., 2005). The effect of compositions in the formulation and the effect of ellagic acid extract on nanoemulsion formation and its stability were also examined. Finally, the release of ellagic acid from nanoemulsion and the skin permeation of ellagic acid through newborn pig skin were also investigated.

Objectives

The purposes of this study were as follows:

1. To compare the methods of ellagic acid extraction from pomegranate rind for ellagic acid content and purity in crude extract.

2. To investigate the effect of oil and surfactant types on the saturated solubility of ellagic acid extracted from pomegranate rind.

3. To investigate the effect of the amounts and types of oils and surfactants on nanoemulsion formation and its physical stability in stress conditions.

4. To investigate the effect of ellagic acid extracted from pomegranate rind on nanoemulsion formation and its physicochemical stability in stress conditions.

5. To study the release of ellagic acid from nanoemulsion formulation.
6. To evaluate the in vitro pig skin permeation of ellagic acid loaded in nanoemulsion.

CHAPTER II

LITERATURE REVIEWS

Ellagic acid

1. Activities and sources of ellagic acid

Ellagic acid is a polyphenolic acid which antioxidant (Aviram et al., 2008; Priyadarsini et al., 2002), antiinflammatory (Panichayupakaranant, Tewtrakul and Yuenyongsawad, 2010), and anticarcinogenic properties (Susanne, Mertens and Susan, 2005) are its outstanding properties. Jimenez et al. (2006) also affirmed that ellagic acid protects skin fibroblast against enzymatic degradations. In addition, another research reported that ellagic acid could inhibit tyrosinase enzyme, leading to decrease of skin pigment synthesis (Yoshimura et al., 2005). Therefore, ellagic acid has been considered as a skin-whitening agent. Ellagic acid usually exists in fruits and plants. Ellagic acid is found in strawberries, pears, peaches, plums, grapes, apples, kiwis (Daniel et al., 1989) and pomegranates (Seeram et al., 2006). Moreover, ellagic acid exists in leaves and barks of plants (Baipai et al., 2005). In general, ellagic acid exists in two forms, i.e. free form as ellagic acid and bound form as ellgitannins. Free ellagic acid is naturally exists in low quantity as presented in fruits and vegetables (Seeram et al., 2006). Lei, Jervis, and Helm (2001) showed that ellagic acid exists in oak wood only 0.2% w/w. As well as Jordão et al. (2005), they also found the amount of ellagic acid in wood which was approximately 80 mg/L. Ellagic acid has been found in a small amount in wood but to a lesser extent in fruits. The amount of ellagic acid in nature, however, depends on cultivar (Maas, Wang and Galletta, 1991), ripening stages (Williner, Pirovani, and Güemes, 2003), seasonal changes (Feeny and Bostock, 1968), and storage time (Zafrilla, Ferreres, and Tomás-Barberán, 2001).

2. Extraction method of ellagic acid

Besides environmental conditions affecting ellagic acid content, extraction method of such compound also affects the amount of ellgic acid obtained from fruits or plants. Because of the existence in low amount of free ellagic acid in fruits or plants, the extraction of such free ellagic acid can yield in a low quantity.

From the past to the present, the investigators preferably extract free ellagic acid by solvent extraction and partition with organic solvent (Panichayupakaranant, Itsuriya and Sirikatitham, 2010), or by solid phase extraction method (Amakura et al., 2000). This approach yielded insubstantial amount in the final crude extract less than expected. Therefore, the serious attempt to extract ellagic acid in a large quantity is required. A large number of studies have declared that pomegranate rind is an abundant source of ellagitannins as a precursor to prepare ellagic acid (Larrosa, Tomãs-Barberãn, and Espìn, 2006). Seeram et al. (2006) have shown that pomegranate husk mostly contains 80-85% w/w of ellagitannins. This provokes many researchers to interest the extraction of ellagic acid from that high polyphenolic compound fruit. Ellagic acid percentage in crude extract can be increased by the hydrolysis of ellagitannins (Lu and Yuan, 2008; Yoshimura et al., 2005; Zhou, Yuan, and Lu, 2011). Ellagitannins must be extracted by organic solvent-water mixture and then the resulting ellagitannins was subsequently hydrolyzed by strong acid (such as sulfuric acid or hydrochloric acid). Acid hydrolysis could yield ellagic acid through spontaneous lactonization (Larrosa et al., 2006). Yoshimura et al. (2005) employed the reflux technique to extract ellagitannins by using 50% w/w ethyl alcohol in water and then hydrolyzed those ellagitannins to release ellagic acid. In this case, crude extract gave ellagic acid approximately 90% w/w. Lu and Yuan (2008) also used the same method and yielded the same percentage of ellagic acid. However, recrystallization by methanol was an additional process in that study.

3. Formulation of ellagic acid

Both pure ellagic acid and crude extract have the strong antioxidant effect (Aviram et al., 2008; Priyadarsini et al., 2002; Panichayupakaranant, Tewtrakul and Yuenyongsawad, 2010; Susanne et al., 2005). This conception initiates many investigators and commercial industries to have more attraction of using this compound in preparations for miscellaneous therapeutic and cosmetic intentions. However, the critical problem of incorporating ellagic acid in the formulation is the water solubility. Bala et al. (2006) investigated the solubility of ellagic acid in various solvents. They found that solubility in water of ellagic acid was only 9.7 μg/mL. In contrast, ellagic acid was more soluble in methanol (671.7 μg/mL). Moreover, it could be solubilized in alkaline conditions by using N-methyl pyrrolidone (NMP). Salt formation of ellagic acid by using triethanolamine (TEA) could be achieved to increase solubility of ellagic acid. There are a few

techniques of incorporating ellagic acid in formulation. Murugan et al. (2009) incorporated ellagic acid into the formulation via complexation with hydrogenated soy phosphatidyl choline (HSPC). Optimization of solvent before dissolving ellagic acid was studied by Sharma et al. (2007). Egawa and Marui (2000) incorporated ellagic acid in formulation by increasing the dispersability of ellagic acid by reducing particle size of ellagic acid powder. Furthermore, Ishida et al. (1992) dispersed polyvalent metal salt of ellagic acid in ethyl alcohol, oils and fats before making cream, foundation, and milky lotion. For all techniques, the complexity of incorporating process is involved. Easier method to incorporate ellagic acid is needed.

Nanoemulsion

1. Nanoemulsion formation

Nanoemulsion is a class of emulsion, one liquid is dispersed in another immiscible liquid. The major difference between emulsion and nanoemulsion is the average droplet size. Typically, nanoemulsion has average droplet diameter in the range of 20-500 nm (Solans et al., 2004; Guglielmini, 2008). However, the definition of droplet size range depends on each author's definition. Nanoemulsion is a thermodynamically unstable system which cannot be formed spontaneously. Thus, energy input is required to make the internal phase to be small droplets (Mason et al., 2006). Nanoemulsion formation can be examined by the Equation 1 (Tadros et al., 2004).

$$\Delta G = \Delta A\gamma - T\Delta S \qquad \text{Eq. 1}$$

Where ΔA is the surface area difference between the area of bulk oil and the new established surface area, γ is the interfacial tension. As small globules are dispersed, the high discrepancy of the surface area between such droplets and bulk phase takes place, therefore providing positive free energy of formation (ΔG), which is not compensated by the small entropy ($T\Delta S$). To overcome this occurrence, high energy input is needed in order to defeat the presence of additional free energy of emulsification for disrupting the big oil droplets to the nanoscale.

2. Nanoemulsion preparation

In general, nanoemulsion production can be classified into high energy emulsification methods and low-energy emulsification methods. High energy emulsification methods employ energy input into the system, while low energy emulsifications employ internal energy. Both methods have different advantages and disadvantages. High energy emulsification can produce nanoemulsion easily but they can make high cost of production. The high performance of machine is needed for this method. In contrast, for low energy emulsification techniques, low cost of production can be attained because of no complexity of preparation.

2.1 High energy emulsification

For high energy emulsification, the energy depends on the source of energy from the emulsification process. In recent years, various high energy emulsification techniques were extensively used in many research fields with the following methods.

2.1.1 High pressure homogenization

High pressure homogenization technique is the most frequently applied method to generate nanoscale droplets. The intended energy is mainly taken from the turbulence exaggerated by hydrolic pressure input which can disperse coarse emulsion into tiny droplets. (Malmsten, 2002), as in Figure 2.

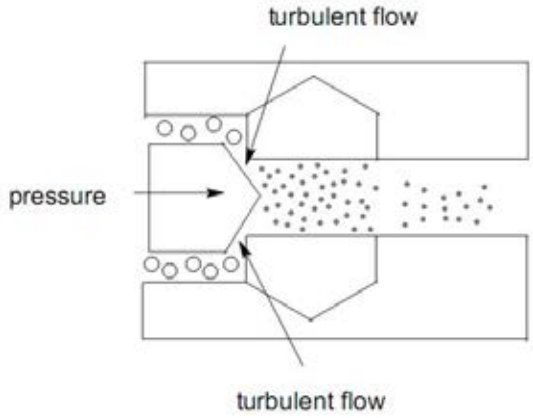

Figure 2 Turbulent flow in the high pressure homogenizer (Malmsten, 2002)

After coarse emulsion is filled into the chamber, the high pressure pump dramatically presses the emulsion under high pressure condition. As a consequently, high shear, impact, and cavitation occur, which potentially results in the nano-range emulsion.

2.1.2 Microfluidizer

To improve droplet size reduction efficiency, microfluidizer is a more advantage technological equipment that was developed from the high pressure homogenizer. The source of energy of this equipment obtained from two-way high pressure stream collision. Emulsion is added in the reservoir through high pressure pump, and then the emulsion is separated into two ways and finally is collided with a high speed velocity approximately 400 m/s. As a result, this technique creates high shear, impact and cavitation and subsequently generates fine emulsion droplets with narrow size distribution (Conroy, 2011), as can be seen in Figure 3.

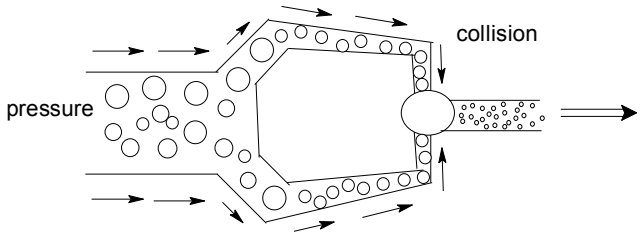

Figure 3 Emulsion droplets collision in the microfluidizer chamber (Conroy, 2011)

2.1.3 Ultrasonication

The principle of this method is to initiate energy through the intense ultrasound supplies. This technology corresponds the imploding of cavitated bubbles, resulting in high velocity of liquid jet which reduces emulsion droplet size (Hielscher, 2005).

2.2 Low-energy emulsifications

Low-energy emulsifications are the interesting processes for producing ultrafine emulsions because of low energy usage, low production cost, and easier to scale-up for industry. Low-energy emulsifications also need energy to make such small droplets, but the source of energy comes from the intrinsic chemical energy stored in the system which is diverted to reach the nano-size droplets. There are two categories of low-energy emulsifications as follows.

2.2.1 Self-emulsification

Nanoemulsion can be made by direct emulsification, or so called self-emulsification method. This method uses a dilution process without any phase inversion, and the final emulsion

types are obtained as same as the primary ones. This procedure can be achieved by blending oil, surfactant and solvent (oil phase), and then water phase is mixed into the oil phase under gentle stirring (Bouchemal et al., 2004; Rang and Miller, 1999; Wang et al, 2007). Fundamentally, the mechanism involves with the energy release into system interrelating with solvent migration from the initial phase into the dispersion medium while the two phases are contacting (Solans et al., 2009). This method does not employ any phase inversion step. It differs from the other methods, the phase inversion emulsification method.

2.2.2 Phase inversion emulsification

The second category of a low energy emulsification is the emulsion phase inversion from water in oil (w/o) to oil in water (o/w) or vice versa. This inversion depends on a surfactant curvature which changes during emulsification. The change of surfactant curvature is induced either by the changes of temperature (phase inversion temperature) or by the changes of composition (phase inversion composition).

2.2.2.1 Phase inversion temperature (PIT) technique

Phase inversion temperature technique has been used extensively. Generally, the inversion of surfactant curvature is occurred by the change of nonionic surfactant characteristics. This alteration is usually induced by the change of temperature. The source of the internal energy is directly obtained from the surfactant curvature changes during emulsification. The mechanism of PIT emulsification is the conversion of surfactant film curvature at the interface between oil and water domain with the temperature change as shown in Figure 4.

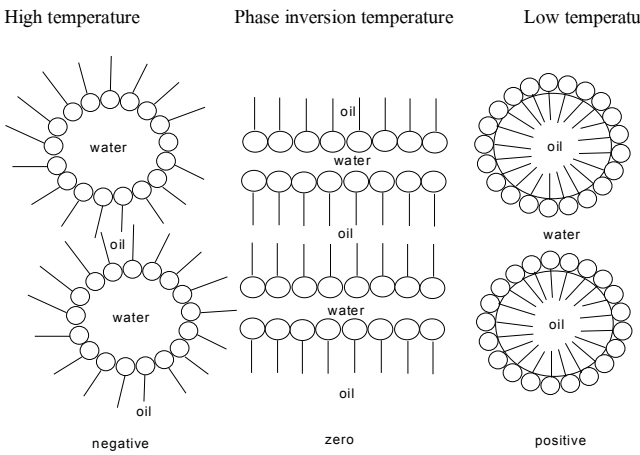

Figure 4 Spontaneous surfactant curvature changes in PIT technique (Solans et al., 2009)

At high temperature, the hydrophilic group of surfactant is dehydrated. This causes the change of surfactant curvature toward a negative direction. When the temperature is subsequently decreased, the negative curvature of surfactant film is changed to positive one. This caused by the relative increase of hydration force between polyoxyethylene groups and OH groups of water. Therefore, it makes surfactant curvature to change. At the PIT point, the surfactant curvature is balanced because the lamellar phase or the bicontinuous phase is oriented at this temperature. From such orientation, the very low interfacial tension is obtained (Engels, Förster, and Rybinski, 1995). In relation, it is promoted to emulsify although the low energy is used. As a result, submicroscopically small oil droplets are easily attained (Kunieda and Friberg, 1981).

PIT phase inversion can make both oil in water and water in oil nanoemulsion. With respect to oil in water nanoemulsion, oil, emulsifiers and water are combined and shaken near the PIT point which are scrutinized before emulsion preparation. After shaking, the resulting emulsion is suddenly cooled in an ice bath (Izquierdo et al., 2005; Galindo-Alvarez et al., 2011; Anton and Vandamme, 2009; Roger, Cabane, and Olsson, 2010; Mei, Xu, and Sun, 2010). For water in oil nanoemulsion, the initial emulsion is continuously cooled until reaching 0 ^{o}C, and then immediately heated to temperature above the PIT with continuous agitation (Esquena, Sankar, and Solans, 2003). This process can instantly change surfactant curvature toward a negative direction and water in oil nanoemulsion is generated as expected.

The PIT point can be evaluated by using conductivity execution. First, emulsion is prepared as a simple emulsion by simple mixer, and then the conductivity of emulsion is measured as a function of temperature. As the temperature steadily increases, the emulsion conductivity dramatically increases until reaching the maximum value and tends to decrease continuously until the minimum value. The PIT point can be calculated from the mean conductivity value by using the maximum and the minimum values (Mei et al., 2010).

2.2.2.2 Phase inversion composition (PIC) technique

PIC method has excited many researchers interest in recent years, in cosmetics, pharmaceutics, academics and industries, because low temperature is used in the process to emulsify oil and water. Therefore, this technique can protect heat-labile substances

from thermal instability. Both PIT and PIC methods employ the same mechanism of emulsification, the phase inversion. The slight differences between PIT and PIC methods are factors influencing the change of surfactant curvature. In the case of PIT, the change of surfactant curvature is induced by the temperature change. In the case of PIC, the change of surfactant curvature is induced by the change of hydration interaction between poloxyethylene groups of surfactant and OH groups of water while the composition of water is being changed (Solans et al, 2009). Phase inversion composition method can be prepared by blending oil and surfactants (oil phase) until homogeneous, and then the water is added dropwisely into the oil phase (Liu et al., 2006).

3. Factors affecting nanoemulsion formation

Nanoemulsion formation by the low energy emulsification methods depends on various variables, including compositions and method of preparation. Therefore, all factors are the critical parameters which are needed to be concerned with the preparation of nanoemulsion by this technique. Many researchers have investigated the factors affecting nanoemulsion formation and its stability as we stated herein.

There are many factors that affect the formation of nanoemulsion. However, those factors depend on each emulsification technique. In this study, the PIC technique is in our interested. Therefore, factors affecting the formation of nanoemulsion by this technique were reviewed, as described below.

3.1 Factors of composition

3.1.1. Hydrophilic Lipophilic Balance (HLB)

The HLB value is an important parameter among other factors affecting nanoemulsion formation. Liu et al. (2006) investigated the effect of the varied HLB values of surfactant mixture on nanoemulsion formation using paraffin oil (HLB 10-12) as an oil phase. This finding indicated that emulsion droplet size was varied according to the changes of HLB mixed values of surfactant admixture. In addition, nanoemulsion could be generated with the size less than 300 nm when the HLB of emulsion system was near the HLB value of oil, or so called “optimum HLB”. Nonetheless, HLB value could be altered by the change of preparation temperature. Evidently, this conclusion was also in agreement with Dai et al. (1997). They also

found that nanoemulsion composed of paraffin oil and nonionic surfactant could be constructed with droplet size less than 500 nm when the optimum HLB was close to the HLB of the oil. Furthermore, nanoemulsion could be prepared by using only one surfactant if the HLB of that surfactant was near the HLB of oil. Sadurní et al. (2005) reported that the use of Cremophor®EL as an emulsifier in emulsion system could emulsify emulsion to a small droplet, since the HLB of Cremophor®EL (HLB = 12-14) was close to the HLB of castor oil (HLB=14). In the same manner, the use of Solutol®HS (HLB=14-16) as a surfactant and Miglyol®812 (HLB=15) as an oil component could produce tiny globule emulsion. Wang et al. (2007) similarly showed that using decane (HLB=10) as an oil constituent and Laureth®-5 (HLB=10.5) as a surfactant could be easily attained nanoemulsion with the droplet size around 200 nm.

3.1.2. Surfactant concentration

Besides the HLB system manipulating nanoemulsion formation, the concentration of surfactant is an important factor generating scrutiny of emulsion droplet as well. Most scientists discovered that surfactant concentration is the key element of controlling emulsion droplet size (Depraétere et al., 1980; Liu et al., 2006; Sajjadi, 2006; Fernandez et al., 2004). The study of Liu et al (2006) demonstrated that when the concentrations of surfactant were increased from 3-8% w/w, the size of emulsion tended to decrease from 300 nm to 100 nm. In agreement with Sajjadi's study (2006), it revealed that formulation containing surfactant concentration lower than 3% w/w could not reduce emulsion droplet size to the nano-scale but an increase of surfactant concentration up to 5% w/w remarkably decreased droplet size to 500 nm. Furthermore, this study also showed that the small droplet size commonly accompanied with the narrow size distribution. The reason of that phenomenon might be occurred from the decreased interfacial tension corresponding to the increased surfactant concentration, which enhanced emulsification more than the presence of low surfactant amount. According to the ultra-low interfacial tension, it could facilitate surfactant curvature changes and result in the small droplet size. In addition, the viscosity which was risen up by the increased surfactant concentrations might reduce droplet coalescence, when the emulsion system suddenly passed through the ultralow interfacial tension (Fernandez et al., 2004). Therefore, the final nanoemulsion still remained in the same size as in the ordinary state and could also improve droplet size distribution.

3.1.3 Surfactant structure

Middle phase structure, bicontinuous or lamellar liquid crystalline, is one part of the mechanism of nanoemulsion formation. The configuration of those associations including the arrangement and the strength of them own can affect the production of nanoemulsion, whether promoting the surfactant curvature to change or not (Engels et al., 1995; Morales et al., 2003). In that event, the organization of such phase, therefore, depends directly on surfactant structure used in a formulation. Evidence from literature indicated that the differences in surfactant structures of the surfactant mixtures contained in emulsion system could lead nanoemulsion to form easier, as compared to the use of the same surfactant structure. Dai et al. (1997) reported that the utilization of surfactant mixture with the same alkyl chain lengths in molecule (Tween®80: Span®80) could induce nanoemulsion to form harder than the use of the different carbon chain lengths in surfactant mixture (Tween®80:Span®20). Moreover, the higher difference in surfactant structures was, the easier small droplet diameter could be attained. In this paper, the discussion of this factor can be explained by the surfactant film structure. While the surfactant film composed of the different surfactant structures was positioning at the interfaces of the two opposing liquid, this arrangement tended to form a loosening and flexible structure which is in convenience to be induced for changing directions of surfactant curvature. For the overall process, nanoemulsion can be obtained.

3.1.4 Oil concentration

The concentration of oil is also one of the parameters that affect nanoemulsion formation. In general, effect of oil concentration accompanies with surfactant concentration. Therefore, oil effect must be considered as oil/surfactant ratio (o/s ratio). As can be seen in some research papers, Pey et al. (2006) investigated the effect of o/s ratio on the size of nanoemulsion comprised of paraffin oil and Tween®20:Span®20 as a surfactant mixture. They found that when o/s ratio increased from 2 to 3, the size of emulsion droplet increased apparently from 81 nm to 145 nm. In agreement with Maestro et al. (2006), they demonstrated that the ratio of hexane/oleic acid-C12E10 increased from 30/70 to 50/50, the final emulsion droplet was increased from 8 to 20 nm. Similarly, high o/s ratio of n-decane/Brij®30 as oil and surfactant, respectively, made droplet size of nanoemulsion increased from 50 to 300 nm (Forgiarini et al., 2001). In contrast, Wang et al. (2007) concluded that nano-scale droplet could be accomplished at the optimum o/s

ratio. Those investigators have found that formulation containing o/s ratio less than the "optimum point" resulted in big droplets. In the same way, o/s ratio more than the optimum point, the larger emulsion globules were produced. It could be interpreted by concerning with the relationship between oil and surfactant proportion. At o/s ratio less than optimum point, the ratio of surfactant seems to be increased and may be contribute to create the discrete surfactant structure at the outer phase. Therefore, this separation of a lamellar liquid crystal may increase droplet size distribution and average nanoemulsion droplet size (Morales et al., 2003). Additionally, the excess oil seemed to be remained at the outside of the lamellar structure when o/s ratio far from the optimum point. That excess oil could be exactly emulsified only by agitation energy, resulting in the inhomogeniety of emulsification and increasing of the mean droplet size.

3.1.5 Oil type

Although the effect of oil type on nanoemulsion formation is not widely studied, there is a concern about this factor on some publications. Forgiarini et al. (2006) investigated the effect of different oil types (hydrocarbon oil and vegetable oil) in formulation on o/w nanoemulsion formation through emulsion phase inversion method. In this study, liquid paraffin and soy bean oil represented hydrocarbon oil and vegetable oil, respectively. In addition, surfactant types were also used as an indicator for monitoring oil type effect. The result appeared that liquid paraffin oil could form nanoemulsion with all surfactants that have different HLB values, i.e. Tween®80:Span®80 (HLB 10.6), Tween®80:Span®60 (HLB 11.2), Tween®80:Span®20 (HLB 12). Nevertheless, the use of soybean oil generated nanoemulsion only with particular surfactant type mixtures, i.e. Tween®80:Span®80, Tween®80:Span®60. They suggested that the difficulty of nanoemulsion formation using with vegetable oil came from the higher solubility of surfactant in vegetable oil than hydrocarbon oil.

3.2 Factors of preparation method

Since nanoemulsion is a thermodynamically unstable system, the procedure of emulsification also affects the final nanoemulsion characteristics. There are some publications evaluating the effect of the emulsification process on nanoemulsion formation, with the following subjects.

3.2.1 Agitation and addition rate

Besides compositions of formulation affecting the formation of nanoemulsion, preparation variables, i.e. mixing rate and rate of water addition, also affect the formation of nanoemulsion. In general, factors of composition and preparation method have an interaction to each other. Bilbao-Sainz et al. (2010) revealed that the high stirring speed during emulsion system passed through emulsion inversion point could reduce the droplet size of the inverted emulsion. In agreement with the study of Solè et al. (2006), it further suggested that slow addition rate and high agitation speed would be preferred for making small droplet emulsion. This is probably because the sufficient time and energy are needed to incorporate oil component into the liquid crystalline phase, before the further drop will be added. There is another instrumental factor that must be carefully examined for this interpretation as described by Solè et al. (2010). The effect of addition rate on nanoemulsion formation can be seen apparently at particular geometry of mixing vessel. If the shape of vessel is convenient for mixing all compositions throughout the container perfectly, the addition rate would not be a critical factor. On the contrary if the vessel body is improper, the addition rate will effect on the final droplet size. In this study, they concluded that the problem of blending took place from the high viscosity of emulsion resulting from the existence of liquid crystalline phase.

3.2.2 Order of addition

The kinetic process is one of the elements controlling nanoemulsion formation. Therefore, the suitable order of addition of each component is highly required in order to attain nano-scale droplet radius. The study of Forgiarini et al. (2001) demonstrated that addition of oil component was added into an aqueous phase containing surface active agent (method A) made o/w emulsion droplet size only 6 μm although amount of surfactant was increased. Whereas the droplet size of emulsion in order of 50 nm was achieved by the reverse method (method B), that was the water phase was added into an oil phase containing emulsifying agent. To understand this finding deeply, the phase diagram of those three components (oil, surfactant, and water), PIT point and interfacial tension value were carefully examined. From phase diagram study corresponding to method A, it seems that there is no phase inversion while oil component was being added into liquid lamellar phase in water. While method B performed phase transition from isotropic liquid phase to multiphase region, and the change of surfactant curvature was attained.

Consequently, the proper order of addition finally yields emulsion with small globule, narrow size distribution, and bluish appearance.

Nanoemulsion stability

The stability of conventional emulsion associates with a large number of processes, such as creaming, flocculation, coalescence, and Ostwald ripening. For the process of creaming, the difference of size distribution makes a separation of emulsion. On the contrary, nanoemulsion stands over the progress of creaming because the energy of Brownian movement of such small droplets overcomes the gravitational force which is the fundamental cause of emulsion instability. As well as the other two processes, flocculation and coalescence, the effect of small droplet size of nanoemulsion is dominant. Therefore, flocculation and coalescence cannot exist over the long time period. The only important of nanoemulsion instability is Ostwald ripening (Izquierdo et al., 2002; Pons et al., 2003; Izquierdo et al., 2005; Solé et al., 2006; Al-Edresi and Baie, 2009; Peng et al., 2010; Rao and Mcclements, 2010). Teo et al. (2010) showed that nanoemulsion containing palm oil ester and Tween®80:Pluronic®F-68 exhibited Ostwald ripening since the droplet size appeared to be increased with time. This was similar to the study of Sonneville-Aubrun et al. (2004) in case of nanoemulsion consisting of isopropyl palmitate/PEG-8 isostearate:disodium stearoyl glutamate. The main cause of destabilization is that the differences in droplet size leads to the growth of droplet radius by the expense of the small droplets (Wooster, Goding, and Sanguansri, 2008). Nevertheless, Ostwald ripening rate intimately depends on the solubilizing nature of oil in aqueous medium as explained by Lifshitz-Slyozov-Wagner (LSW) theory. Therefore, the molecular structure of oil plays a part in the rate of Ostwald ripening. Sonneville-Aubrun et al. (2004) have illustrated that nanoemulsion using low molecular weight oil as oil component had Ostwald ripening rate higher than high molecular weight oil. On the other hand, the presence of insoluble oil makes nanoemulsion stable over 2 months at 45 ^{0}C. Also in agreement with Izquierdo et al. (2002), Ostwald ripening rate rapidly increased by decane (oil soluble in continuous phase) more than the lower oil solubilizing potential (dodecane, tetradecane, hexadecane). Accordingly, Laplace's pressure difference between the small and the big globules provides molecular diffusion through the continuous phase, although there is a small distinction between the two droplet sizes. Therefore, the soluble oil could facilitate oil migration through the outer phase. Practically, this instability could be overtaken by incorporating the

second insoluble oil into the formulation which could reduce the driving force of the soluble oil. Isocetyl isostearate (Sonneville-Aubrun, 2004), squalene (Al-Edresi and Baie, 2009), peanut oil (Wooster et al., 2008), and corn oil (McClements, 2010; Ziani, 2011) are classified as the insoluble oil. In addition, the other dominant factor governing nanoemulsion instability is surfactant concentration. Izquierdo et al. (2002) found that the further increased surfactant concentration favored Ostwald ripening, which was also in agreement with the studies of Weiss (2000) and Binks et al. (1999). This study could be responsible for the micellar structure presumably exists in dispersion medium in order of magnitude of surfactant which would increase solubility of oil component.

Nanoemulsion as a drug delivery system for the skin

Nanoemulsion has been extensively employed for skin products, since they have unique physical characteristics: transparency, fluidity and small particle size. The main reason is that nanoemulsion provides more skin feel than conventional emulsion. In addition, nanoemulsion has ability to deliver active substances into the skin. There are numerous evidences indicated that dermatological drugs incorporated in nanoemulsions could improve skin treatment significantly (Shakeel et al., 2008; Abu-Elyazid et al., 2011; Sakeena et al., 2010). The mechanism of skin penetration enhancer is due to the increasing in drug content at the skin surface with respect to high surface area of nanoemulsion droplets. Schwarz, Weisspapir and Friedman (1995) studied the influence of emulsion droplet size on the efficacy of diazepam when applied to the skin of convulsive rats. The result found that nanoemulsion with 100 nm in diameter dramatically increased diazepam activity compared to the conventional emulsion (5 μm). However, the activity of diazepam depended on the oil type used in formulation. It could be shown that the low polar oil resulted in diazepam activity less than the high polar oil. This may be because diazepam is more favorably soluble in high polar oil. Additionally, not only pharmacological drugs can be incorporated in nanoemulsion, but nanoemulsion blank can also take advantages for cosmetic purposes. The study of the effect of three different blank vehicles on skin hydration disclosed that nanoemulsion enhanced skin hydration more than either milk bath or body water (Sonneville-aubrun et al., 2004). Because of the premium properties of nanoemulsions, they have been increasingly patented for cosmetic purposes, typically containing with natural substances. For example, commercial industry used nanoemulsion technology incorporating with gingseng

saponin for skin care products (Yoo et al., 2003). This study has shown that gingseng saponin metabolite loaded in nanoemulsion penetrated into skin more than solution preparation significantly and hence extremely induced collagen biosynthesis as well. Not only in economical industries but also in pharmaceutical fields employ nanoemulsion technology for skin treatment. Baker et al. (2009) suggested that the use of nanoemulsion as drug delivery system for the treatment of onchomycosis has increased antifungal activity more than the typical antifungal drug treatment.

CHAPTER III

MATERIALS AND METHODS

Materials

Absolute Ethanol, AR grade (RCI Lab Scan Co., Ltd., Thailand, lot no. 09020045)

Conductivity calibration solution (Eutech Instrument Pte Ltd., Singapore, batch no. S06812)

Disodium hydrogen phosphate (Asia Pacific chemicals Limited, batch no. F2F136)

Ellagic acid Standard (Sigma, USA, lot no. E2250)

Isopropanol, HPLC grade (RCI Lab Scan Co., Ltd., Thailand, lot no. 11010375)

Isopropyl Myristate (Namsiang Group, Thailand, lot no. 12390H)

Methanol, HPLC grade (RCI Lab Scan Co., Ltd., Thailand, batch no. 11060197)

Mineral oil (Namsiang Group, Thailand, batch no. 2010112222)

Oleic acid (Panreac, Spain, lot no. 0000140886)

pH calibration solution (Thermo Electron Corporation, England, lot no. NMP1)

Polyoxyethylene 10 oleyl ether (Brij®97) (Generous gift from CRODA, Thailand, lot no. 0000213011)

Polyoxyethylene 2 oleyl ether (Brij®93) (Generous gift from CRODA, Thailand, lot no. 59645)

Polyoxyethylene 20 sorbitan monoolaurate (Tween®20) (Namsiang Group, Thailand, lot no. JP0070d)

Polyoxyethylene 20 sorbitan monooleate (Tween®80) (Generous gift from CRODA, Thailand, lot no. 16526)

Polyoxyethylene 4 lauryl ether (Brij®30) (Generous gift from CRODA, Thailand, lot no. 61135)

Polyoxyethylene 40 castor oil (Cremophor RH®40) (Namsiang Group, Thailand, lot no. 0020010)

Potassium dihydrogen phosphate (Merck, Germany, batch no. 1102146)

Propyl paraben (Srichand, Thailand, batch no. 20100202)

Rice bran oil (TROPICALIFE, Thailand, lot no. 250609)

Sodium Chloride, AR grade (Merck, Germany, lot no. K41653304049)

Sorbitan laurate (Span®20) (Generous gift from CRODA, Thailand, lot no. 58476)

Sorbitan oleate (Span®80) (Namsiang Group, Thailand, lot no. 0060010)

Squalene (Namsiang Group, Thailand, lot no. 00700d)

Sweet orange oil (Namsiang Group, Thailand, lot no. 159803)

Xanthan gum (S. Tong Chemical Co., Ltd., Thailand, lot no. 1L2763K)

Equipments

Analytical balance (Model AX105, Mettler Toledo, Switzerland)

Conductivity meter (Model C535, Consort, Belgium)

Dialysis membrane (Regenerated cellulose tubular membrane MWCO=12000-14000, Membrane Filtration Product, Inc., USA)

Disposable syring nylon filter 13 mm, 0.45 µm

Heating mentle (Germany)

High performance liquid chromatography system (Shimadzu, Japan) equipped with

- Automatic sample injector (SIL-20AC HT)
- Communications bus module (SPD-M20A)
- Column (BDS Hypersil C18, 5µm, 250mm x 4.6mm)
- Precolumn (µBondpack C18, 5µm, 125 A^{o}, Water Corporation, Ireland)
- PDA-detector (SPD-M20A)
- Column oven (CTO-20A)

Light microscope (KHC, Olympus, Japan)

Magnetic stirrer (CAT, Germany)

Mircopipette (Pipetman, Gilson, Inc., France)

Modified Franz diffusion cells (Crown Glass Company, USA)

pH meter (Sartorius, USA)

Photon correlation spectroscopy (Nano ZS, Malvern, UK)

Reflux condenser

Refrigerated centrifuged (Beckman, USA)

Refrigerated incubator (FOC 225I, VELP Scientifica, Italy)

Rotary evaporator (Buchi heating bath B-490, Switzerland)

Sonicator (Model TP680DH, Elma, Germany)

Stability cabinet (Memert, Germany)

UV-spectrophotometer (UV-1601, Shimadzu, Japan)

Vortex mixer (Vortex Ginies-2, Scientific Industries, USA)

Water bath (Model WB22, Becthai Co., Ltd., Thailand)

Methods

1. Extraction of ellagic acid in dried pomegranate rind

In this study, the two extraction methods (Lu and Yuan, 2008 and Yoshimura et al., 2005) were compared in order to identify the suitable extraction procedures for ellagic acid. These two methods were selected because the purity of ellagic acid, the ability of extraction in lab-scale, the small amount of organic solvent used and the similar processes. Both of extraction methods began with the extraction of ellagitannins and then hydrolysis. The parameters used in this step of extraction were slightly different. The next process was divided into two procedures; with and without recrystallization by methanol (Method A and B, respectively). The parameters used in each method of extraction were shown in Figure 5. The suitability of extraction process was determined by no complexity, less organic solvent used and, high percentage yield and high percentage purity. The extractions were all carried out in triplicates.

1.1 Sample preparation

Pomegranate fruits were purchased from Thai local market and were then cleaned with tap water. The outer peel was manually separated from fresh sacs and cut into slices. The peel was dried in hot air oven at 60 ^{o}C for overnight and subsequently grounded to powders. The homogenized powders were passed through sieve no.6 before being used in both extraction methods.

1.2 Extraction methods

1.2.1 Method A (Lu and Yuan, 2008)

Forty grams of dried powders were accurately weighed and dispersed into 200 mL of ethanol. The dispersion was then shaken in water bath for 2 hours. After that, the residue was separated by centrifuging at 4000 rpm for 30 min. The extraction of this residue was repeated twice. The pooled supernatant was then concentrated by rotary evaporator at 40 ^{o}C until 0.25 mL of the resulting extract was reached. For hydrolysis, the concentrated extract was made up to 150 mL by distilled water and sulfuric acid was added to a concentration as indicated in Figure 5.

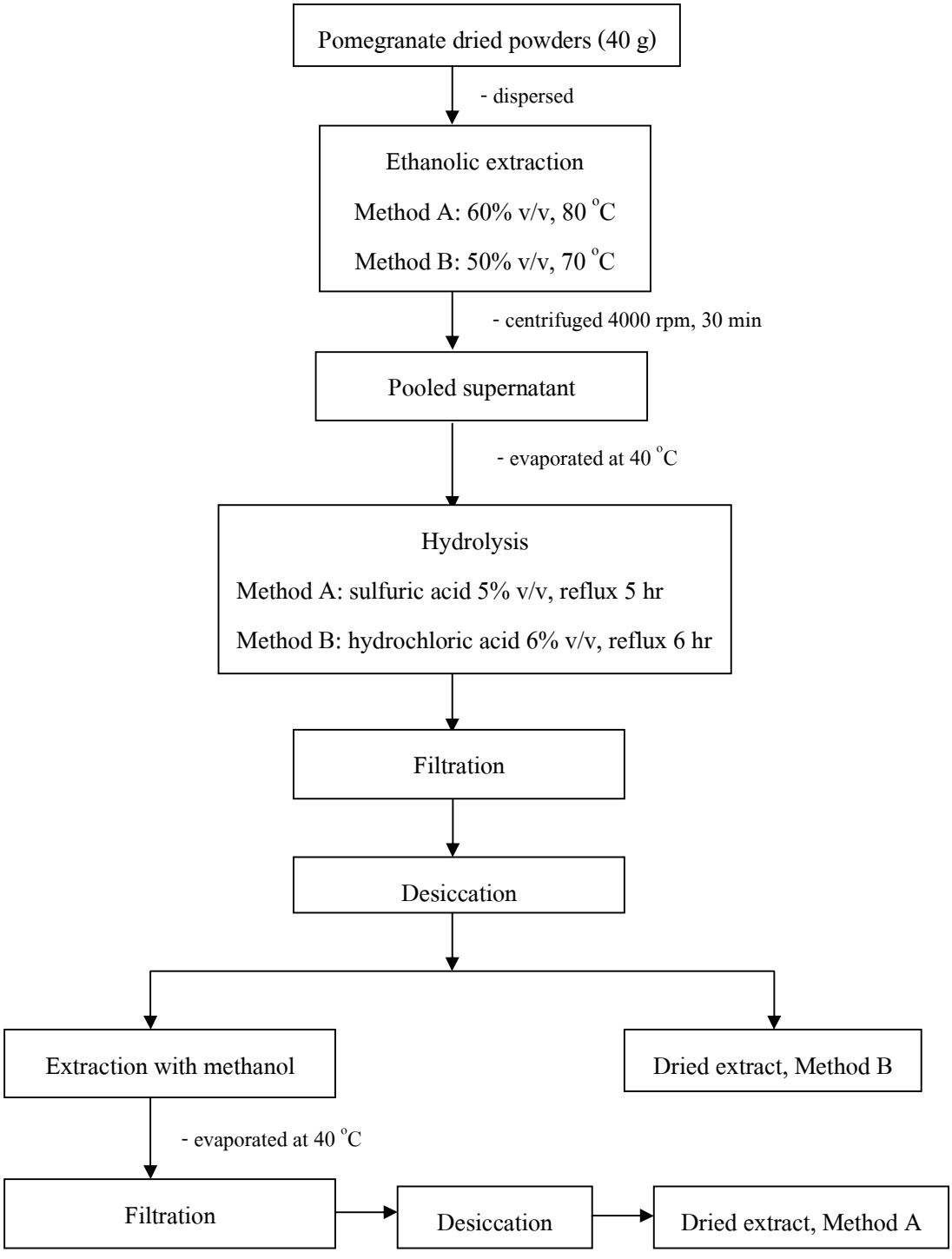

Figure 5 Schematic diagram of extraction method A and B

This mixture was then refluxed at 105 ^{o}C for 5 hours in the oil bath to control the temperature. After the hydrolysis reaction, the precipitates were removed and kept in desiccators for 2 days to dryness before using in the purification step. The dry residue was further suspended in methanol (30 mL/g residue) and then shaken in water bath (at 45 ^{o}C for 2 hours). The insoluble particles were then re-extracted in twice. The supernatant was concentrated by rotary evaporator at 40 ^{o}C. The residue was then filtered and kept in desiccators until dryness.

1.2.2 Method B (Yoshimura et al., 2005)

For the method B, the same amounts (40 g) of dried powders were accurately weighed and suspended into 200 mL of ethanol and shaken for 2 hours. The insoluble portion was re-extracted with ethanolic solution in thrice. The combined ethanolic extract was centrifuged. The pooled supernatant was then concentrated by rotary evaporator at 40 ^{o}C until 0.25 mL of the resulting extract was reached. Then, the concentrate was adjusted up to 150 mL by distilled water and hydrochloric acid was added to a concentration as described in Figure 5. After that, the extract was refluxed for 6 hours at 100 ^{o}C. Eventually, the resulting sediment was filtered and kept in desiccators to dryness.

1.3 Comparison of the two extraction methods

To compare the efficiency of each extraction procedure, the following evaluations were studied.

1.3.1 Total yield of dried extract

The percentage of total yield (% w/w) obtained from both methods was carried out according to the following equation:

$$\text{Percentage of total yield} = \frac{Wt_{final}}{Wt_{inital}} \times 100 \qquad \text{Eq. 2}$$

Where,

Wt_{final} is the total weight of dried solid extract (g), obtained at the end of extracting process.

Wt_{inital} is the total weight of dried powders from pomegranate rind (g), added before process of extraction.

1.3.2 Thin Layer Chromatography (TLC)

To verify the existence of ellagic acid, TLC was carried out by modifying from Jeganathan and Kannan (2008). The stationary phase was commercial precoated silica gel 60 F_{254} which was cut into 4.5x8 cm and marked the starting line above the lower edge of the plate about 1 cm. Both samples of the crude extract were dissolved in methanol (0.5 mg dried extract/mL) and spotted onto an analytical TLC plate paralleled with a standard ellagic acid solution (1 μg/mL methanol). The TLC plate was then developed using toluene:ethyl acetate:formic acid:methanol (6:6:1.6:0.4 v/v) as the mobile phase. After development, the spots were examined under UV radiation (254 nm). The characteristics of spot or band were observed and the distances of spots were measured to calculate the R_f values. And the R_f values of each dried extract were compared with the reference standard.

1.3.3 Ultraviolet (UV) spectroscopic method

UV-spectroscopy is used for identifying of ellagic acid and measuring percentage of purity of the dried extracts. Each of dried extract was done in triplicate. UV-spectroscopic method was validated using the guideline in the USP 32/NF 27 (United Stated Pharmacopeia, 2010). The validations for specificity, linearity, accuracy, and precision were tested as described in Appendix A.

1.3.3.1 Identification by UV-spectrum

UV-spectrum was used to confirm the identification of ellagic acid in dried extract. Each of dried extract was dissolved in methanol (27 μg/mL) and the UV-spectrum between 200-800 nm was scanned by UV-spectrophotometer (UV1601, shimadzu). The resulting spectrum was then compared with the spectrum of standard solution of ellagic acid (2.5 μg/mL in

methanol). The wavelength of maximum absorption (λ_{max}) was determined and used in the analysis of percentage purity.

1.3.3.2 Percentage purity

- Preparation of standard solutions

Standard solution (1 mg/mL) of ellagic acid was prepared by dissolving standard ellagic acid 1 mg in methanol in 10 mL volumetric flask. Working standard solutions were prepared by diluting the stock solution at the concentration of 1.5-4 μg/mL in methanol. Then the absorbance of these solutions was measured at maximum absorption wavelength obtained from Section 1.3.3.1 and calibration graph was prepared by plotting absorbance against concentration.

- Preparation of samples

Ellagic acid content in dried extract was determined. 0.5 mg of dried extract was weighted and dissolved in 10 mL methanol in volumetric flask. The appropriate dilutions were made in the range of 1.5-4 μg/mL of ellagic acid. The absorbance was then recorded at maximum absorption wavelength obtained from Section 1.3.3.1 and the amount of ellagic acid in sample was calculated according to a calibration curve.

1.3.4 High Performance Liquid Chromatographic (HPLC) method

HPLC technique was used to confirm the percentage purity of the dried extract. Each of dried extract was determined in triplicate. A reversed phase HPLC assay was developed for the determination of ellagic acid and validated as same as described in Section 1.3.3. The methods of validation were explained in Appendix B.

- Preparation of standard solutions

One milligram of ellagic acid was accurately weighed and dissolved in methanol in 10 mL volumetric flask. The mixture was swirled until ellagic acid was completely dissolved and then adjusted to the final volume by methanol. The stock solution had a final concentration of 100 μg/mL. Standard solutions with the known concentrations of 0.8-3.3 μg/mL were then prepared by the dilution of the stock solution with methanol.

- Preparation of internal standard solution

One milligram of propyl paraben was accurately weighted and dissolved in methanol in 10 mL volumetric flask. The mixture was swirled until propyl paraben was completely dissolved and then adjusted to the final volume by methanol. The stock solution had a final concentration of 100 µg/mL. Standard solution with a known concentration of 1.762 µg/mL was then prepared by the dilution of the stock solution with methanol.

- Preparation of samples

0.5 mg of dried extracts was accurately weighted and dissolved in methanol in 10 mL volumetric flask. The mixture was swirled until the dried extract was completely dissolved and then adjusted to the final volume by methanol. This solution was diluted with an appropriate amount of methanol to obtained peak area ratio in the range of standard curve. The amount of internal standard (0.2 µg/mL) was added to the sample solution prior to the HPLC analysis. The amount of ellagic acid in sample was calculated according to calibration curve. Chromatographic condition for determination of ellagic acid was as follow:

Column	: BDS Hypersil® C18, 5 µm, 250x4.6 mm
Precolumn	: µBondapack C18, 10 µm, 125 A^0
Mobile phase	: 0.2% phosphoric acid: methanol (45:55 v/v)
Injection volume	: 10 µL
Flow rate	: Isocratic, 0.8 mL/min
Detector	: PDA detector at 255 nm
Temperature	: 30 ^oC

Percentage purity of dried extract was calculated as in Equation 3:

$$\text{Percentage purity} = \frac{\text{gram of ellagic acid}}{\text{gram of dried extract}} \times 100 \qquad \text{Eq. 3}$$

Where, percentage purity is the content of ellagic acid in dried extract 100 gram, gram of ellagic acid is gram of ellagic acid calculated from Section 1.3.3 and 1.3.4 respectively, gram of dried extract is gram of dried extract which is used in each analysis method (UV and HPLC). The method that gave a high percentage yield and purity was then selected. The pomegranate peel was then extracted by the selected method in this study. All dried extracts were then pooled, and percentage purity was analyzed by HPLC method as described above. The pooled extract was then used in further studies.

2. Saturated solubility study of ellagic acid in various oils and surfactants

To screen components used in formulations, the saturated solubility study of ellagic acid in various oils and surfactants were conducted for achieving a high loading capacity of ellagic acid.

2.1 Saturated solubility study in different oils

Rice bran oil as natural triglyceride, sweet orange oil as essential oil, oleic acid as unsaturated fatty acid, isopropyl myristate as fatty ester, squalene as synthetic hydrocarbon and mineral oil as natural hydrocarbon were used in this study. The saturated solubility study of ellagic acid in those oils was modified from the study of Azeem et al. (2009). An excess amount of a pooled extract was added into each oil (4 g) and mixed thoroughly. The mixtures were then shaken continuously at 25±2 ^{o}C for 72 hours. Saturated solutions were filtered with 0.22 μm syringe filter and diluted by appropriate solvents to the concentration in the range of calibration curve in Section 1.3.3.2. Ellagic acid was used as a marker and analyzed by validated UV-spectroscopy (see Appendix A). The amount of ellagic acid was analyzed by absorbance measurement at maximum absorption wavelength obtained from Section 1.3.3.1 and interpreted by using calibration curve. The saturated solubility of dried extract was calculated from the amount of ellagic acid, and percentage purity of the pooled extract. The amount of ellagic acid was divided by the percentage purity of the pooled extract, before being used in Equation 4. The percentage purity of the pooled extract was determined as described in Section 1.3.4. The top three solubilities of dried extracts in the oils were then chosen for Section 3.1.

$$\text{The solubility of dried extract (μg/g oil)} = \frac{\text{the amount of ellagic acid in pooled extract}}{\text{gram of oil}} \qquad \text{Eq. 4}$$

2.2 Saturated solubility study in different surfactants

Non-ionic surfactant was included in this study because this type of surfactant does not cause irritation to the skin. The investigated groups of non-ionic surfactants were polyoxyethylene sorbitan fatty acid ester, sorbitan fatty acid ester, polyoxyethylene alkyl ether and polyoxyethylene castor oil derivatives. Each surfactant was selected from the representative of each group of surfactants. The selected surfactants were Tween®20 and Tween®80 for polyoxyethylene sorbitan fatty acid ester, Span®20 and Span®80 for sorbitan fatty acid ester, Brij®30, Brij®93, and Brij®97 for polyoxyethylene alkyl ether, and Cremophor® RH 40 for polyoxyethylene castor oil derivative. Saturated solubility of ellagic acid and the calculated solubility of dried extract in each surfactant were determined as same as in Section 2.1. The surfactants were selected according to the high solubility. Each surfactant was then matched for the study in Section 3. The criteria of coupling were the structure of each surfactant, the solubility of ellagic acid and the HLB values of oils with the HLB values of surfactants. The matching surfactant structures were classified into the same and different structures. The definition of the same surfactant structure is the first and the second surfactants of surfactant mixtures must be in the same class of surfactants. These two surfactants must have the same number of carbon atoms at surfactant tail also. An example of a pair of surfactant is Tween®20 and Span®20. The definition of the different surfactant structures is divided into two classes. In the first case, the first and the second surfactants of surfactant mixtures must be in the same class of surfactants, but the number of carbon atoms must be different. For example, the mixture of surfactants was Tween®20 and Span®80. In the second class, the first and the second surfactants of surfactant mixtures must be in different classes of surfactants. For example, a pair of surfactant mixture was Tween®20 and Brij®97. Considering the HLB values, the first surfactant must had a HLB value greater than the value of the HLB of oils used in formulations. A HLB value of the second surfactant must be less than the value of the HLB of oils to control the HLB_{mix} of the matching surfactants equal the HLB of the oils.

3. Formation of o/w nanoemulsion by low energy emulsification method

The main factors influencing the formation and the stability of nanoemulsion are the types and the amounts of oils and surfactants. To optimized formulation of nanoemulsion, the effect of

those factors on nanoemulsion formation and its stability were studied. Prior to prepare nanoemulsion, the key point is the HLB value of surfactant mixtures and the HLB value of oil. Nanoemulsion can be formed easily and has high stability when the HLB value of surfactant mixtures close to the HLB of oil (Dai et al., 1997; Liu et al., 2006; Li et al., 2010). Therefore, the HLB of selected oil from Section 2.1 were studied as follow.

3.1. Determination of HLB values of oils

The HLB values of selected oils were investigated according to Morais et al. (2006). Emulsions were prepared at different values of HLB_{mix} of surfactant mixtures. The values of HLB_{mix} were selected from the value of HLB in literature±2. The surfactant mixture used in this study was Tween®80 and Span®80 because this combination of surfactants makes the most stable emulsion (Lu and Rhodes, 200). If the HLB value of Tween®80 could not be set for HLB_{mix} over the value of HLB of the oil, Tween®20 (HLB 16.7) and Span®20 (HLB 8.6) were used as a pair of surfactants to determine the HLB of that oil. The value of HLB_{mix} was calculated as follow.

$$HLB_{mix} = (HLB_T)(\%T) + (HLB_S)(\%S) \qquad \text{Eq. 5}$$

Where HLB_T and HLB_S were HLB values of Tween® and Span® respectively, %T and %S were percentages of Tween® and Span® respectively. The total amount of surfactant mixtures was determined at 10% w/w. After calculating the amount of Tween® and Span®, Span® was added in an oil phase and Tween® was added into the water phase. The oil phase and water phase were heated separately at 60 and 65 C^o respectively. The water phase was then slowly added into the oil phase with agitation. The HLB of the oil was evaluated from the stability of emulsion immediately after preparation. The stability of emulsion was continued monitored until phase separation was apparently seen. The value of HLB_{mix} that made the most stable emulsion was determined as the HLB value of the oil.

3.2 Effect of types and amounts of oils and surfactants on nanoemulsion formation

Formation of nanoemulsion by low energy emulsification depends on the compositions used in formulations. Therefore, the types and the amounts of oils and surfactants can affect nanoemulsion formation. In this study, the effects of oil (selected from Section 2.1) and

surfactant (selected from Section 2.2) types and the amounts of oils (10, 20, 30% w/w) and surfactants (5, 10, 15% w/w) to nanoemulsion formation were studied.

Nanoemulsion was prepared by the study of Liu et al. (2006) with slight modification. The preparation process of nanoemulsion was described as follows. Briefly, the oil and surfactants were mixed by changing ratio of surfactant mixtures according to the HLB of selected oil obtained from Section 3.1. The water phase was added at 0.2 mL/min with continuous stirring by a magnetic bar at 400 rpm. When the viscosity of formulation increased, the rate of water was immediately changed to 1 mL/min. Then, the formulation was continued stirring for 20 min.

After that, the formation of nanoemulsion and the physical stability were evaluated. Formation of oil in water nanoemulsion was also examined. The obtained formulation was subsequently characterized on the physical properties of nanoemulsion as described follow.

- Visualization (Shafiq-un-Nabi et al., 2007)

The appearance of formulation was first visualized, and the formulation must not be separated after emulsion was prepared.

- Particle size determination (Shafiq-un-Nabi et al., 2007).

The average particle size was measured by photon correlation spectroscopy (NanoZiser ZS, Malvern, UK) after the formulation was left overnight. Samples (50 μL) were diluted with water (3 mL) before analysis. The experiments were done in triplicate. Average particle sizes must be less than 500 nm.

- Type of emulsion

- Dilution test (Allouche et al., 2003)

The formulations (200 μL) were diluted with water or oils used in formulations. If the formulation was easily dispersed in water, the formulation was defined as oil in water. If the formulation was dispersed in oils, the formulation was determined as water in oil. The formulations were done in triplicate. The formulations must be dispersed in water.

- Conductivity (Morales et al., 2003)

Conductivities of the formulations were measured using conductivity meter. To indicate oil in water type of formulations, the formulations must have conductivity. The measurements were done in triplicate.

To optimize the formulation of nanoemulsion, the physical stability was used for screening the formulation for the study in Section 4. The physical stability was determined as follow.

3.3 Physical stability of formulations in accelerated conditions (Shafiq et al. (2007)

The physical stability of the nanoemulsions selected from Section 3.2 were tested in three steps, i.e. centrifugation, heating cooling cycles and freeze thaw cycles respectively. The stable nanoemulsions were evaluated as described in Section 3.2 in each step. The accelerated stability tests were as follows:

3.3.1 Centrifugation

The selected nanoemulsions were subjected to centrifugation at 3500 rpm for 30 min. The stable formulations with no phase separation and with no change of particle size were then selected for heating cooling cycles.

3.3.2 Heating cooling cycles

Passed formulations were kept at 4 ^{o}C for 48 hours and 45 ^{o}C for 48 hours respectively. This step was repeated for 6 cycles. The stable formulations were then subjected to freeze thaw cycles.

3.3.3 Freeze thaw cycles

Passed formulations were kept at -21 ^{o}C for 48 hours and 25 ^{o}C for 48 hours respectively. This step was repeated for 3 cycles. The stable formulations were then selected for Section 4.

4. Investigation of ellagic acid loaded nanoemulsion

4.1 Effect of ellagic acid loading on nanoemulsion formation

To investigate the effect of ellagic acid loading on nanoemulsion formation, the selected formulations from Section 3.3 were prepared as described in Section 3.2. The amount of dried extracted was added in formulation according to its saturated solubility in an oil/surfactant mixture. This saturated solubility study was carried out according to Section 2.1. Some impurities in dried extract remained in formulation after added in the form of insoluble particles. Therefore, the oil phase was filtered before preparation. The chromatographic condition for determination of ellagic acid in each oil phase was as follow:

Column : BDS Hypersil® C18, 5 µm, 250x4.6 mm

Precolumn : µBondapack C18, 10 µm, 125 A^0

Mobile phase : Gradient system

Solution A: 0.2 %v/v phosphoric acid,

Solution B: Methanol

Injection volume : 10 µL

Flow rate : 0.8 mL/min

Detector : PDA detector at 255 nm

Temperature : 35 ^oC

Nanoemulsion formation was evaluated as described in Section 3.2 and precipitation of ellagic acid was examined under microscopy technique. Determination of ellagic acid content was analyzed by validated HPLC method (see Appendix B) as described above.

4.2 Effect of ellagic acid loading on physical stability

Physical stability of nanoemulsion was studied after ellagic acid loading. The selected formulations from Section 4.1 were centrifuged at 3500 rpm for 30 min. Physical stability was evaluated as described in Section 3.2. Formulations with no precipitation were then kept at stress condition (45 ^oC) for 3 months. The physical stability was evaluated as described in Section 3.2, and the precipitation of ellagic acid was evaluated as same as in Section 4.1. The chemical

stability was evaluated by determination of ellagic acid content at 0, 1, 2 and 3 months. The most stable formulation was then selected for Section 5.

5. In vitro release study

The release of ellagic acid from formulation selected from Section 4 was studied. The release profiles of ellagic acid solution in phosphate buffer saline (pH 7.4) was compared and plotted between the percentage of cumulative amounts of ellagic acid released and time. The release study was performed by modified Franz diffusion cells with internal diameter 1.70-1.75 cm. The effective permeable surface area of the cell was 2.27-2.41 cm^2. The donor and receptor compartments were separated by dialysis membrane (cellulose tubular membrane, Cellu-Sep®) with a molecular cut-off of 12,000-14,000. The cellulose membrane was hydrated in purified water for 24 hours and then washed by hot water. Before the cellulose membrane being used, the membrane was soaked in Phosphate buffer saline pH 7.4 for 1 hour. Phosphate buffer saline pH 7.4 was selected as receiver medium. The receptor compartment was equipped with a magnetic stirring bar. The rotating rate was fixed at 600 rpm. The temperature of the receiver medium was kept at 37 ^{o}C by circulating water though a jacket surrounding the cell body throughout the experiments. The receptor fluid and the membrane were equilibrated to the desired temperature for 30 min. After equilibration, 2.0 mL of the selected formulation was placed onto the membrane surface of each cell and the cell was then tightly covered by paraffin film. The receptor fluid 3.0 mL was removed 0.5, 1, 2, 3, 4, 8, 12, 16 and 24 hours and replaced with an equal volume of prewarmed (37 ^{o}C) fresh medium. The receptor fluid was diluted at appropriate concentration and measured by using HPLC condition as in Section 4.1. The percentage of ellagic acid released was calculated by the following equation

$$\% \text{ Ellagic acid released} = (A_t/A_0) \times 100 \qquad \text{Eq. 6}$$

Where A_t is the cumulative amount of ellagic acid released at a particular time; A_0 is the initial amount of ellagic acid in 2 mL of each formulation. The release study for each formulation was performed in quadruplicate.

6. In vitro permeation study

The permeation was investigated utilizing modified Franz diffusion cell. The abdominal skin of newborn pig was used (Cilurzo, Minghetti, and Sinico, 2007).

6.1 Preparation of newborn pig skin membrane

The skin was completely removed subcutaneous fat and extraneous tissue using forcepts and scissors to obtain a full-thickness abdominal skin membrane. The separated skin was cleaned in purified water. Then it was wrapped in aluminum foil and stored in a freezer (-20 ^{o}C). The frozen skin was thawed and left to rehydrate by immersing in phosphate buffer saline pH 7.4 for 1 hour before being used.

6.2 Permeation study

The procedure of permeation study was the same as release study from Section 5 except that the membrane used in this study was newborn pig skin. The excised newborn pig skin was covered with stratum corneum facing the donor compartment and the dermal side facing the receptor fluid. The skin and the receptor fluid were equilibrated to 32 ^{o}C and 37 ^{o}C, respectively, for 30 min. After equilibration, 2 mL of formulation or 1mL of control solution was added onto donor compartment of each cell. Control solution is a solution of dried extract in phosphate buffer saline pH 7.4. All formulations were freshly prepared before being used. At 24 hours, donor, skin, and receiver medium were then immediately analyzed by HPLC with the same condition of Section 5. Each set of experiments was performed in triplicate.

6.3 Skin retention of ellagic acid

At the end of permeation study, the skin surface and the donor cap were washed 5 times with isopropyl alcohol (IPA) for formulations and with phosphate buffer pH 7.4 for control solution. Each sample was appropriated diluted and analyzed by validated HPLC method. The skin was then removed. The skin was cut into small pieces and extracted with IPA by vortexing for 5 minutes, sonicating for 5 min, and shaking at ambient temperature overnight. Each sample was then centrifuged and the supernatant was then analyzed by validated HPLC method.

7. Statistical analysis

Statistical analysis to compare treatment means was performed on SPSS version 13.0. The statistical difference of all experiment data were tested with a significant level at 95 % ($p<0.05$). Average particle size of formulations before and after centrifugation was tested with Paired t-test. Average particle size of formulations at heating cooling and freeze thaw cycle were performed with one-way ANOVA. For post hoc analysis, Tukey's HSD or Dunnett T3 test was used if the distribution of data did not deviate significantly from normality.

CHAPTER IV

RESULTS AND DISCUSSION

1. Extraction of ellagic acid in dried pomegranate rind

The existence of ellagic acid in each dried extract was determined by TLC. The TLC chromatograms of both dried extract samples showed similar pattern to the reference standard of ellagic acid as depicted in Figure 6. Moreover, the equal R_f values of dried extract from method A (0.37), method B (0.37) and reference standard (0.37) were obtained. Therefore, the equal R_f values and the same characteristic of the TLC patterns among method A, method B and reference standard indicated the presence of ellagic acid in both dried extracts from method A and B.

Figure 6 Thin-layer chromatograms of dried extract samples obtained from pomegranate rind (method A and B) compared to the reference standard . Each spot was identified as, **S**:reference standard, **A**:dried extract obtained from method A, and **B**:dried extract obtained from method B, respectively

The presence of ellagic acid in each dried extract was also confirmed by UV-spectroscopy. The result revealed that the spectra of dried extracts from both method A and B were similar to

the spectrum of reference standard (Figure 7). The existing peak of ellagic acid exhibited at 255 nm. These spectra supported that the dried extracts from method A and B contain ellagic acid. The maximum absorption was found at 255 nm, which is in agreement with Bala et al. (2006).

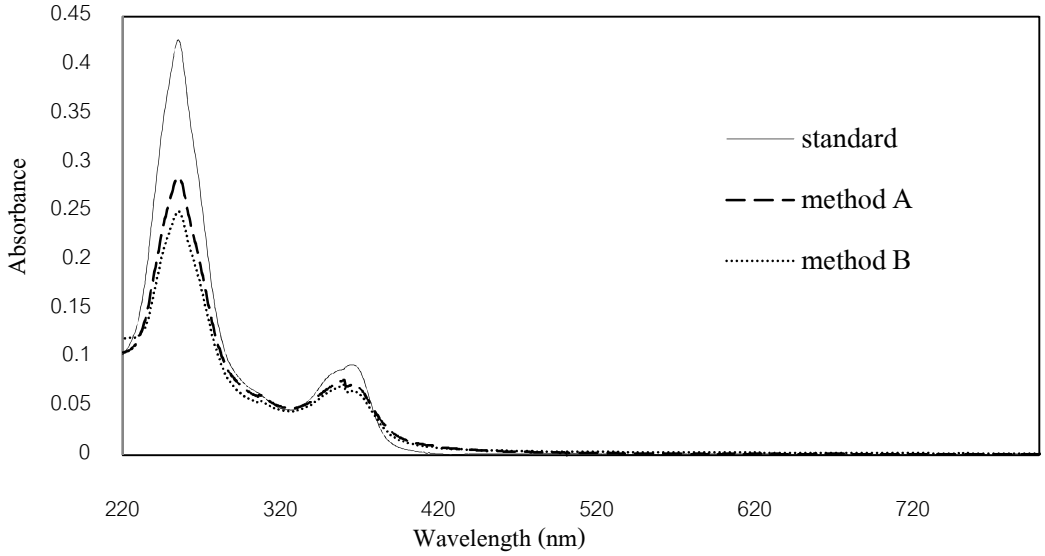

Figure 7 Ultraviolet spectra of dried extracts from method A (- - -) and method B (·····) along with the standard solution of ellagic acid (——)

The percentages of yield and purity from both method A and B were determined. The percentage of yield was calculated from equation 2 as described in Chapter 3. The percentage of purity was determined by UV-spectroscopy and confirmed by HPLC. The specificity, linearity, accuracy, and precision were passed in all criteria as described in Appendix A and B for UV and HPLC analysis respectively. The percentages of yield and purity of both extraction methods were shown in Table 1. The results demonstrated that percentage yield of method B (6.28±1.66%) was higher than method A (0.71±0.11%). However, the purity percentage of method A (77.70±5.37%) gave a higher purity percentage than method B (25.99±1.34%) with UV analysis. In addition, the percentage of purity analyzed by HPLC confirmed the result of the percentage purity analyzed by UV-spectroscopy. The difference of method A and B was the procedure of extraction. Method B used only one step of extraction but method A involved in two steps. For method B, the hydrolysis was only used and then finished in the process, while method A started with hydrolysis and used the recrystallization for the next step. In the hydrolysis reaction process, punicalagin from pomegranate rind produces hexahydroxydiphenic acid (HHDP) and glucose. Then ellagic acid is released from HHDP by spontaneous lactonization (Häkkinen et al., 2000).

Therefore, the impurities in method B might come from those reactions. In the recrystallization process, ellagic acid was separated from impure dried extract by suspending the dried extract in methanol. Ellagic acid is then dissolved in methanol but the contaminating substances remained. When methanol was evaporated, ellagic acid was less soluble and precipitated to the crystal form with the higher purity. Therefore, the recrystallization process of method A could help ellagic acid become purer. In this study method A used the hydrolysis and the recrystallization as same as in the study of Lu and Yuan (2008), and method B used only the hydrolysis as same as in the study of Yoshimura et al. (2005). Nevertheless, both dried extracts in this study have both a lower purity and yield percentage than the study of Lu and Yuan (2007) and Yoshimura et al. (2005). This may be due to the dissimilarity of environmental conditions of disparate sources of pomegranate fruits causes different contents of polyphenolic compound (Borochov-Neori et al., 2009). This can make a different of percentage yield and purity of ellagic acid.

Table 1 Percentages of yield and purity (average value±SD, n=3) of ellagic acid from different extraction methods

Method	%Yield	%Purity	
		UV	HPLC
A	0.71±0.11	77.70±5.37	67.04±1.74
B	6.28±1.66	25.99±1.34	26.05±2.50

In comparison of method A and B, method B gave a high percentage yield with a low percentage purity while method A gave a low percentage yield with a high percentage purity. From the purity of the dried extract, method A was selected for extraction in this study.

2. Saturated solubility study of ellagic acid in various oils and surfactants

2.1 Saturated solubility study in different oils

The saturated solubility of dried extract in various oil types was studied. The ellagic acid content was used as a marker and determined by UV-spectroscopy. The validation of UV-spectroscopy was passed in all criteria as described in Appendix A. The results of the saturated solubility of dried extract were calculated from equation 4 as described in Chapter 3. The purity

percentage of the pooled extract was 48.80±0.69% w/w. From Table 2, rice bran oil had the strongest solubilizing power for dried extract. Sweet orange oil and oleic acid had the second and the third strongest solubilizing power, respectively. The solubility of the last three of dried extracts was obtained in squalene, isopropyl myristate and mineral oil, respectively. This result was similar to the study of Bala et al. (2006).

Table 2 Saturated solubility of dried extract in different oils

Oil types	**Ellagic acid (µg/g)**	**Calculated dried extract (µg/g)**
Rice bran oil	278.97±4.12	571.65±8.45
Sweet orange oil	91.52±2.39	187.54±4.90
Oleic acid	61.18±2.45	125.37±5.03
Squalene	9.51±0.49	19.44±0.97
Isopropyl myristate	5.06±2.49	10.38±5.10
Mineral oil	2.84±0.06	5.83±0.13

They found that the solubility of ellagic acid increased by solvents containing functional group that has an ability to form hydrogen bonds. In this case, polyethylene glycol 400 (PEG 400) with 9 polyoxyethylene groups showed the high solubility of ellagic acid. Hydrogen bonding can be formed between two functional groups acted as hydrogen bond donor and hydrogen bond acceptor respectively. The hydrogen bond donor group is the H atom attached to the electronegative atoms (O, N, S, F, Cl, Br, I, and C), and the hydrogen bond acceptor group is the electronegative atom or π-bond of unsaturated hydrocarbon (Gilli and Gilli, 2009). Rice bran oil has a triglyceride oil as the main component. Triglyceride oil is the oil containing many O atoms. Therefore, the high O atoms acted as the hydrogen bond acceptors of triglyceride oil (Figure 8) may be responsible for the highest solubility of ellagic acid caused by hydrogen bonding with the OH atoms acted as the hydrogen bond donors of ellagic acid (Figure 1). In the case of sweet orange oil and oleic acid, sweet orange oil has a large number of hydrogen bond acceptors with π-bonds and oleic acid has the hydrogen bond acceptor with π-bonds and hydrogen bond acceptor with O atoms (see Appendix C). Therefore, these functional groups can be responsible for the high solubility of ellagic acid. In the case of mineral oil, there is no atom that can form hydrogen bonds. This may be responsible for the lowest solubility of ellagic acid.

Shruthi and Ramachandra (2011) found that ellagic acid had an ability to form hydrogen bonds. This supported the ability of hydrogen bonding of ellagic acid. From this study, it can be concluded that ellagic acid is more soluble in rice bran oil (triglyceride oil), sweet orange oil (essential oil), and oleic acid (fatty acid), respectively. Therefore, those oils were selected for Section 3.

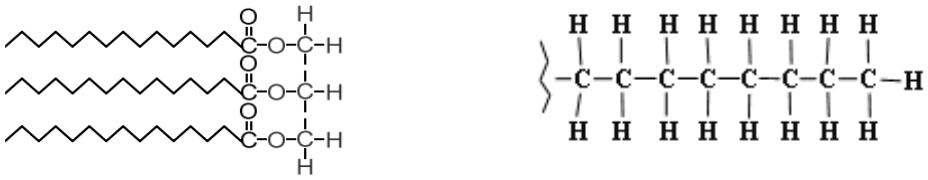

Figure 8 Structures of triglyceride (left) and mineral oil (right)

2.2 Saturated solubility study in different surfactants

The effect of surfactant types on saturated solubility of dried extract was studied. From Table 3, the order of dried extract solubility in various surfactants was Tween®80~Tween®20> Brij®97~Brij®93>Span®80~Cremophor RH®40>Span®20> Brij®30. The saturated solubility of dried extract was high with polyoxyethylene sorbitan fatty acid ester group. This may be caused by the high O atoms at ethylene oxide groups (20 units) (see Appendix C) providing hydrogen bonding with the OH groups of ellagic acid (Figure 1). Brij®30 showed the lowest saturated solubility of dried extract. This may be due to saturated C-12 in the carbon chain which could not bond with ellagic acid (see Appendix C). In contrast, Brij®97 and Brij®93 have unsaturated C-18 in the carbon chain (see Appendix C) which cause hydrogen bonding and is responsible for the high solubility of ellagic acid. Therefore, Brij®30 was not included in further studies. In this study, Tween®80, Tween®20, Brij®97, Brij®93, Span® 80, Cremophor RH®40 and Span®20 were selected. This selection was based on the same and different structures of surfactants which had a good saturated solubility of dried extract. Consequently, the same and different structures of surfactants were matched for Section 3 as explained in Chapter 3. Before coupling, the values of HLB of oils were investigated as in Section 3.

Table 3 Saturated solubility of dried extract in different surfactants

Surfactant groups	Surfactant types	Ellagic acid (µg/g)	Calculated dried extract (µg/g)
Polyoxyethylene sorbitan fatty acid ester	Tween®80	272.51±12.59	558.42±25.80
	Tween®20	245.00±18.88	507.88±38.70
Polyoxyethylene alkyl ether	Brij®97	154.05±6.94	315.68±14.23
	Brij®93	133.55±7.65	273.67±15.68
	Brij®30	25.33±5.49	51.91±11.25
Sorbitan fatty acid ester	Span®20	48.05±8.22	98.46±16.85
	Span®80	105.87±16.01	216.94±32.82
Polyoxyethylene 40 castor oil	Cremophor RH®40	104.67±22.10	214.50±47.14

3. Formation of nanoemulsion by low energy emulsification method

Formation of nanoemulsion by low energy emulsification depends on the types and amounts of oils and surfactants. In this study, the effects of the types and amounts of oils (10, 20, 30% w/w) and surfactants (5, 10, 15% w/w) to nanoemulsion formation were studied. The studied oils were rice bran oil, oleic acid, and sweet orange oil, respectively. The studied surfactants were matched as explained in Section 2.2. Nanoemulsions were prepared and the formation of nanoemulsion and its stability were then evaluated as described in Chapter 3.

3.1 Determination of HLB values of oils

Nanoemulsion can be easily formed when the value of HLB_{mix} of surfactant mixtures is close to the value of HLB of oil (Dai et al., 1997; Liu et al., 2006; Li et al., 2010). Therefore, the values of HLB of rice bran oil, oleic acid, and sweet orange oil were determined. The HLB values in literature for rice bran oil, sweet orange oil and oleic acid were 7 (Bernardi et al., 2011), 13 (Wolf and Havekotte., 1989) and 16 (Mahato and Narang, 2012) respectively. Therefore, the investigated values of HLB_{mix} for rice bran oil were 5, 6, 7, 8 and 9, for sweet orange oil were 11, 12, 13, 14 and 15, respectively. For oleic acid, the values of HLB_{mix} were selected from the value

of HLB in literature-2. This is because the highest HLB value of surfactants used in this study could not be set for HLB_{mix} over the value of HLB of oleic acid. In this case, Tween®20 (HLB 16.7) and Span®20 (HLB 8.6) were used as a pair of surfactants to determine the HLB. Therefore, the investigated values of HLB_{mix} for oleic acid were 14, 15 and 16, respectively. For rice bran oil, HLB 7 made emulsion more stable than the other HLB values after two days of preparation, while phase separation occurred with HLB 5, 6, 8, and 9 respectively. For oleic acid, HLB 16 made stable emulsion after preparation while phase separation occurred with HLB values of 14 and 15 respectively. HLB value of 14 made stable emulsion with sweet orange oil, but HLB values of 11, 12, 13, and 15 could not (Figure 9). Therefore, HLB values of rice bran oil, sweet orange oil, and oleic acid were 7, 14 and 16, respectively. This result is slightly different to other literature (Burnadi et al., 2011(rice bran oil 7); Wolf and Havekotte., 1989 (sweet orange oil 13); Mahato and Narang, 2012 (oleic 16)). It may be due to the difference of raw materials which cause a variation of HLB from the other studies. The HLB of rice bran oil (7), oleic acid (16), and sweet orange oil (14) were then used in Section 3.2.

Rice bran oil, at 2 days of preparation

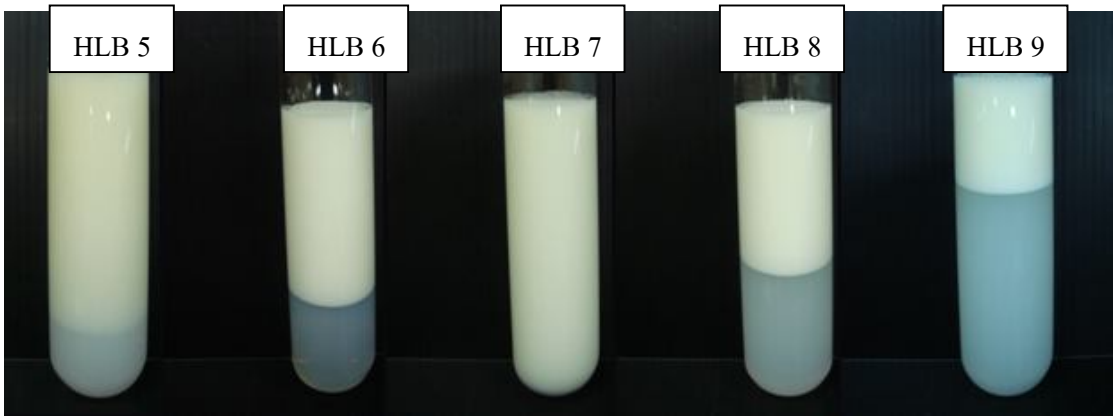

Figure 9 (continue) Emulsion at various HLB_{mix} values of Tween®80:Span®80 (for rice bran oil and sweet orange oil) and HLB_{mix} values of Tween®20:Span®20 (for oleic acid), at 10% w/w of oil and 10% w/w of total surfactant mixtures.

Oleic acid, at 7 days of preparation

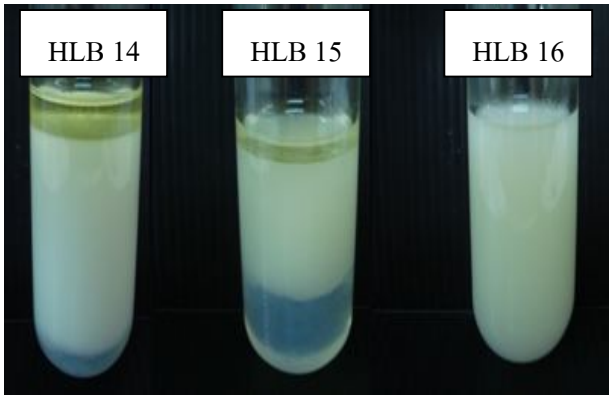

Sweet orange oil, at 1 days of preparation

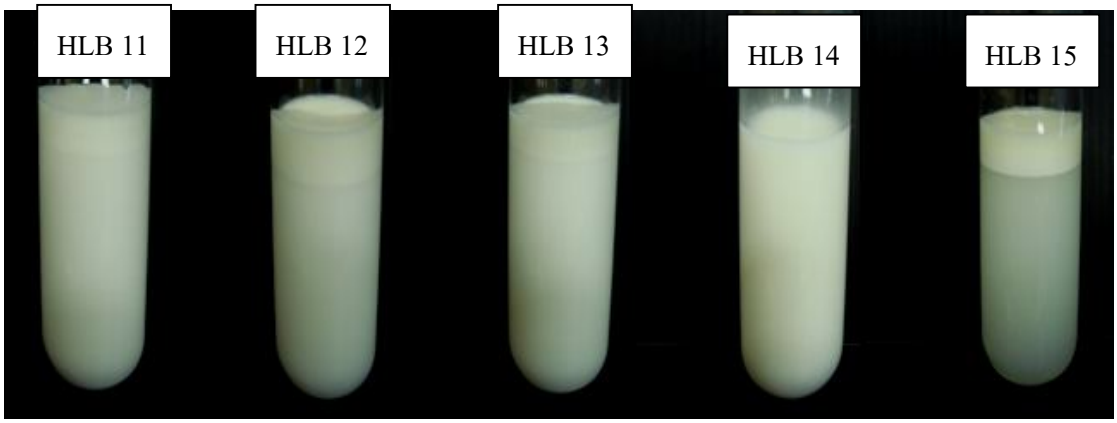

Figure 9 (continue) Emulsion at various HLB_{mix} values of Tween®80:Span®80 (for rice bran oil and sweet orange oil) and HLB_{mix} values of Tween®20:Span®20 (for oleic acid), at 10% w/w of oil and 10% w/w of total surfactant mixtures

3.2 Effect of types and amounts of oils and surfactants on nanoemulsion formation

The surfactants were matched based on the HLB of oils. The HLB values were 7, 16 and 14 for rice bran oil, oleic acid and sweet orange oil, respectively. For matching surfactants, the principle emulsifier must have a HLB value above the HLB of oil, and co-emulsifier must have a HLB value below the HLB of oil. The HLB values of surfactants were described in Appendix C. The same structures of surfactants are based on the same group of surfactants and the same number of carbon chain lengths (see Appendix C). For example, Tween®20 was matched with Span®20 (see Appendix C). The different surfactant structures are based on the difference of surfactant groups between the two surfactant mixtures or the difference of number of carbon

chain lengths. For example, Tween®20 was matched with Brij®97 for the different surfactant groups and Tween®20 was matched with Span®80 for the different number of carbon chain lengths. Table 4 illustrates all matching surfactants.

3.2.1 Effect of oil types

The effect of oil types on nanoemulsion formation was investigated in this study. The results indicated that rice bran oil and oleic acid make difficult to form nanoemulsion compared to sweet orange oil. As can be seen in Table 5, 6 and 7, the Y regions of nanoemulsion formation with rice bran oil and oleic acid are less than sweet orange oil.

Table 4 Coupling of matching surfactants with the same and different structures

Oil types	**Same structures**	**Different structures**
Rice bran oil	Tween®80:Span®80 Brij®97:Brij®93	Tween®80:Brij®93 Tween®20:Span®80 Tween®20:Brij®93 Brij®97:Span®80
Oleic acid	Tween®20:Span®20	Tween®20:Span®80 Tween®20:Brij®93 Tween®20:Brij®97 Tween®20:Cremophor RH®40
Sweet orange oil	Tween®80:Span®80 Tween®20:Span®20	Tween®20:Span®80 Tween®20:Brij®93 Tween®20:Brij®97 Tween®80:Brij®97

Table 5 Formation of nanoemulsions containing rice bran oil at different concentrations (10, 20, 30% w/w) with various surfactant types and amounts (5, 10, 15% w/w). N represent nanoemulsion was not formed and Y represent nanoemulsion was formed.

Rice bran oil

Surfactant types	**T8S8**			**B97B93**			**T2S8**			**T2B93**			**T8B93**			**B97S80**		
% Surfactant / % Oil	**5**	**10**	**15**	**5**	**10**	**15**	**5**	**10**	**15**	**5**	**10**	**15**	**5**	**10**	**15**	**5**	**10**	**15**
10	N	N	N	N	N	N	N	N	N	N	N	N	N	N	N	N	N	N
20	N	N	N	N	N	N	N	N	N	N	N	N	N	N	N	N	N	N
30	N	N	N	N	N	N	N	N	N	N	N	N	N	N	N	N	N	N

Note: T8S8(Tween®80:Span®80), B97B93(Brij®97:Brij®93), T2S8(Tween®20:Span®80), T2B93(Tween®20:Brij®93), T8B93(Tween®80: Brij®93), B97S80(Brij®97:Span®80)

Table 6 Formation of nanoemulsions containing oleic acid at different concentrations (10, 20, 30% w/w) with various surfactant types and amounts (5, 10, 15% w/w). N represent nanoemulsion was not formed and Y represent nanoemulsion was formed.

Oleic acid

Surfactant types	**T2S2**			**T2S8**			**T2B93**			**T2B97**			**T2C40**		
% Surfactant / % Oil	**5**	**10**	**15**	**5**	**10**	**15**	**5**	**10**	**15**	**5**	**10**	**15**	**5**	**10**	**15**
10	N	N	N	N	N	N	N	N	N	N	N	N	N	N	N
20	N	N	N	N	N	N	N	N	N	N	N	N	N	**Y**	N
30	N	N	N	N	N	N	N	N	N	N	N	N	N	N	N

Note: T2S2(Tween®20:Span®20), T2B97(Tween®20:Brij®97), T2C40(Tween®20:Cremophor RH®40)

Table 7 Formation of nanoemulsions containing sweet orange oil at different concentrations (10, 20, 30% w/w) with various surfactant types and amounts (5, 10, 15% w/w). N represent nanoemulsion was not formed and Y represent nanoemulsion was formed.

Sweet orange oil

Surfactant types	**T8S8**			**T2S2**			**T2S8**			**T2B93**			**T2B97**			**T8B97**		
% Surfactant / % Oil	**5**	**10**	**15**	**5**	**10**	**15**	**5**	**10**	**15**	**5**	**10**	**15**	**5**	**10**	**15**	**5**	**10**	**15**
10	N	N	N	**Y**	N	N	**Y**	**Y**	N	N	**Y**	N	**Y**	**Y**	N	N	N	**Y**
20	N	N	N	N	**Y**	**Y**	N	N	N	N	N	N	N	**Y**	**Y**	N	N	N
30	N	N	N	N	N	**Y**	N	N	N	N	N	N	N	N	N	N	N	N

Note: T8B97(Tween®80:Brij®97)

The mechanism of nanoemulsion formation by low energy emulsification is phase inversion from w/o to o/w emulsion. At the phase inversion point, the very low interfacial tension is obtained from the arrangement of surfactants as a lamellar liquid crystalline phase or a gel phase. The gel phase is then broken and inversed to form o/w nanoemulsion by the increased amount of water. From the mechanism of formation, the viscosity of oil phase may be a considerable factor influencing nanoemulsion formation. In this study, rice bran oil has the highest viscosity (Giap et al., 2009) followed by oleic acid (Noureddini, Teoh and Clements, 1992) and sweet orange oil, respectively. The high viscosity of rice bran oil and oleic acid caused the gel phase more viscous than sweet orange oil. Therefore, this viscous gel phase is difficult to break and results in the difficulty of the phase inversion process. Besides the viscosity of oil, another possible reason is the solubility of oil in the gel phase of surfactant mixture. In this experiment, rice bran oil and oleic acid were less soluble in the gel phase. It could be observed from the turbidity of the gel phase (Figure 10). This turbidity is caused by the excess oil which is insoluble in the gel phase. When a small quantity of oil is soluble in such a middle phase, the excess oil remains at the outside and a larger oil droplet size is attained (Solan et al., 2009). This is because the source of energy for the emulsification process comes from the two sources (external and internal forces). The emulsification process of the excess oil directly depends on the external forces. Big droplets are then obtained. However, the soluble oil in the gel phase is emulsified by the internal forces from the low interfacial tension of the system, where the gel phase is formed. The obtained droplet sizes are then small. In this study, the emulsion with the droplet size more than 1000 nm was not considered as a nanoemulsion. The two mechanisms of emulsification were evident from the size profile as shown in Figure 11, where the bimodal size distribution was obtained.

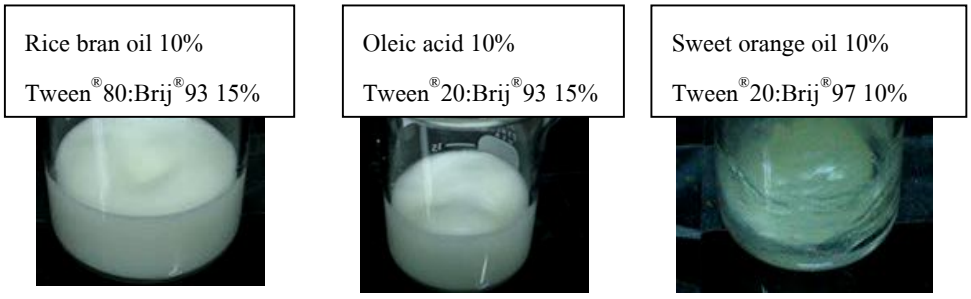

Figure 10 The turbidity of the gel phase of rice bran oil (left), oleic acid (middle), and sweet orange oil (right

The small droplets (size < 1000 nm) are obtained from the internal forces and the big droplets (>1000 nm) are obtained from the external forces. From the clear gel phase of sweet orange oil, it was indicated that sweet orange oil is completely soluble in the gel phase. Therefore, the mechanism of emulsification is directly dependent on the internal forces. The resulting small droplets (size < 1000 nm) were obtained without any droplet size more than 1000 nm (Figure 11 below). The solubility of oil in a gel phase can be considered with the molar volume of oil. The solubility of oil in gel phase decreases with the high molar volume of oil (Uddin, Kunieda and Solans, 2003). In this study, rice bran oil (triglyceride oil) has a higher molar volume than oleic acid and sweet orange oil, respectively. This may be responsible for the difficulty of formation of nanoemulsion for rice bran oil.

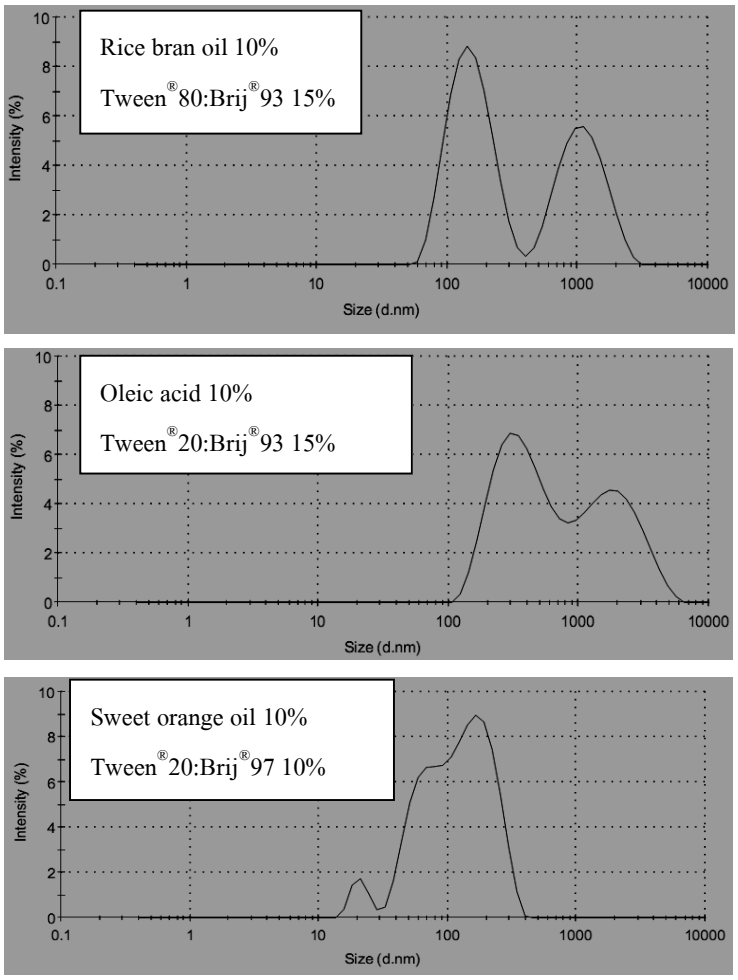

Figure 11 The size profile of rice bran oil(top), oleic acid and(middle) sweet orange oil(below)

It can be concluded from this study that triglyceride (rice bran oil) and fatty acid (oleic acid) formed a nanoemulsion which is harder than essential oil (sweet orange oil).

3.2.2. Effect of surfactant types

The effect of surfactant types was investigated. The results were shown in Table 5, 6 and 7. The type of surfactant took an effect on nanoemulsion formation only with sweet orange oil, while regarding rice bran oil and oleic acid, the type of surfactant could not affect nanoemulsion formation. For rice bran oil, both the same and different surfactant structures could not form nanoemulsion (Table 5). For sweet orange oil, the different surfactant structures formed nanoemulsion easier than the same surfactant structure, as in the case of Tween®20:Span®80, Tween®20:Brij®93, Tween®20:Brij®97 and Tween®80:Brij®97 (Table 7). At the phase inversion point, the arrangement of surfactant film was an important factor influencing nanoemulsion formation. The surfactant film can be flexible or rigid, depending on the structures of surfactant mixture at the interfaces. If two surfactants in surfactant mixture have similar structure, the film is rigid. If two surfactants have different structures, the film is flexible (Dios, Barrao and Tojo, 2011). In addition, the arrangement of the flexible surfactant film enhances the surfactant film to be inversed easily (Butt, Graf, and Kappl, 2003). In contrast, the arrangement of rigid surfactant film decreases the ability of the inversion. From the experimental results in this study, the different structures of surfactant mixtures have an ability of arrangement in loosening character. Therefore, this flexible film can be induced easily to inverse at the phase inversion point and nanoemulsion can be attained. This study was similar to the study of Dai et al. (1997). They studied the effect of the different numbers of carbon chain lengths between the pair of surfactant mixtures on nanoemulsion formation. The result was that the high difference of carbon numbers (Tween®80, C18:Span®20, C12) made the nanoemulsion form easily compared to the low difference of carbon numbers (Tween®80, C18:Span®40, C16). However, the same structure of surfactant mixture could also form nanoemulsion, as in the case of Tween®20:Span®20 (Table 7). Although Tween®20:Span®20 has the same structure from the same surfactant group and the same number of carbon chains, there is a difference among the other types with the same structure of surfactant mixtures (Tween®80:Span®80). Tween®20 and Span®20 have a fewer number of carbon atoms at carbon chain lengths (12 carbon atoms) while Tween®80 and Span®80 have more carbon atoms (18 carbon atoms). Therefore, the short carbon chain length of surfactants has

enough flexibility of surfactant films compared to the high carbon chain length. The surfactant film is then easily inversed and nanoemulsion is attained. For oleic acid, nanoemulsion could be formed with particular different structures of surfactant mixture. In this case, only Tween®20:Cremophor RH®40 could form nanoemulsion. The possible explanation was that this couple of surfactants has the most different surfactant structures compared to the other couple of surfactants for oleic acid (Table 4). This is because the hydrocarbon tails of Cremophor RH®40 is the castor oil which is highly different among Span®80, Brij®93 and Brij®97, which is the straight hydrocarbon chain in surfactant tails. From the most different of surfactant structures, it makes the most flexible film at the interface and enhances the inversion of this film. Hence, surfactant curvature is easily changed to a positive direction and then makes small droplets (Solan, 2009). Consequently, nanoemulsion is easily obtained.

3.2.3 Effect of amounts of oils and surfactants

Besides the type of oil and surfactant which can influence nanoemulsion formation, the amounts of surfactants and oils are also considerable factors. Therefore, the effect of surfactant and oil amounts to nanoemulsion formation was studied. The effect of oil and surfactant concentration was interpreted as the oil to surfactant (o/s) ratio. The formation of nanoemulsion could be attained at the optimum o/s ratio. However, the optimum ratio depended on the type of oils and surfactants. In the case of rice bran oil, there was no the optimum ratio with all surfactant types (Table 8). For oleic acid, nanoemulsion could be obtained only at o/s ratio equal to 2:1 with Tween®20:Cremophor RH®40 as the surfactant mixtures (Table 9). Nevertheless, nanoemulsion could be attained at the wider range of the optimum o/s ratio for sweet orange oil (Table 10) but this optimum ratio must not be more than 2:1. This result was in agreement with Wang et al. (2007).

Table 8 Nanoemulsion formations of rice bran oil with different surfactant types and o/s ratios

o/s ratio / Surfactant types	2:3	1:1	4:3	2:1	3:1	4:1	6:1
T8S8	N	N	N	N	N	N	N
B97B93	N	N	N	N	N	N	N
T2S8	N	N	N	N	N	N	N
T2B93	N	N	N	N	N	N	N
T8B93	N	N	N	N	N	N	N
B97S80	N	N	N	N	N	N	N

Table 9 Nanoemulsion formations of oleic acid with different surfactant types and o/s ratios

o/s ratio / Surfactant types	2:3	1:1	4:3	2:1	3:1	4:1	6:1
T2S2	N	N	N	N	N	N	N
T2S8	N	N	N	N	N	N	N
T2B93	N	N	N	N	N	N	N
T2B97	N	N	N	N	N	N	N
T2C40	N	N	N	**Y**	N	N	N

Table 10 Nanoemulsion formations of sweet orange oil with different surfactant types and o/s ratios

o/s ratio / Surfactant types	2:3	1:1	4:3	2:1	3:1	4:1	6:1
T8S8	N	N	N	N	N	N	N
T2S2	N	N	**Y**	**Y**	N	N	N
T2B93	N	**Y**	N	N	N	N	N
T2B97	N	**Y**	**Y**	**Y**	N	N	N
T2S8	N	**Y**	N	**Y**	N	N	N
T8B97	**Y**	N	N	N	N	N	N

From the results, it suggests that the o/s ratio should not be more than 2:1 to reduce the interfacial tension which is resulted from the high amount of oil. Consequently, the small droplets can be attained. In addition, the o/s ratio should not be less than 1:1 to prevent the separation of a lamellar liquid crystalline phase which may increase droplet size distribution. Therefore, nanoemulsion can be obtained (Morales et al., 2003).

After investigation of the effects of types and amounts of oils and surfactants, thirteen nanoemulsions were obtained (Table 12). All formulations had high conductivity and could disperse in water but could not disperse in oil. Therefore, all nanoemulsions were oil in water type. To optimize these nanoemulsions, the physical stability was used for screening the formulations for the study in Section 4. Formulation codes were defined as follows.

1	2	3	4

Where, 1 is oil type, 2 is concentration of oil, 3 is surfactant type, and 4 is concentration of surfactant. Abbreviations were listed below in Table 11.

Table 11 List of abbreviations

Name	**Code**
Rice bran oil	R
Oleic acid	O
Sweet orange oil	S
5 % w/w concentrations	5
10 % w/w concentrations	10
15 % w/w concentrations	15
20 % w/w concentrations	20
30 % w/w concentrations	30
Tween®20	T2
Tween®80	T8
Span®80	S8
Brij®93	B93

Table 11 (continue) List of abbreviations

Name	Code
Cremophor RH® 40	C40

For example, O20T2C4010 is oleic acid 20% w/w with Tween®20: Cremophor RH®40 10% w/w.

Table 12 All thirteen nanoemulsion formulations and conductivity values

Oil groups	Formulations	Conductivity (µs/cm)
Oleic acid	O20T2C4010	39.5-41.4
Sweet orange oil	S10T2S205	65.0-66.1
	S20T2S210	118.0-122.0
	S20T2S215	149.0-150.0
	S30T2S215	122.0-123.0
	S10T2S805	87.3-97.6
	S10T2S810	166.0-170.0
	S10T2B9310	102.0-104.0
	S10T2B9705	83.1-89.5
	S10T2B9710	157.0-159.0
	S20T2B9710	140-143
	S20T2B9715	182.0-185.0
	S10T8B9715	129.0-131.0

3.3 Physical stability of nanoemulsions in accelerated conditions

The physical stability of all nanoemulsions from Table 12 was investigated. The accelerated stresses of physical stability tests were centrifugation, heating cooling, and freeze thaw cycle respectively as described in Chapter 3. For centrifugation, 9 formulations showed creaming and 4 formulations were stable. For creaming, it may be due to wide size distribution.

As can be seen in Figure 12, the wider size distribution occurred after centrifugation. This caused emulsion creaming from Stokes' law (Hill, 1998). With stable formulations, there was no phase separation and average particle sizes were not changed after centrifugation ($p>0.05$) for S10T2S810, S10T2B9710 and S20T2S215 (Figure 13). Although statistics of the average particle size of O20T2C4010 was changed significantly ($p<0.05$), the particle sizes was in the range of nanometers (Figure 13). For O20T2C4010, the stability may be due to the optimum o/s ratio (Table 9). O20T2C4010, S10T2S810, S10T2B9710 and S20T2S215 were then subjected to the heating cooling cycle. All four stable formulations were kept at 45 ^{o}C for 48 hours and 4 ^{o}C for 48 hours respectively. This was repeated for 6 cycles. Only O20T2C4010 remained stable. Formulations of S20T2S215 and S10T2S810 were cracking (Table 13). It is possible that o/s ratios of these formulations far from the optimum ratio and hence increase the instability. In case of S10T2B9710, there was gel formation at the first two cycles (Figure 14). However, the gel was formed only at a temperature of 45 ^{o}C.

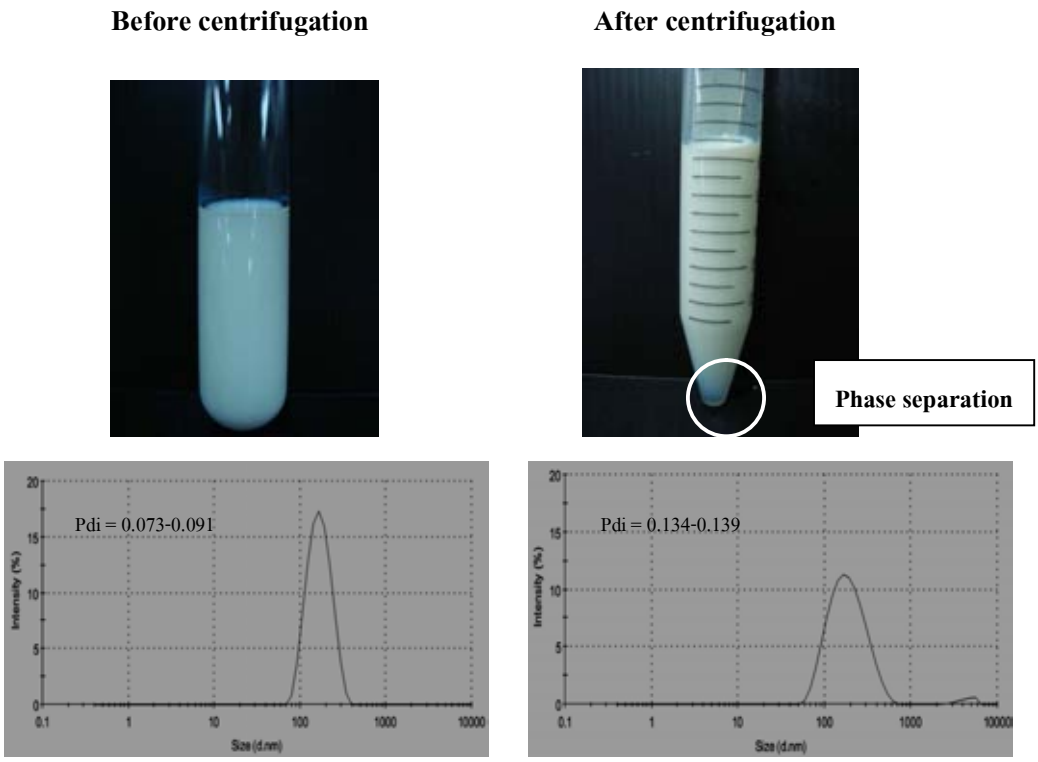

Figure 12 Nanoemulsion formulations of S10T2S205 before and after centrifugation

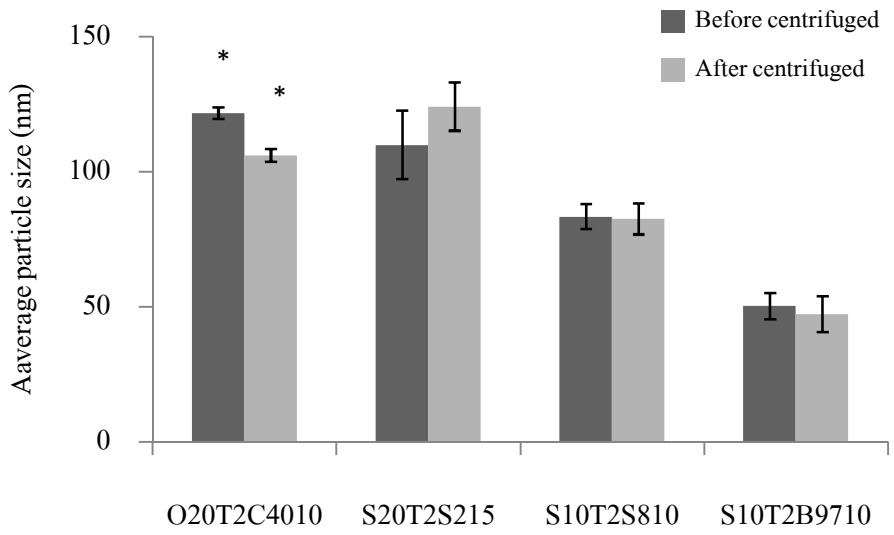

Note: * statistical significant ($p<0.05$)

Figure 13 Particle sizes of formulations before and after centrifugation

Table 13 Particle sizes (average±SD) and physical stability of nanoemulsions after passing through 6 heating-cooling cycles

Cycle numbers	Formulations			
	O20T2C4010	**S20T2S215**	**S10T2S810**	**S10T2B9710**
0	123.17±18.51	154.1±0.87	89.36±7.22	68.55±6.14
1	101.58±11.90	cracking	216.5±3.73	58.42±3.11†
2	86.32±1.65	cracking	301.83±29.65	40.54±1.56†
3	103.5±10.20	cracking	cracking	31.18±4.70
4	105.7±1.10	cracking	cracking	24.75±1.33
5	104.17±0.32	cracking	cracking	37.89±2.42
6	98.93±3.52	cracking	cracking	48.91±1.17

Note: † gel formation

After S10T2B9710 was left at room temperature (25 ^{o}C) the gel phase disappeared. This may be due to the properties of Brij$^{®}$97 which change when the temperature changes (Amar, Aserin and Garti, 2010). When the temperature is increased, the POE groups of Brij$^{®}$97 are

dehydrated. This dehydration makes the POE groups have a small volume and results in the rearrangement of surfactant curvatures to the mesophase or the gel phase. At outside the oven, when the temperature of formulation was decreased to room temperature, the POE groups were rehydrated and the volume of POE groups was bigger. This makes the curvatures of surfactant rearrange again to the same position as before being heating. Therefore, the gel phase disappeared. However, the fluctuation of these surfactant curvatures will result in the change of nanoemulsion property. As can be seen in Figure 14, S10T2B9710 was turbid after passing through 6 cycles compared to the initial condition at cycle 0. This turbidity is resulted from the increase of size distribution, which can be observed from the size profiles. The particle size tends to increase from cycle 0 to cycle 6. This result might be attributed to the fluctuation of temperature. Thus, O20T2C4010 was then subjected to the freeze thaw cycles.

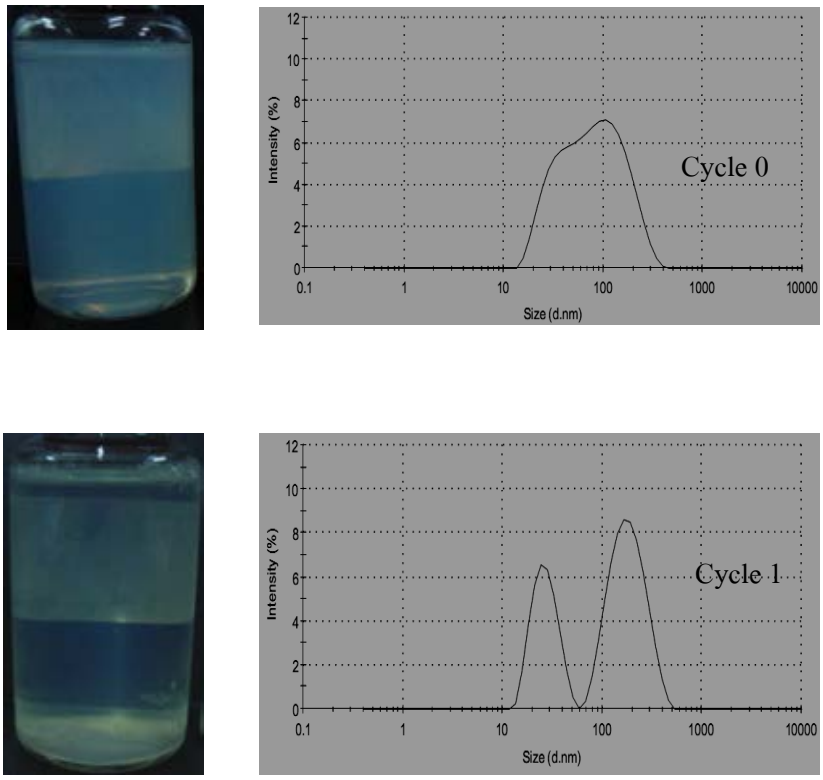

Figure 14 The physical appearance and particle size distribution of S10T2B9710 at different cycle

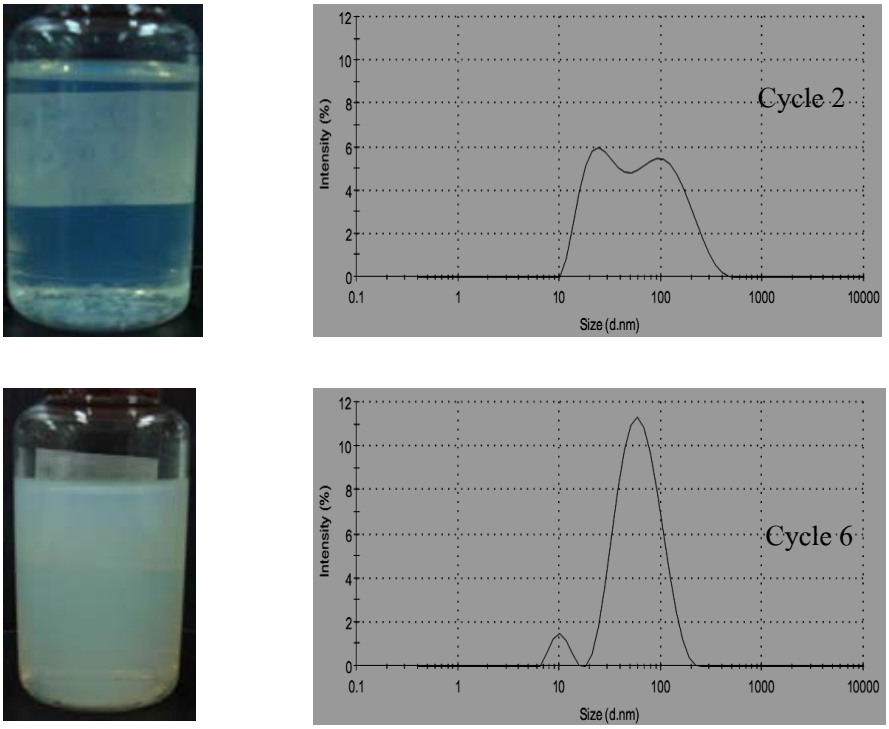

Figure 14 (continue) The physical appearance and particle size distribution of S10T2B9710 at different cycles

After O20T2C4010 was kept in the freeze thaw cycles as described in Chapter 3, this formulation was stable. There was no phase change, and particle size slightly changed after 3 cycles ($p<0.05$) but still in the range of nanoemulsion (Figure 15). There are two possible reasons for the highest stability of this formulation. The first reason may be due to the fact that the high viscosity of this formulation prevents the collision of the droplets, and hence increases the stability. The second reason may be due to the high sterric property of long chain head groups (Kim, Shin, and Oh, 2005) with 20 POE groups of Tween®20 and 40 POE groups of Cremophor RH®40. Normally, the POE side chain of non-ionic surfactant is absorbed at the interfaces between the droplets, and the carbon tail is located at the oil side. A long chain of POE groups can make the sterric effect and hence prevents the droplets coming close together. Therefore, this can prevent droplet collisions and hence increase its stability (Swarbrick, Rubino, and Rubino, 2006).

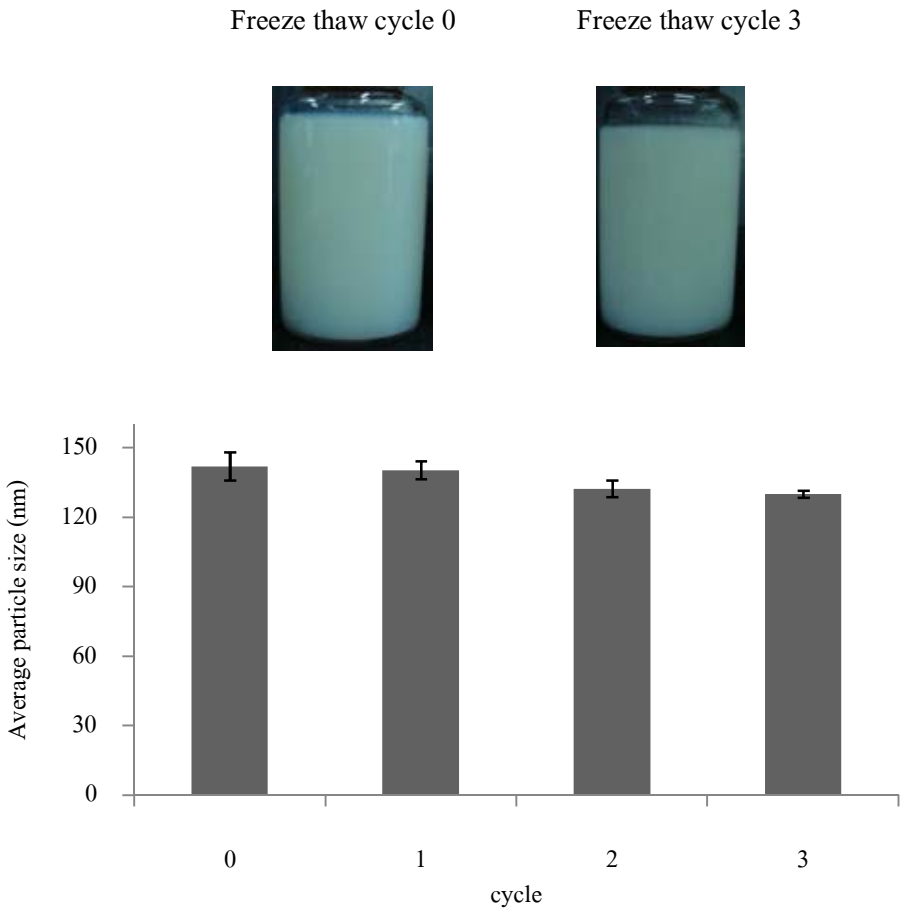

Figure 15 Appearance and particle size of O20T2C4010 after freeze thaw 3 cycles

From all physical stability studied, there was only one stable formulation of O20T2C4010. The main cause of instability is the collision between the droplets. When the two droplets come close together, each individual drop is attached to form the loose assemblies of particles, or the so called floccules. These floccules tend to make an emulsion creaming. If these floccules are joined to form a bigger one, it makes coalescence and increases in size distribution. If this coalescence continues, the emulsion is cracking. Therefore, the increase of viscosity can reduce the chance of droplet collision and make emulsion more stable (Hasenhuette, 2008). 0.5% w/w xanthan gum was then selected to increase viscosity of the unstable nanoemulsions. The selected formulations were S10T2B9310, S10T2S810, and S10T2S210. For S10T2B9310, this formulation was selected from the centrifugation test in Section 3.3. This selection is based on

the tendency of good stability if the viscosity is increased. The more homogeneity of size distribution (single peak, Figure 16) and the less oil concentration in formulation (10% w/w), the more stable of nanoemulsion can be achieved. The homogeneity of size distribution reduces the rate of creaming from Stokes'law. The low concentration of oil can facilitate the surfactants to accumulate around droplets and thus increase the thickness of surfactant film at the interfaces. As a result, this film thickness can prevent the collision of the two droplets and increase stability.

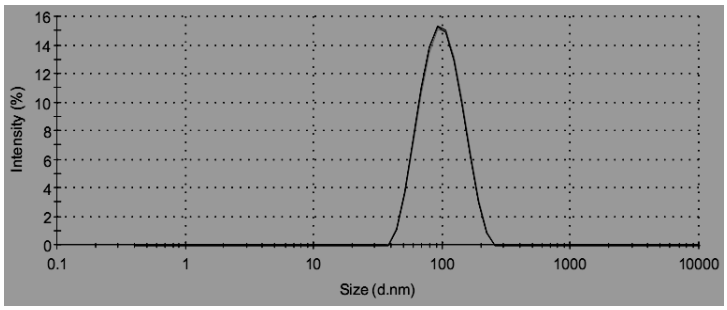

Figure 16 The particle size distribution of S10T2B9310

S10T2S810 was chosen based on the heating cooling cycle since it took 3 cycles for the instability from a total of 6 cycles. The longer the cycle is, the more stable the formulation is. Therefore, this formulation tends to be stable if the viscosity of formulation is increased. For S10T2S210, it was selected from Table 7 since this formulation tends to form nanoemulsion if droplet coalescence can be prohibited. From Figure 17, there was a small number of droplets larger than 1000 nm, and it indicated a small number of droplet coalescence. Therefore, the increasing viscosity of such formulation may reduce the chances of droplet collision and coalescence.

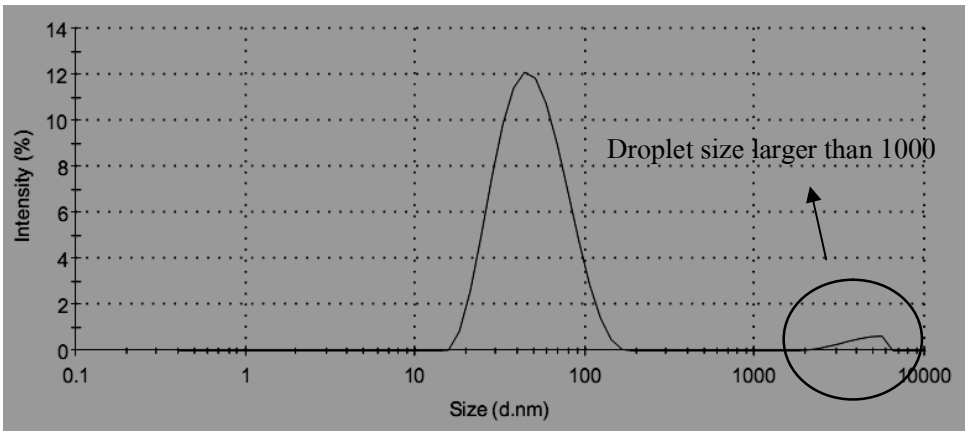

Figure 17 The particle size distribution of S10T2S210

Xanthan gum gel 1% w/w was prepared by dispersing xanthan gum in water and stirring with a 4-bladed propeller. The stirring continued until xanthan gum was mixed completely. This dispersion was left overnight before being used. After three formulations were selected, the formulations were prepared as described in chapter 3, and 1% w/w xanthan gum was added immediately to make a concentration of 0.5% w/w xanthan gum in formulation. To evaluate the stability of selected formulations, physical stability was investigated the same as in Section 3.3.

To show xanthan gum component in formulation code, X is added at the last position of the formulation codes After S10T2B9310X, S10T2S810X, and S10T2S210X were centrifuged; all formulations were stable (Figure 18). From this result, it is indicated that xanthan gum can enhance their stability. For S10T2S210X, xanthan gum could prevent droplet coalescence (Troy, 2006) as can be seen in Figure 19. There is no big droplet size more than 1000 nm after xanthan gum was added.

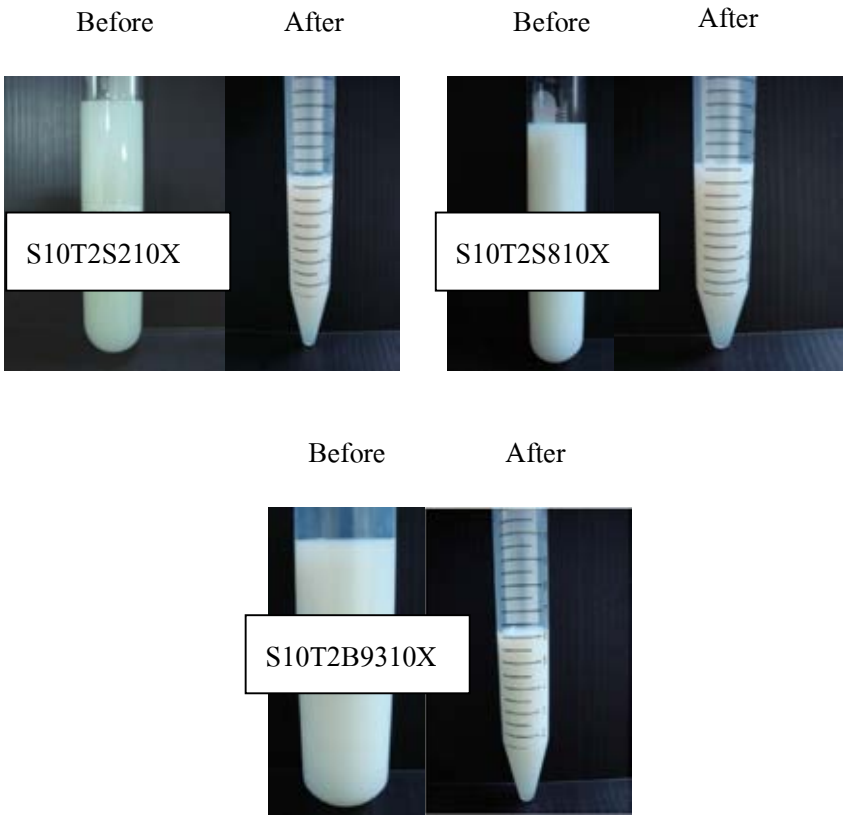

Figure 18 Appearance of S10T2S210X, S10T2S810X and S10T2B9310X before and after centrifugation

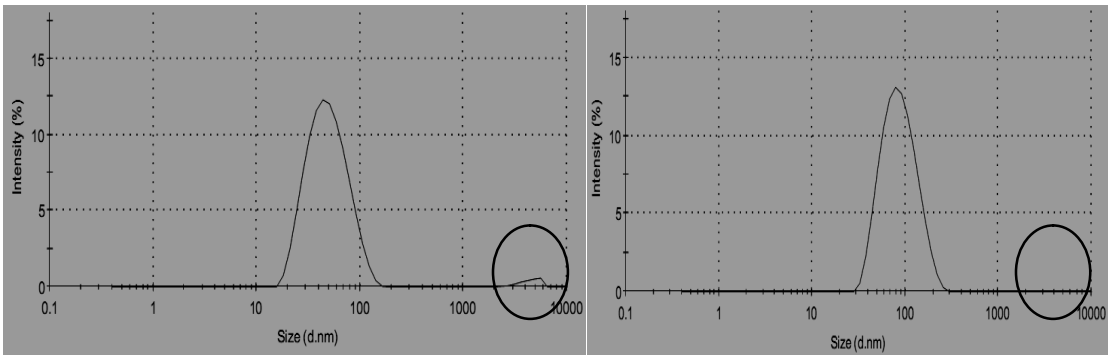

Before After

Figure 19 Size distributions of S10T2S210X before and after adding 0.5% w/w xanthan gum

After centrifugation test, all three formulations were subjected to the heating cooling cycle. The data is shown in Table 14. S10T2S210X and S10T2S810X showed creaming after 6 cycles. However, S10T2S810X showed creaming instead of cracking as shown in Table 13.

Table 14 Particle sizes and physical stability of nanoemulsions with 0.5% w/w xanthan gum after passing through 6 heating-cooling cycles.

Cycle numbers	**Formulations**		
	S10T2B9310X	**S10T2S810X**	**S10T2S210X**
0	80.85±3.92	90.27±39.55	82.8±2.30
1	118.27±3.37	90.27±39.55	84.43±6.56
2	144.47±3.39	179.23±12.92	creaming
3	162.9±3.27	201.63±11.77	creaming
4	180.43±2.05	215.63±6.39	creaming
5	196.97±2.84	creaming	creaming
6	201.9±0.66	creaming	creaming

Therefore, 0.5% w/w xanthan gum can be a stabilizer for nanoemulsion. For S10T2B9310X, there was no phase separation, and particle size was increased after 6 cycles ($p<0.05$). However, average particle size was in the range of nanoemulsion. Therefore, S10T2B9310X was subjected to the freeze thaw cycle. After S10T2B9310X was kept in the freeze thaw cycle, there was no phase separation but particle size more than 1000 nm occurred (Figure 20). Therefore, freeze thaw cycle may be a high stress condition compared to the centrifugation and heating cooling cycles. The droplets were forced to collide immediately after the water phase was freezed (Golding and Pelan, 2008). In contrast with the heating cooling cycles, the collision of droplets is less due to the random motions of Brownian motion effects.

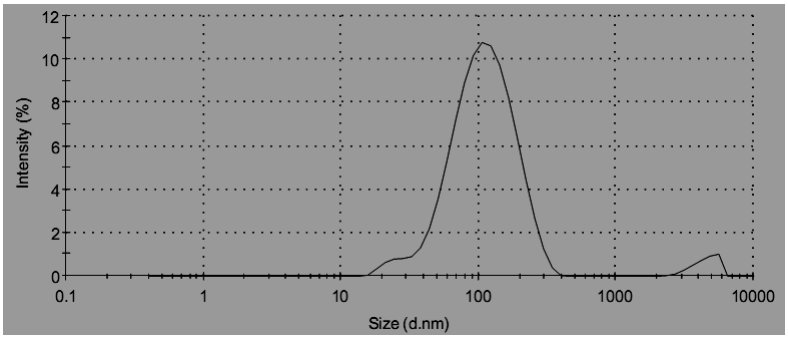

Figure 20 Size distribution of S10T2B9310X at 3 freeze thaw cycles

From such high stress conditions of the freeze thaw cycle, the stable formulations which passed through heating cooling cycles were then selected for Section 4. For O20T2C4010, it was the most stable nanoemulsion. For S10T2B9710, it tends to be stable if there is no fluctuation of temperatures at heating cooling cycle. For S10T2B9310X, it was stable at the heating cooling cycle. Therefore, three formulations (O20T2C4010, S10T2B9710, and S10T2B9310X) were chosen in order to study the effect of ellagic acid loading.

4. Investigation of ellagic acid loaded nanoemulsion

4.1 Effect of ellagic acid loading on nanoemulsion formation

The effect of ellagic acid loading on nanoemulsion formation was studied. To show ellagic acid in formulation code, EA is added at the last position of the code of formulations. The O20T2C4010EA, S10T2B9710EA and S10T2B9310XEA were prepared as described in Chapter 3. The amount of dried extract was added into the oil phase according to ellagic acid solubility in that oil. However, this adding made emulsion more turbid. Therefore, the saturated solubility of dried extract in oil and surfactant mixture was investigated. The solubilities of dried extract in the oil and surfactant mixtures of O20T2C40EA, S10T2B9310XEA and S10T2B9710EA were 21.10, 41.07 and 17.16 µg/mL, respectively. The dried extract was then added in each formulation, and the formulations were then prepared as described in Chapter 3. Ellagic acid content in each formulation was in the range of 8.94-9.20 µg/g by calculation. However, it reduced approximately 56.09-61.86% after filtering process. Therefore, the amount of ellagic acid in each formulation was in the range of 3.41-4.04 µg/g as described in Table 15.

Percentage of label amount for each formulation is also shown in Table 15. All formulations had no phase separation and precipitation of dried extract.

Table 15 Content of ellagic acid in formulations (average±SD) and %label amount

Formulation codes	**Ellagic acid in formulation (µg/g)**	**% Label amount**
O20T2C4010EA	3.41±0.12	97.26-103.70
S10T2B9310XEA	4.04±0.12	107.92-115.32
S10T2B9710EA	3.59±0.14	108.86-117.73

Table 16 Particle sizes (nm±SD) of blank, ellagic acid loaded formulations at room temperature before and after centrifugation.

	Particle size		
		Ellagic acid loaded formulations	
Formulations	**Blank**	**Before centrifugation**	**After centrifugation**
O20T2C4010	121.74±2.15	123.54±14.98	164.16±56.58
S10T2B9310X	87.95±14.7	86.63±5.90	86.95±8.26
S10T2B9710	43.32±4.27	64.54±18.26	62.81±19.25

All ellagic acid loaded nanoemulsions had the same appearance and average particle sizes compared to blank formulations ($p>0.05$) (Table 16). It is indicated that dried extract does not affect nanoemulsion formation. This is because dried extract can be incorporated into the core of oil (Gaonkar and Bagwe, 2005). At phase inversion point, surfactant curvatures can change in the same manner as in formulation before dried extract was added. Therefore, surfactant curvature does not interfere with such location of ellagic acid.

4.2 Effect of ellagic acid loading on physical stability

The preparations of the selected nanoemulsions from Section 4.1 and their blank formulations were further examined for physical stability under ICH guideline. Nanoemulsions were subjected to screen and confirm their suitability by using centrifugation test. Physical stability was evaluated as phase separation, particle size determination and drug precipitation. After centrifugation, there was no precipitation and particle size did not change (Table 16). All formulations were then stored at 45 ^{o}C for 3 months and the physical stability was examined at each time interval. In this study, all formulations were cracking after storage for 1 month. To select the formulation for the further studies, all formulations were kept at 45 ^{o}C and examined the change of average droplet size at day 0, 5, 7, 9, 12 and 17, respectively. The less change of particle size is, the more stable formulation is. As can be seen from Figure 21B, the particle sizes of O20T2C4010EA and S10T2B9310XEA increased over time. It was also found that the formulation of O20T2C4010EA was cracking while S10T2B9310EA was creaming after storage for 7 days (Figure 22). For S10T2B9710EA, there was a gel formation at the seventh day. In consideration of all blank formulations, the average particle size was increased the same as the EA loaded in formulations (Figure 21A). Therefore, the instability of formulations was not caused by adding the dried extract into formulation. It is noticeable that O20T2C4010 passed through the centrifugation, heating cooling, and freeze thaw cycle as described in Section 3.1 However, it could not remain stable in this study where the average particle size was dramatically increased when the formulation was kept at 45 ^{o}C and cracking at the seventh day of storage.

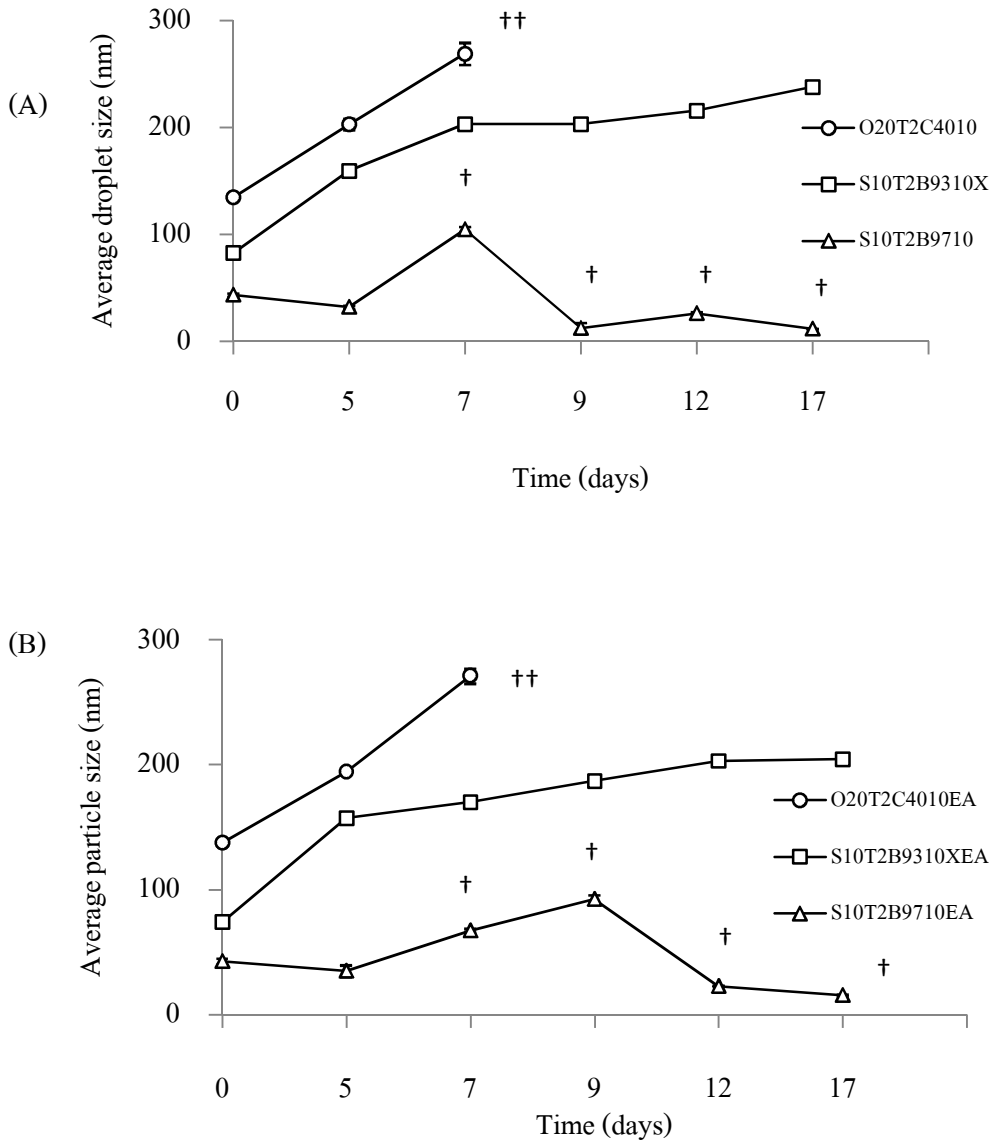

Note: †† cracking, †gel

Figure 21 Average droplet size of blank (A) and ellagic acid-loaded in formulation (B) as a function of time (day), n=3.

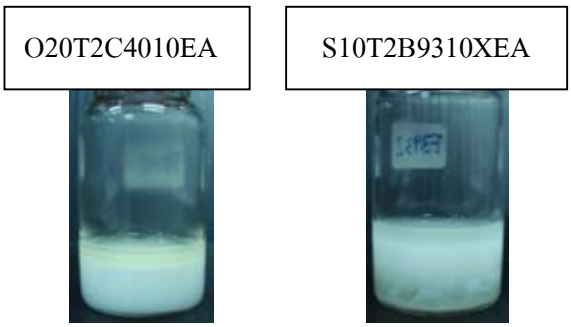

Figure 22 The physical appearance of O20T2C4010EA (cracking) and S10T2B9310XEA (creaming) after storage for 7 days

Comparing of S10T2B9310X and S10T2B9710, O20T2C4010 had the most instability. This may be due to the high viscosity of O20T2C4010 could prevent droplet coalescence at heating cooling cycle and freeze thaw conditions. This high viscosity may be obtained from the cubic phase of middle phase surfactant (Rodríguez, Shigeta, and Kunieda, 2000). When O20T2C4010 was kept at 45 ^{o}C for several days, this middle phase melted (Solans et al., 2004) and hence the viscosity was decreased. This made a possible of droplet collision which results in the break of surfactant film. The emulsion was then cracking. For S10T2B9710, the average particle size increased sharply at the seventh day when compared to S10T2B9710EA. Considering the appearance of formulation, blank of S10T2B9710 had turbid gel phase more than its loaded formulation of S10T2B9710EA (Figure 23). The more turbid gel phase formation, the high average particle size obtained. From three formulations, S10T2B9710EA was chosen for further studies. This because the particle size of such formulation was slightly changed over time, the high amount of ellagic acid could be added and the gel phase could be disappeared at room temperature.

S10T2B9710EA Blank S10T2B9710

Figure 23 Gel formation of S10T2B9710EA and S10T2B9710 after storage for 7 days

5. In vitro release study

To study release behavior of ellagic acid containing in nanoemulsion, in vitro release study was carried out. The amount of ellagic acid released into a receiver medium was analyzed by the reverse-phase HPLC. The HPLC method used in this study was validated. The specificity, accuracy, precision, and linearity meet all requirements (see Appendix B). The release of ellagic acid from solution was also studied for comparison. The profiles of ellagic acid released from S10T2B9710EA and solution are illustrated in Figure 24. S10T2B9710EA gave slow ellagic acid release compared to solution. The formulation gradually released ellagic acid over 24 hours. The release of ellagic acid was about 68-86% over 24 hours. The slow release of hydrophobic compounds from nanoemulsion system was also found in other studies (Sakulku et al., 2009; Ruktanonchai et al., 2009; Ammar, Salama, and Mahmoud, 2008; Bali, Ali, and Ali, 2010). This may be due to ellagic acid is being located in the oil core of nanoemulsion droplets. This makes the slow diffusion of ellagic acid into the medium.

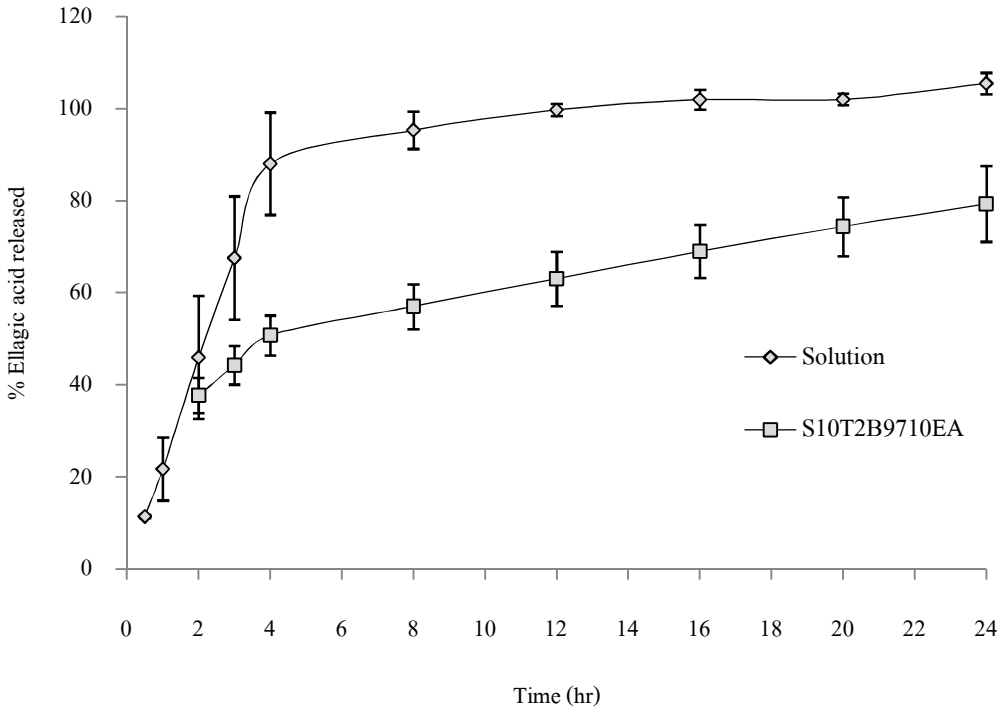

Figure 24 The release profiles of ellagic acid from nanoemulsion and saturated solution (mean±SD, n=4)

6. In vitro permeation study

To study the efficiency of nanoemulsion to deliver ellagic acid through skin, in vitro skin permeation study was carried out. Table 17 shows ellagic acid content in donor, skin, and receiver compartment, respectively. Almost ellagic acid was contained in the donor part (91.42-93.66 %). Ellagic acid content in the skin and receiver part could not be detected due to limitation of HPLC assay or there is some certain substances from skin interfered this analysis.

Table 17 Ellagic acid contents at donor, skin, and receiver component of Franz-diffusion cell at 24 hours. N/D = not detected.

Formulations	**% Ellagic acid**		
	Donor	Skin	Receiver
Solution	90.77±3.29	N/D	N/D
S10T2B9710EA	92.54±1.12	N/D	N/D

To clarify the performance of HPLC, ellagic acid standard solution at LOQ (0.2 µg/mL) was spiked into phosphate buffer pH 7.4 as the receiver medium used in this study. The result form Figure 25 showed that HPLC has an ability to detect ellagic acid at LOQ concentration at retention time equal to 17.131 minutes. Therefore, HPLC has sufficient ability to detect ellagic acid at LOQ.

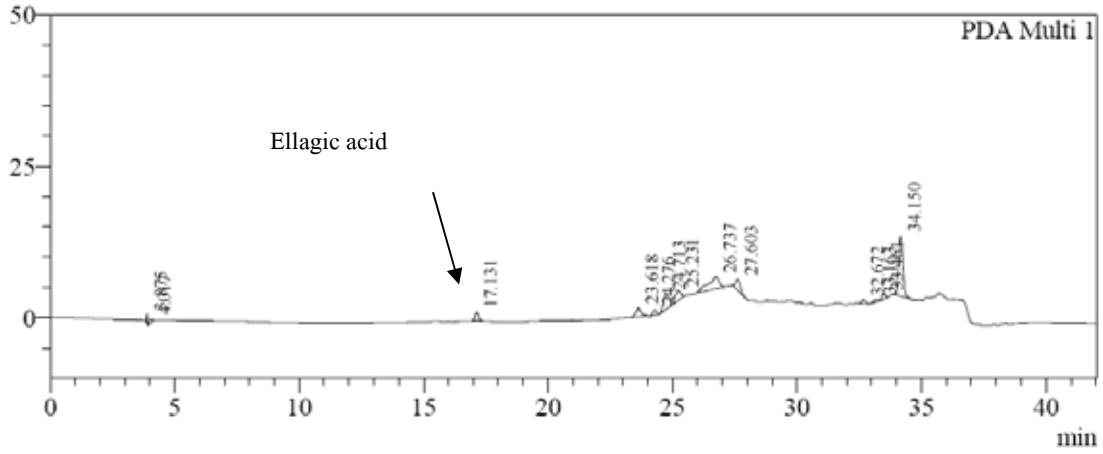

Figure 25 Chromatogram of standard of ellagic acid in phosphate buffer solution, pH 7.4 at LOQ (0.2 µg/mL), peak of ellagic acid is at 17.131 minutes.

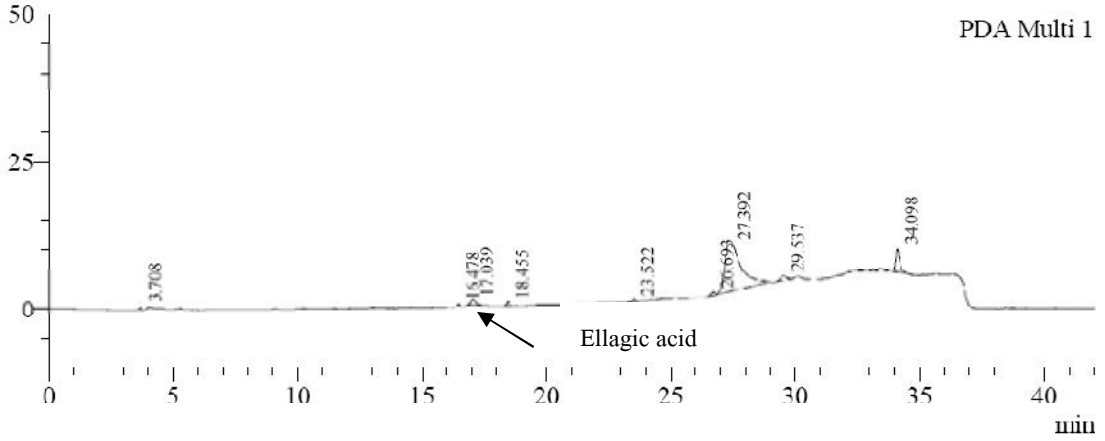

Figure 26 Chromatogram of standard of ellagic acid solution at LOQ (0.2 µg/mL) spiked in blank receiver medium

To clarify the interference of some substances from skin, ellagic acid standard solution at LOQ concentration was spiked into blank receiver medium after the experiment was run over 24 hours. The data showed that there was a peak at 17.039 minutes (Figure 26). To clarify the peak identity, UV spectrum of this peak was analyzed by a PDA detector. The data showed that there was not ellagic acid peak (Figure 27) when compared to the spectrum of standard ellagic acid in phosphate buffer, pH 7.4 (Figure 28). It was indicated that some substances from skin released in receiver medium and it may interacted with ellagic acid.

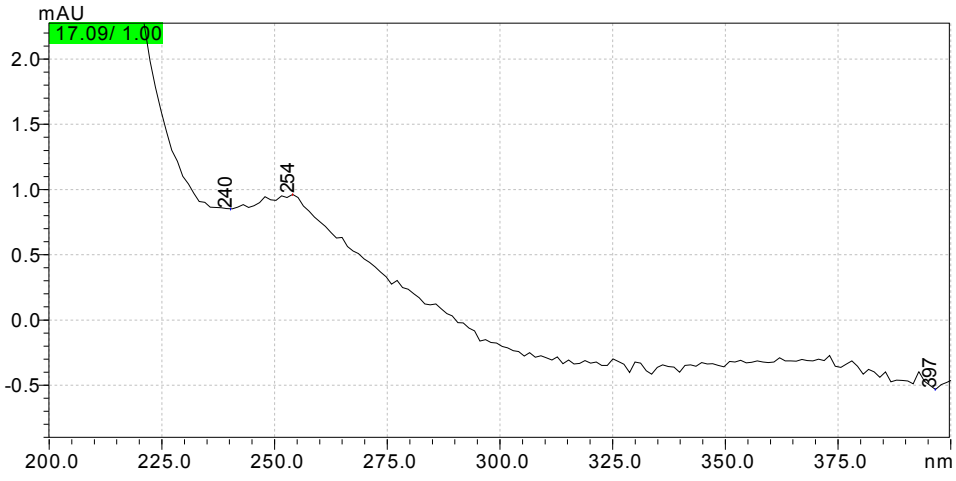

Figure 27 UV-spectrum of the peak at 17.039 minutes of spiked standard solution into blank receiver medium

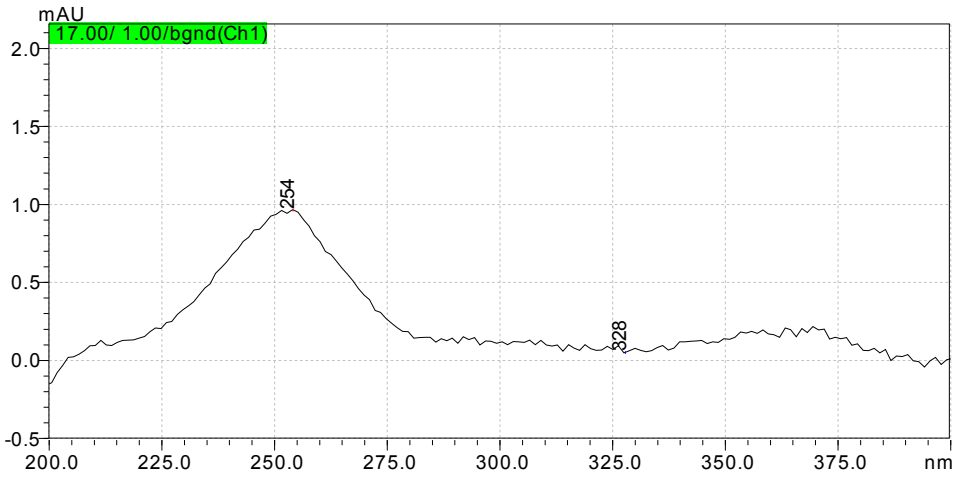

Figure 28 UV-spectrum of the peak at 17.131 minutes of spiked standard solution into phosphate buffer solution pH 7.4

To elucidate this assumption, the high concentration of standard ellagic acid solution (4 µg/mL) was spiked into blank receiver medium and phosphate buffer pH 7.4 solution. These solutions were then injected into chromatography column and then the chromatographics were then interpreted. The data showed that the peak area of ellagic acid in the blank receiver medium (Figure 29) was reduced when compared to the peak area of standard solution in phosphate buffer pH 7.4, at the same concentration of standard ellagic acid (Figure 30). It clarified that there were some substances from skin combined with ellagic acid. Therefore, ellagic acid in receiver medium could not be detected at low concentration.

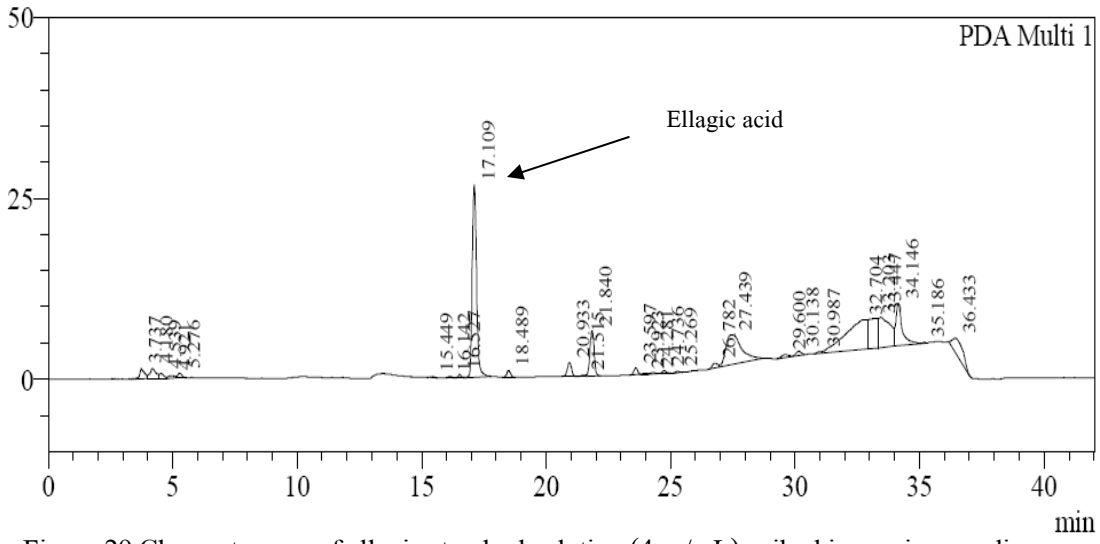

Figure 29 Chromatogram of ellagic standard solution (4µg/mL) spiked in receiver medium

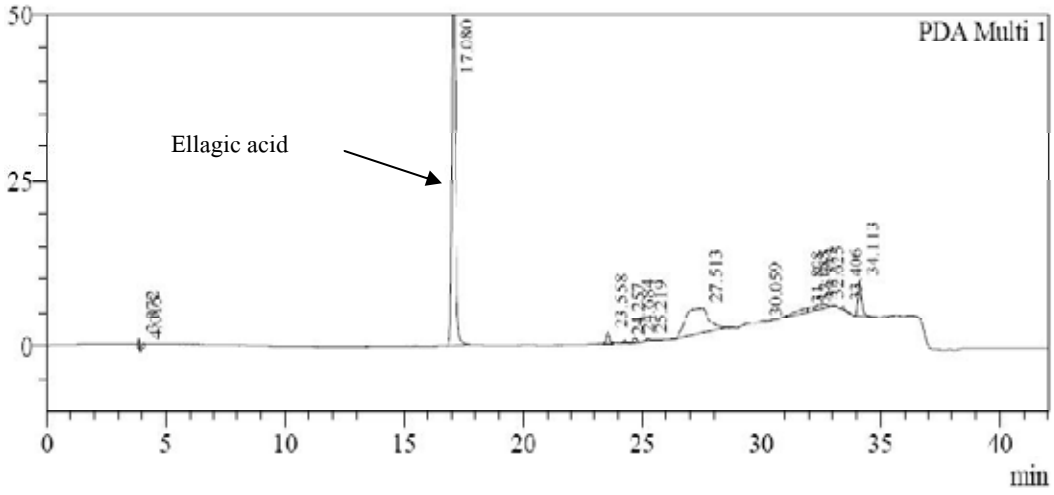

Figure 30 Chromatogram of standard ellagic acid solution (4µg/mL) in phosphate buffer pH 7.4, peak of ellagic acid is at 17.080

CHAPTER V

CONCLUIONS

Pomegranate rind is one of the rich source of polyphenolic compound especially ellagic acid which is a potent antioxidant. This study focused on the development of ellagic acid loaded in nanoemulsion, which was produced by low energy emulsification technique for skin delivery. The suitable extraction method for producing ellagic acid extract with high percentage yield and high percentage purity was investigated. Effect of the types of oils and surfactants on the saturated solubility of dried extract was also studied. Factors affecting nanoemulsion formation, including oil types, surfactant types, and oil and surfactant amounts were investigated. The physical stability of nanoemulsion was evaluated to screen the formulations. Effect of dried extract on nanoemulsion formation was studied. Release profile of ellagic acid extract loaded in nanoemulsion and skin permeation of ellagic acid extract were also studied. Conclusions can be drawn from these studies as follows:

1. The extraction methods (method A and B) could produce ellagic acid, which were indicated by the equal R_f values and the same spectra between the dried extracts and standard solution of ellagic acid. In addition, the extraction with recrystallization technique (method A) was the suitable method for producing high percentage purity of ellagic acid. The percentage purities of ellagic acid were 77.70±5.37 and 67.04±1.74 for UV and HPLC analysis, respectively.

2. Ellagic acid could be dissolved in oils and surfactants that have functional groups to form hydrogen bond. The oils were rice bran oil, sweet orange oil and oleic acid. The surfactants were Tween®80, Tween®20, Brij®97, Brij®93, Span®20, Span®80 and Cremophor RH®40, respectively.

3. The factors affecting nanoemulsion formation by low energy emulsification were types of oils and surfactants and the amounts of oils and surfactants. For the oil types, rice bran oil (triglyceride oil) made difficult to form nanoemulsion compared to oleic acid (fatty acid) and sweet orange oil (essential oil), respectively. For the types of surfactants, the different structures of surfactant mixtures formed nanoemulsion easily. Oil and surfactant concentrations also

affected nanoemulsion formation. Nanoemulsion could be formed at the optimum oil to surfactant ratio (2:1).

4. Nanoemulsions could be prepared by using low energy method and showed mean particle sizes in nanometer ranges. The ellagic acid could be incorporated in nanoemulsions at 0.35-0.60 mg %w/w which depended on each formulation.

5. The present study showed the slower ellagic acid release from nanoemulsion than that from solution.

6. For the permeation study, ellagic acid was mainly located at the donor part (92.51±1.12%) and it could not be detected in the skin and receiver medium. There were some components interfered the HPLC assay.

In this present work, the prepared nanoemulsions might be of benefit for developing nanoemulsions containing other compounds that possess similar property of ellagic acid. For future investigation, the optimization of extraction process should be conducted in more detail in order to obtain high percentage of yield. Furthermore, the use of solubilizer and enhancer such as propylene glycol or polyethylene glycol may be added in the nanoemulsion to increase ellagic acid loading in nanoemulsion. In vitro enzyme assay should also be used to verify the antioxidant activity of ellagic acid in receiver medium. In addition, in vivo study should be investigated further in animal to determine the possibility for human use.

REFERENCES

Abu-Elyazid, S.K., Kassem, A.A., Samy, A.M., and Gomaa, M.E. 2011. Evaluation of skin permeation and pharmacological effects of tenoxicam nanoemulsion in topical formulations. Asian Journal of Pharmaceutical and Health Sciences 1(3): 99-105.

Al-Edresi, S., and Baie, S. 2009. Formulation and stability of whitening VCO-in-water nano-cream. Pharmaceutical Nanotechnology 373: 174-178.

Allouche, J., Tyrode, E., Sadtler, V., Choplin, L., and Salager, J.L. 2003. Emulsion morphology follow up simultaneous in situ conductivity and viscosity measurements during a dynamic termperature-induced transitional inversion. The 3rd International Symposium on Food Rheology and Structure, ETH Zurich.

Amakura, Y., Okada, M., Tsuji, S., and Tonogai, Y. 2000. Studied on procedure for sample preparation of ellagic acid in several kinds of foodstuffs. Kokuritsu Iyakuhin Shokuhin Eisei Kenkyusho Hokoku 118: 100-2.

Amar-Yuli, I., Aserin, A., and Garti, N. 2010. Some characteristics of lyotropic liquid-crystalline mesophase. In T. F. Tadros (ed.). Self-organized surfactant structure, pp. 89-272. Germany: Wiley-VCH.

Ammar, H.O., Salama, H.A., Ghorab, M., and Mahmoud, A.A. 2009. Nanoemulsion as a potential ophthalmic delivery system for dorzolamide hydrochloride. AAPS PharmSciTech 10(3): 808-819.

Anton, N., and Vandamme, T.F. 2009. The universality of low-energy nano-emulsification. International Journal of Pharmaceutics 377: 142-147.

Aviram, M., et al. 2008. Pomegranate phenolics from the peels, arils, and flowers are antiatherogenic: studies in vivo in atherosclerotic apolipoprotein E-deficient (E^0) mice and in vitro in cultured macrophages and lipoproteins. Journal of Agricultural and Food Chemistry 56: 1148-1157.

Azeem, A., Ahmad, F., Khar, R., and Talegaonkar, S. 2009a. Nanocarrier for the transdermal delivery of an antiparkinsonian drug. AAPS PharmSciTech 10: 1093-1103.

Azeem, A., et al. 2009. Nanoemulsion components screening and selection: a technical note. AAPSPharmSciTech 10(1): 69-76.

Bae, J.Y., Choi, J.S., Kang, S.W., Lee, Y.J., Park, J., and Kang, Y.H. 2010. Dietary compound ellagic acid alleviates skin wrinkle and inflammation induced by UV-B I radiation. Experimental Dermatology 19: e182-e190.

Baipai, M., Pande, A., Tewari, S.K., and Dhan, P. 2005. Phenolic contents and antioxidant activity of some food and medicinal plants. International Journal of Food Sciences and Nutrition 56(4): 287-291.

Baker, J.R., Flack, M.R., Ciotti, S., and Sutcliffe, J.A. 2009. US *patent No*. 0269394 A1:Methods and composition for treating onchomycosis, NanoBio Corporation, United Stated: 1-67.

Bala, I., Bhardwaj, V., Hariharan, S., and Kumar, M.N. 2006. Analytical methods for assay of ellagic acid and its solubility studies. Journal of Pharmaceutical and Biomedical Analysis 40(1): 206-210.

Bali, V., Ali, M., and Ali, J. 2011. Nanocarrier for the enhanced bioavailability of a cardiovascular agent: In vitro, pharmacodynamic, pharmacokinetic and stability assessment. International Journal of Pharmaceutics 403: 46-56.

Bernardi, D.S., Pereira, T.A., Maciel, N.R., Bortoloto, J., Viera, G.S., Oliveira, G.C., and Rocha-Filho, P.A. 2011. Formation and stability of oil-in-water nanoemulsions containing rice bran oil: in vitro and in vivo assessments. Journal of Nanobiotechnology 9(44): 1-9.

Bilbao-Sáinz, C., Avena-Bustillos, R.J., Wood, D.F., Williams, T.G., and Mchugh, T.H. 2010. Nanoemulsions prepared by a low-energy emulsification method applied to edible films. Journal of Agricultural Food Chemistry 58: 11932-11938.

Binks, B.P., Clint, J.H., Fletcher, P.D., and Rippon, S. 1999. Kinetics of swelling of oil-in-water emulsions stabilized by different surfactants. Langmuir 15: 4495-4501.

Borochov-Neori, H., et al. 2009. Seasonal and cultivar variations in antioxidant and sensory quality of pomegranate (*Punica granatum* L.) fruit. Journal of Food Composition and Analysis 22: 189-195.

Bouchemal, K., Briançon, S., Perrier, E., and Fessi, H. 2004. Nano-emulsion formulation using spontaneous emulsification: solvent, oil and surfactant optimisation. Pharmaceutical Nanotechnology 280: 241-251.

Butt, H.J., Graf, K., and Kappl, M. 2003. Physics and chemistry of interfaces. Germany: Wiley-VCH.

Chouksey, R., Jain, A.M., Pandey, H., and Maithil, A. 2011. Development and bioavailability studies of atorvastatin nanoemulsion. International Journal of Pharmacy & Lifesciences 2(8): 982-988.

Cilurzo, F., Minghetti, P., and Sinico, C. 2007. Newborn pig skin as model membrane in vitro drug permeation studies: A technical note. AAPS PharmSciTech 8(4): E1-E4.

Conroy, J.W. How it works [online]. 2011. Avaiable from: http://www. microfluidicscorp.com/index.php?option=com_content&view=article&id=49&Itemid=18 0 [2011, November 14]

Dai, L., Li, W., and Hou, X. 1997. Effect of the molecular structure of mixed nonionic surfactants on the temperature of miniemulsion formation. Colloids and Surfaces A: Physicochemical and Engineering Aspects 25(1): 27-32.

Daniel, E.M., Krupnick, A.S., Heur, Y.H., Blinzler, J.A., Nims, R.W., and Stoner, G.D. 1989. Extraction, stability, and quantitation of ellagic acid in various fruits and nuts. Journal of Food Composition and analysis 2(4): 338-349.

Delaney, J.S. 2004. Estimating aqueous solubility directly from molecular structure. Journal of Chemical Information and Computer Sciences 44: 1000-1005.

Depraétere, P., Florence, A.T., Puisieux, F., and Seiller, M. 1980. Some properties of oil-in-water emulsions stabilized with mixed non-ionic surfactants (Brij®92 and Brij®96). International Journal of Pharmaceutics 5: 291-304.

Dios, M., Barrao, F., and Tojo, C. 2011. A simulation study on the structure of bimetallic nanoparticles synthesized in microemulsion. In F. Kremer, and W. Richtering (ed.). Progress in colloid and polymer science: trends in colloid and interfaces science, pp. 155-159. New York: Springer-Verlag BerlinHeidelberg.

Egawa, M., and Marui, Y. 2000. US *patent No*. 6,066,312. Topical composition for application to the skin containing an ellagic acid-based compound or salt thereof, Lion Corporation, Japan: 1-20.

Engels, T., Förster, T., and Rybinski, W.V. 1995. The influence of coemulsifier type on the stability of oil-in-water emulsions. Colloids and Surfaces A: Physicochemical and Engineering Aspects 99: 141-149.

Esquena, J., Sankar, G.R., and Solans, C. 2003. Highly concentrated w/o emulsions prepared by the PIT method as templates for solid foams. Langmuir 19: 2983-2988.

Feeny, P.P., Bostock, H. 1968. Seasonal changes in the tannin content of oak leaves. Phytochemistry 7(5): 871-880.

Fernandez, P., André, V., Rieger, J., and Kühnle, A. 2004. Nano-emulsion formation by emulsion phase inversion. Colloids and Surfaces A: Physicochemical Engineering Aspects 251: 53-58.

Forgiarini, A., Esquena, J., González, C., and Solans, C. 2001. Formation of nano-emulsions by low-energy emulsification methods at constant temperature. Langmuir 17: 2076-2083.

Forgiarini, A., Marquez, L., Celis, M.T., and Salager, J.L. Nano-emulsions of triglyceride by means of a inversion method[online]. 2006. Avaiable from: http://www.firp.ula.ve/CV _profesores/06_CME4_Forgiarini.pdf [2011, November 14]

Galindo-Alvarez, J., et al. 2011. Miniemulsion polymerization templates: A systematic comparison between low energy emulsification (Near-PIT) and ultrasound emulsification methods. Colloids and Surfaces A: Physicochemical and Engineering Aspects 374(1-3): 134-141.

Gaonkar, A.G., and Bagwe, R.P. 2005. Microemulsion in Foods: Challenges and applications. In K. L. Mittal, and D. O. Shah (ed.). Adsorption and aggregation of surfactants in solution, pp. 368-388. New York: Marcel Dekker.

Giap, S.G.E., Nik, W.M.N.W., Ahmad, M.F., and Amran, A. 2009. The assessment of rheological model reliability in lubricating behavior of vegetable oils. Engineering e-Transaction 4(2): 81-89.

Gilli, G., and Gilli, P. 2009. The nature of the hydrogen bond outline of a comprehensive hydrogen bond theory. 1st ed. United Kingdom: Oxford university.

Golding M., and Pelan, E. 2008. Application of emulsifiers to reduce fat and enhance nutritional quality. In G. L. Hasenhuettl, and R. W. Hartel (ed.). Food emulsifiers and their applications, pp. 327-348. New York: Springer Science+Business Media.

Guglielmini, G. 2008. Nanostructured novel carrier for topical application. Clinics in Dermatology 26: 341-346.

Häkkinen, S.H., Kärenlampi, S.O., Mykkänen, H.M., Heinonen, I.M., and Törrönen, A.R. 2000. Ellagic acid content in berries: influence of domestic processing and storage. European Food Research and Technology 212: 75-80.

Hielscher, T. 2005. Ultrasonic production of nano-size dispersions and emulsions. Proceedings of European Nanosystems Conference ENS'05: 1-6.

Hill, S.E. 1998. Emulsion and foam. In S. E. Hill, D. A. Ledward, and J. R. Mitchell (ed.). Functional properties of food macromolecules, pp. 311-312. Great Britain: Aspen Publishers.

Ishida, K., Sato, Y., Egawa, M., and Takeuchi, K. 1992. US *patent No*. 5,141,741: Anti-sunburn skin-care preparation, Lion Corporation, Japan: 1-12.

Izquierdo, P., et al. 2002. Formation and stability of nano-emulsions prepared using the phase inversion temperature method. Langmuir 18: 26-30.

Izquierdo, P., et al. 2005. The influence of surfactant mixing ratio on nano-emulsion formation by the pit method. Journal of Colloid and Interface Science 285(1): 388-394.

Jeevana, J.B., and Sreelakshmi, K. 2011. Design and evaluation of self-nanoemulsifying drug delivery system of flutamide. Journal of Young Pharmacists 3(1): 4-8.

Jeganathan, N.S., and Kannan, K. 2008. HPTLC method for estimation of ellagic acid and gallic acid in *Triphala churanam* formulations. Research Journal of Phytochemistry 2(1): 1-9.

Jimenez, F., Mitts, T.F., Liu, K., Wang, Y., and Hinek, A. 2006. Ellagic and tannic acids protect newly synthesized elastic fibers from premature enzymatic degradation in dermal fibroblast cultures. Journal of Investigative Dermatology 126: 1272-1280.

Jordão, A.M., Ricardo-da-Silva, J.M., and Laureano, O. 2005. Extraction of some ellagitannins and ellagic acid from oak wood chips (*Quercus pyrenaica* L.) in model wine solutions: effect of time, pH, temperature and alcoholic content. South African Journal for Enology & Viticulture 26(2): 83-89.

Junyaprasert, V.B., Singhsa, P., Suksiriworapong, J., and Chantasart, D. 2012. Physicochemical properties and skin permeation of Span 60/Tween 60 niosomes of ellagic acid. International Journal of Pharmaceutics 423: 303-311.

Kim, D-W., Shin, S-Il., and Oh, S-G. 2005. Preparation and stabilization of silver colloids in aqueous surfactant solutions. In K. L. Mittal, and D. O. Shah (ed.). Adsorption and aggregation of surfactants in solution, pp. 234-246. New York: Marcel Dekker.

Kunieda, H., and Friberg, S.E. 1981. Critical phenomena in a surfactant/water/oil system. Basic study on the correlation between solubilization, microemulsion, and ultralow interfacial tensions. Bulletin of the Chemical Society of Japan 54: 1010-1014.

Larrosa, M., Tomãs-Barberãn, F.A., Espìn, J.C. 2006. The dietary hydrolysable tannin punicalagin releases ellagic acid that induces apoptosis in human colon adenocarcinoma Caco-2

cells by using the mitochondrial pathway. The Journal of Nutritional Biochemistry 17(9): 611-625.

Lei, Z., Jervis, J., and Helm R.F. 2001. Use of methanolysis for the determination of total ellagic acid gallic acid contents of wood and food products. Journal of Agricultural and Food Chemistry 49(3): 1165-1168.

Li, C., Mei, Z., Liu, Q., Wang, J., Xu, J and Sun, D. 2010. Formation and properties of paraffin wax submicron emulsions prepared by the emulsion inversion point method. Colloids and Surfaces A: Physicochemical and Engineering Aspects 356(1-3): 71-77.

Li, Y., Guo, C., Yang, J., Wei, J., Xu, J., and Cheng, S. 2006. Evaluation of antioxidant properties of pomegranate peel extract in comparison with pomegranate pulp extract. Food Chemistry 96: 254-260.

Li, Y., Zheng, J., Xiao, H., and McClements, D.J. 2012. Nanoemulsion-based delivery systems for poorly water-soluble bioactive compounds: Influence of formulation parameters on polymethoxyflavone crystallization. Food Hydrocolloids 27: 517-528.

Liu, W., Sun, D., Li, C., Liu, Q., and Xu, J. 2006. Formation and stability of paraffin oil-in-water nano-emulsion prepared by the emulsion inversion point method. Journal of Colloid and Interface Science 303(2): 557-563.

Lu, D., and Rhodes, D.G. 2000. Mixed composition films of Span and Tween 80 at the air-water interface. Langmuir 16: 8107-8112.

Lu, J.J., and Yuan, Q. 2008. A new method for ellagic acid production from pomegranate husk. Journal of Food Process Engineering 31(4): 443-454.

Maas, J.L., Wang, S.Y., Galletta, G.J. 1991. Evaluation of strawberry cultivars for ellagic acid content. HortScience 26(1): 6668.

Määttä-Riihinen, K.R., Kamal-Eldin, A., and Törrönen, R.A. 2004. Identification and quantification of phenolic compounds in berries of *Fragaria* and *Rubus* species (Family Rosaceae). Journal of Agricultural and Food Chemistry 52:6178-6187.

Maestro, A., Pey, C.M., Gonzalez, C., Solans, C., and Gutiérrez, J.M. 2006. Nano-emulsions preparation by low energy methods in an ionic surfactant system. Colloids and Surface A: Physicochemical and Engineering Aspects 288: 138-143.

Mahato, R.I., and Narang, A.S. 2012. Pharmaceutical dosage forms and drug delivery. London: Taylor & Francis group.

Malmsten, M. 2002. Surfactants and Polymers in drug delivery. New York: Marcel Deckker.

Mason, T.G., Graves, S.M., Wilking, J.N., and Lin, M.Y. 2006. Extreme emulsification: formation and structure of nanoemulisons. Condensed Matter Physics 9(45): 193-199.

McClements, D.J., Henson, L., Popplewell, L.M., Decker, E.A., and Choi, S.J. 2010. Inhibition of Ostwald ripening in model beverage emulsions by addition of poorly water soluble triglyceride oils. Journal of Food Science 0: 1-6.

Mei, Z., Xu, J., and Sun, D. 2010. O/W nano-emulsions with tunable PIT induced by inorganic salts. Colloids and Surfaces A: Physicochemical and Engineering Aspects 375(1-3): 102-108.

Morais, J.M., Santos, O.D.H., Delicato, T., Gonçalves, A.R., and Rocha-Filho, P.A. 2006. Physicochemical characterization of canola oil/water nano-emulsions obtained by determination of required HLB number and emulsion phase inversion methods. Journal of Dispersion Science and Technology 27: 109-115.

Morales, D., Gutirrez, J.M., Garca-Celma, M.J., and Solans, Y.C. 2003. A study of the relation between bicontinuous microemulsions and oil/water nanoemulsion formation. Langmuir 19(18): 7196-7200.

Mou, D., et al. 2008. Hydrogel-thickend nanoemulsion system for topical delivery of lipophillic drugs. Pharmaceutical Nanotechnology 353: 270-276.

Murugan,V., Mukherjee, K., Maiti, K., and Mukherjee, P.K. 2009. Enhanced oral bioavailability and antioxidant profile of ellagic acid by phospholipids. Journal of Agricultural and Food Chemistry 57: 4559-4565.

Negi, P.S., Jayaprakasha, G.K., and Jena, B.S. 2003. Antioxidant and antimutagenic activities of pomegranate peel extracts. Food Chemistry 80: 393-397.

Noureddini, H., Teoh, B.C., and Clements, L.D. 1992. Viscosities of vegetable oils and fatty acids. Journal of the American Oil Chemists' Society 69(12): 1189-1191.

Panichayupakaranant, P., Itsuriya, A., and Sirikatitham, A. 2010. Preparation method and stability of ellagic acid-rich pomegranate fruit peel extract. Pharmaceutical Biology 48(2): 201-205.

Panichayupakaranant, P., Tewtrakul, S., and Yuenyongsawad, S. 2010. Antibacterial, anti-inflammatory and anti-allergic activities of standardized pomegranate rind extract. Food Chemistry 123: 400-403.

Peng, L.C., Liu, C.H., Kwan, C.C., and Huang, K.F. 2010. Optimization of water-in-oil nanoemulsions by mixed surfactants. Colloids and Surfaces A: Physicochemical and Engineering Aspects 370: 136-142.

Pey, C.M., Maestro, A., Solé, I., González, C., Solans, C., and Gutiérrez, J.M. 2006. Optimization of nano-emulsions prepared by low-energy emulsification methods at constant temperature using factorial design study. Colloid and Surface A: Physicochemical Engineering Aspects 288: 144-150.

Pons, R., Carrera, I., Caelles, J., Rouch, J., and Panizza, P. 2003. Formation and properties of miniemulsions formed by microemulsions dilution. Advances in Colloid and Interface Science 106: 129-146.

Priyadarsini, K.I., Khopde, S.M., Kumar, S.S., and Mohan, H. 2002. Free redical studies of ellagic acid, a natural phenolic antioxidant. Journal of Agricultural and Food Chemistry 50: 2200-2206.

Qhattal H.S., Wang, S., Salihima, T., Srivastava, S.K., Liu, X. 2011. Nanoemulsions of cancer chemopreventive agent isothiocyanate display enhanced solubility, dissolution, and permeability. Journal of Agricultural Food and Chemistry 59(23): 12396-404.

Rang, M-J., and Miller, C.A. 1999. Spontaneous emulsification of oils containing hydrocarbon, nonionic surfactant, and oleyl alcohol. Journal of Colloid and Interface Science 209: 179-192.

Rao, J., and Mcclements, D.J. 2010. Stabilization of phase inversion temperature nanoemulsions by surfactant displacement. Journal of Agricultural Food Chemistry 58: 7059-7066.

Rodríguez, C., Shigeta, K., and Kunieda, H. 2000. Cubic phase based concentrated emulsion. Journal of Colloid and Interface Science 233: 197-204.

Roger, K., Cabane, B., and Olsson, U. 2010. Formation of 10-100 nm size-controlled emulsions through a sub-pit cycle. Langmuir 26(6): 3860-3867.

Ruktanonchai, U., et al. 2009. Physicochemical characteristics, cytotoxicity, and antioxidant activity of three lipid nanoparticulate formulations of alpha-lipoic acid. AAPS PharmSciTech 10(1): 227-234.

Sadurní, N.R., Solans, C., Azemar, N.R., and Garca-Celma, M.J. 2005. Studies on the formation of O/W nano-emulsions, by low-energy emulsification methods, suitable for pharmaceutical applications. European Journal of Pharmaceutical Sciences 26: 438-445.

Sajjadi, S. 2006. Nanoemulsion formation by phase inversion emulsification: on the nature of inversion. Langmuir 22(13): 5597-5603.

Sakeena, M.H.F., Yam, M.F., Elrashid, S.M., Munavvar, A.S., and Azmin, M.N. 2010. Anti-inflammatory and analgesic effects of ketoprofen in palm oil esters nanoemulsion. Journal of Oleo Science 59(12): 667-671.

Sakulku, U., Nuchuchua, O., Uawongyart, N., Puttipipatkhachorn, S., Soottita, A., and Ruktanonchai, U. 2009. Characterization and mosquito repellent activity of citronella oil nanoemulsion. International Journal of Pharmaceutics 372: 105-111.

Schwarz, J.S., Weisspapir, M.R., and Friedman, D.I. 1995. Enhanced transdermal delivery of diazepam by submicron emulsion (SME) creams. Pharmaceutical Research 12(5): 687- 692.

Seeram, N.P., Zhang, Y., Reed, J.D., Krueger, C.G., and Vaya, J. 2006. Pomegranate Phytochemicals. In N. P. Seeram, R. N. Schulman, and D. Heber (ed.), Pomegranates ancient roots to modern medicine, pp. 3-30. New York: Taylor & Francis.

Shafiq-un-Nabi, S., Shakeel, F., Talegaonkar, S., Ahmad, F.J., Khar, R.K., and Ali, M. 2007. Development and bioavailability assessment of ramipril nanoemulsion formulation. European Journal of Pharmaceutics and Biopharmaceutics 66: 227-243.

Shakeel, F.S., and Faisal, M.S. 2010. Nanoemulsion: a promising tool for solubility and dissolution enhancement of celecoxib. Pharmaceutical Development and Technology 15(1): 53-56.

Shakeel, F., Baboota, S., Ahuja, A., Ali, J., and Shafiq, S. 2008. Skin permeation mechanism and bioavailability enhancement of celecoxib from transdermally applied nanoemulsion. Journal of Nanobiotechnology 6:8.

Shakeel, F., Ramadan, W., and Shafiq, S. 2009. Solubility and dissolution improvement of aceclofenac using different nanocarriers. Journal of Bioequivalence & Bioavilability 1: 039-043.

Sharma, G., Italia, J.L., Sonaje, K., Tikoo, K., and Ravi Kumar, M.N.V. 2007. Biodegradable in situ gelling system for subcutaneous administration of ellagic acid and ellagic acid loaded nanoparticles: Evaluation of their antioxidant potential against cyclosporine induced nephrotoxicity in rats. Journal of Controlled Release 118(1): 27-37.

Shimogaki, H., Tanaka, Y., Tami, H., and Masuda, M. 2000. In vitro and in vivo evaluation of ellagic acid on melanogenesis inhibition. International Journal of Cosmetic Science 22: 291-303.

Shruthi, S.D., and Ramachandra, Y.L. 2011. RBP-J as a therapeutic target to rheumatoid arthritis- and in silico study. International Journal of Preclinical and Pharmaceutical Research 2(1): 38-44.

Solans, C., Esquena, J., Azemar, N., Rodriguez, C., and Kunieda, H. 2004. Highly concentrated (gel) emulsion: formation and properties. In D. N. Petsev (ed.). Emulsion: structure stability and interactions, pp. 511-767. San Diego: Elsevier.

Solans, C., et al. 2009. Nano-emulsion formation by low-energy methods and functional properties. In H. Á. Roque (ed.), Structure and functional properties of colloidal systems, pp. 457-479. New York: Taylor & Francis.

Solè, I., Maestro, A., Carmen, G., Solans, C., and Gutierrez, J. 2006. Optimization of nano-emulsion preparation by low-energy methods in an ionic surfactant system. Langmuir 22(20): 8326-8332.

Solè, I., et al. 2010. Nano-emulsion prepared by the phase inversion composition method: Preparation variables and scale up. Journal of Colloidal and Interface Science 344: 417-423.

Sonneville-Aubrun, O., Simonnet, J.T., and Alloret, F.L. 2004. Nanoemulsion: a new vehicle for skin care products. Advance in Colloid and Interface Science 108-109: 145-149.

Srivastava, A., Jagan Mohan Rao, L., and Shivanandappa, T. 2007. Isolation of ellagic acid from the aqueous extract of the roots of *Decalepis hamiltonii*: Antioxidant activity and cytoprotective effect. Food Chemistry 103: 224-233.

Susanne, U., Mertens, T., and Susan, S.P. 2005. Ellagic acid and quercetin interact synergistically with resveratrol in the induction of apoptosis and cause transient cell cycle arrest in human leukemia cells. Cancer Letters 218(2): 141-151.

Swarbrick, J., Rubino, J.T., and Rubino, O.P. 2006. Coarse dispersions. In D. B. Troy (ed.). Remington: the science and practice of pharmacy 21st. Maryland: Lippincott Williams & Wilkins.

Tadros, T., Izquierdo, P., Esquena, J., and Solans, C. 2004. Formation and stability of nano-emulsions. Advances in Colloid and Interface Science 108-109: 303-318.

Teo, B.S.X., Basri, M., Zakaria, M.R.S., Salleh, A.B., Rahman, R.N.Z.R.A., Rahman, M.B.A. 2010. A potential tocopherol acetate loaded palm oil esters-in-water nanoemulsions for nanocosmeceuticals. Journal of Nanobiotechnology 8(4): 1-11.

Troy, D.B. 2006. Remington: the science and practice of pharmacy. United Stated: Lippincott Williams & Wilkins.

Uddin, H., Kunieda, H., and Solans, C. 2003. Highly concentrated cubic phase-based emulsions. In K. Esumi, and M. Ueno (ed.). Structure-performance relationships in surfactants. NewYork: Marcel Dekker.

United States Pharmacopeial Convention: The United States Pharmacopeia 32-The National Formulary 27. Mack Publishing: Pennsylvania. 2010.

Wang, L., Li, X., Zhang, G., Dong, J., and Eastoe, J. 2007. Oil-in-water nanoemulsions for pesticide formulations. Journal of Colloid and Interface Science 314: 230-235.

Weiss, J. 2000. Mass transport phenomena in oil-in-water emulsions containing surfactant micelles: Ostwald ripening. Langmuir 16: 6833-6338.

Williner, M.R., Pirovani, M.E., Güemes, D.R. 2003. Ellagic acid content in strawberries of different cultivars and ripening stages. Journal of the Science of Food and Agriculture 83(3): 0022-5142.

Wolf, P.A. and Havekotte, M.J. 1989. Us *patent No*. 4,835,002: Microemulsions of oil in water and alcohol: 1-13.

Wooster, T.J., Goding, M., and Sanguansri, P. 2008. Impact of oil type on nanoemulsion formation and Oswald ripening stability. Langmuir 24: 12758-12765.

Yoo, B.H., et al. 2003. Us *patent No*. 0175315 A1: Nanoemulsion comprising metabolites of gingseng saponin as an active component and a method for preparing the same, and a skin-care composition for anti-aging containing the same: 1-18.

Yoshimura, M., Watanabe, Y., Kasai, K., Yamakoshi, J., and Koga, T. 2005. Inhibitory effect of an ellagic acid-rich pomegranate extract on tyrosinase activity and ultraviolet-induced pigmentation. Bioscience Biotechnology and Biochemistry 69(21): 2368-2373.

Zafrilla, P., Ferreres, F., and Tomás-Barberán, F.A. 2001. Effect of processing and storage on the antioxidant ellagic acid derivatives and flavonoids of red raspberry (Rubus idaeus) Jams. Journal of Agricultural of Food and Chemistry 49(8): 3651-3655.

Zhang, L.L., Xu, M., Wang, Y.M., Wu, D.M., and Chen, J.H. 2010. Optimizing ultrasonic ellagic acid extraction conditions from infructescence of *Platycarya strobilacea* using response surface methodology. Molecules 15: 7923-7932.

Zhou, H., Yuan, Q., and Lu, J. 2011. Preparative separation of punicalin from waste water of hydrolysed pomegranate husk by macroporous resin and preparative high-performance liquid chromatography. Food Chemistry 126: 1361-1365.

Ziani, K., Chang, Y., McLandsborough, L., and McClements, D.J. 2011. Influence of surfactant charge on antimicrobial efficacy of surfactant-stabilized thyme oil nanoemulsions. Journal of Agricultural and Food Chemistry 59: 6247-6255.

APPENDICES

APPENDIX A

Validation of UV spectroscopic method

(The United States Pharmacopieal Convention, 2010)

Validation for the quantitative determination of ellagic acid in methanol by UV spectroscopy

1. Specificity

The absorbance of ellagic acid must not be interfered by others components in sample under spectroscopic condition. The blank methanol, oil, and surfactant (without ellagic acid) and ellagic acid in methanol were prepared. The UV spectrum of the blank were compared with the spectra of the ellagic acid solution

2. Linearity

Six standard solutions of ellagic acid ranging from 1.5-4 μg/mL were prepared and analyzed. Linear regression analysis of the absorbance versus their concentrations was performed. The linearity was determined from the coefficient of determination.

3. Accuracy

Three set of three concentrations (low, medium, high) of ellagic acid at 1.8, 2.8, and 3.8 μg/mL were prepared and analyzed, respectively. The percentage recovery of each concentration was calculated from the estimated concentration to known concentration multiplied by 100.

4. Precision

4.1 Within run precision

The within run precision was determined by analyzed three sets of three concentrations (low, medium, high) of ellagic acid at 1.8, 2.8, and 3.8 μg/mL in the same day. The mean, standard deviation (SD), and the coefficient of variation (%CV) of each standard solution were determined.

4.2 Between run precision

The between run precision was evaluated by comparing each concentration of three sets of standard solution were prepared and analyzed in different days. The mean, standard deviation (SD), and the coefficient of variation (%CV) of each standard solution were determined.

Validation for the quantitative determination of ellagic acid in methanol by spectroscopy

The validation of intended method is the process by which performance characteristics of the method are established to meet the requirements. The analytical parameters used for the assay validation were specificity, linearity, accuracy, and precision.

1.1 Specificity

The specificity of an analytical method is the ability to measure the given analyze accurately and specificity in the presence of other components in the sample. The UV absorption spectra (Figure A2-A13) indicated that the wavelength 255 nm was the optimal wavelength giving the highest sensitivity without interference of substances.

1.2 Linearity

The linearity of an analytical method is the ability to elicit test results that are directly proportional to the concentration of the analyzed in samples within a given range. The standard curve of ellagic acid in methanol was shown in Figure A 1. The standard curves were found to be linear with coefficient of determination 0.9999.

Table A1 Data for calibration curve of ellagic acid in methanol by UV spectroscopy

Concentration	**Absorbance**					
(µg/mL)	**Set 1**	**Set 2**	**Set 3**	**Mean**	**SD**	**%CV**
1.5	0.2675	0.2684	0.2683	0.2681	0.0005	0.18
2	0.3665	0.3560	0.3641	0.3622	0.0055	1.52
2.5	0.4570	0.4481	0.4553	0.4535	0.0047	1.04
3	0.5488	0.5388	0.5470	0.5449	0.0053	0.98
3.5	0.6342	0.6254	0.6304	0.6300	0.0044	0.70
4	0.7170	0.7080	0.7180	0.7143	0.0055	0.77

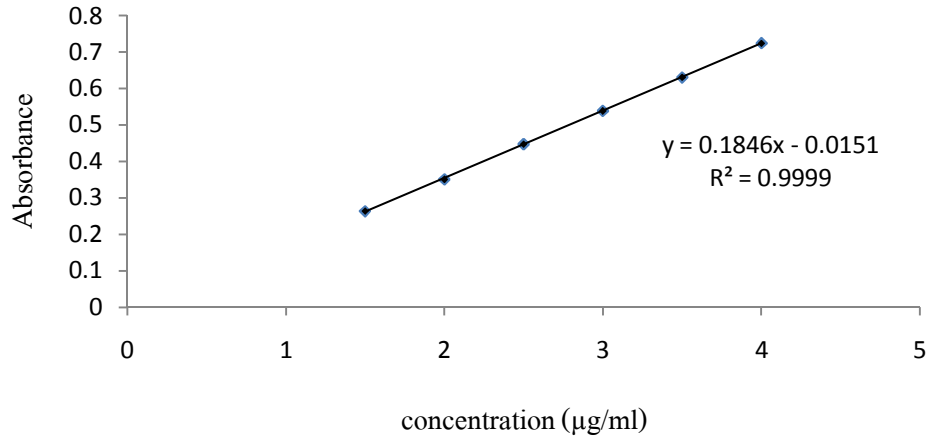

Figure A1 Calibration curve of ellagic acid in methanol by UV spectroscopy

1.3 Accuracy

The accuracy of an analytical method is the closeness of test results obtained by the method to the true value. Accuracy is calculated as percent recovery by the assay of known added amount of analyzes. The percentages of analytical recovery of ellagic acid solution are shown in Table B2. The percentages analytical recovery of ellagic acid solution was in range (98-102 %) of which indicated that this method could be used for analysis in all concentrations studied with high accuracy.

Table A2 The percentage of analytical recovery of ellagic acid in methanol by UV spectroscopy

Concentration (µg/mL)	%Analytical recovery			Mean	SD
	Set 1	Set 2	Set 3		
1.8	99.38	99.17	98.92	99.16	0.23
2.8	98.62	99.86	99.98	99.49	0.75
3.8	98.08	100.88	98.81	99.26	1.45

1.4 Precision

The precision of an analytical method is the degree of agreement among individual test results when the procedure is applied repeatedly to multiple samplings of a homogeneous sample.

The precision of an analytical method is usually expressed as the standard deviation or relative standard deviation (coefficient of variation).

The precision of the analysis of ellagic acid in methanol was determined both within run precision and between run precision as illustrated in Table A3-A4. All percentage coefficient of variation values were lower than 2.00%, indicating that of the UV spectrophotometric method used were precise for quantitative analysis of ellagic acid in the range studied.

Table A3 Data of within run precision of ellagic acid in methanol by UV spectroscopy

Concentration (µg/mL)	**Calculated Conc. (µg/mL)**			**Mean**	**SD**	**%CV**
	Set 1	**Set 2**	**Set 3**			
1.8	1.8112	1.8252	1.8352	1.8239	0.0120	0.66
2.8	2.8235	2.8040	2.7756	2.8010	0.0241	0.86
3.8	3.8413	3.8007	3.8458	3.8293	0.0249	0.65

Table A4 Data of between run precision of ellagic acid in methanol by UV spectroscopy

Concentration (µg/mL)	**Calculated Conc. (µg/mL)**			**Mean**	**SD**	**%CV**
	Set 1	**Set 2**	**Set 3**			
1.8	1.8251	1.8158	1.8338	1.8249	0.0090	0.49
2.8	2.8159	2.8337	2.8469	2.8321	0.0155	0.55
3.8	3.8105	3.8321	3.8349	3.8258	0.0134	0.35

In conclusion, the analysis of ellagic acid in methanol by UV spectrophotometric method developed in this study showed good specificity, linearity, accuracy, and precision.

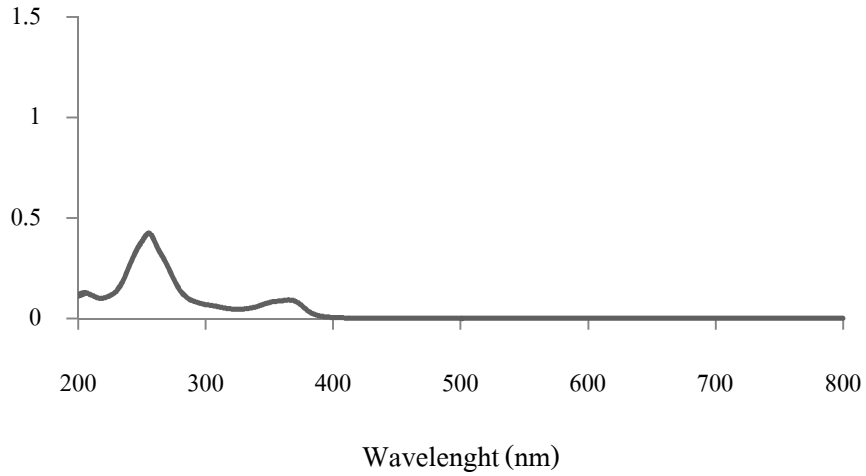

Figure A2 Absorption spectrum of ellagic acid in methanol

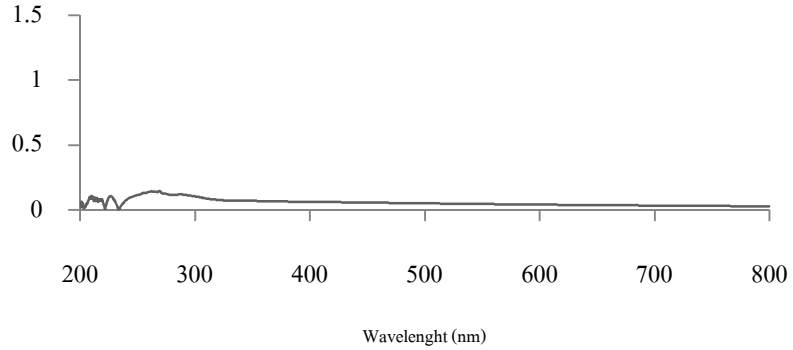

Figure A3 Absorption spectrum of mineral oil in methanol

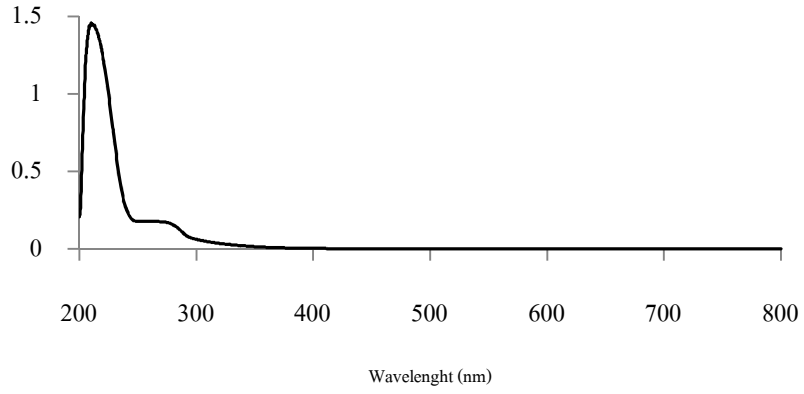

Figure A4 Absorption spectrum of Span®80 in hexane

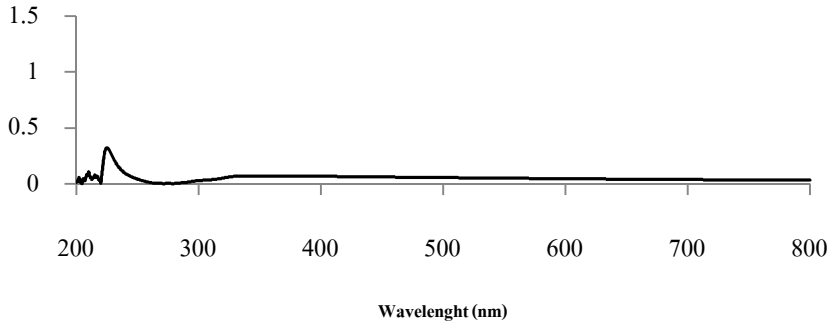

Figure A5 Absorption spectrum of squalene in hexane

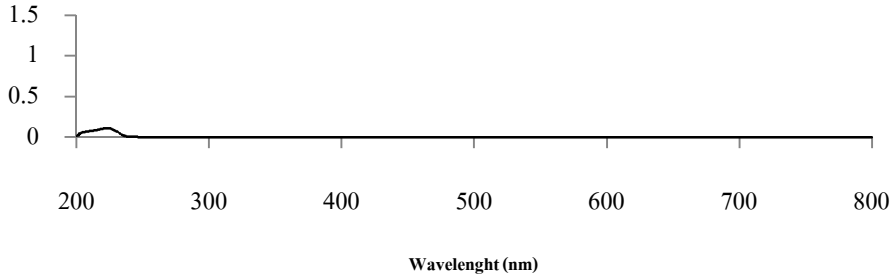

Figure A6 Absorption spectrum of Tween® 20 oil in methanol

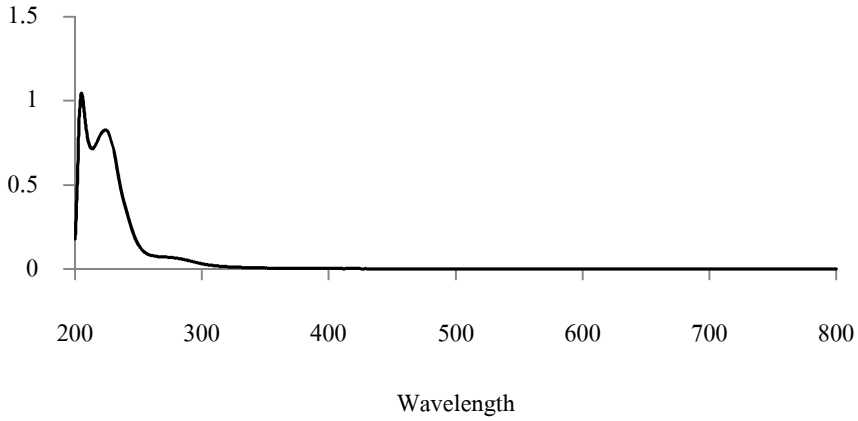

Figure A7 Absorption spectrum of Brij® 30 in methanol

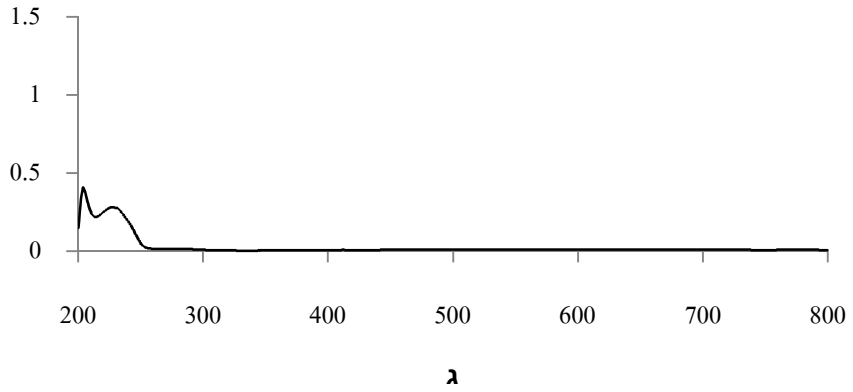

Figure A8 Absorption spectrum of Brij® 93 in methanol

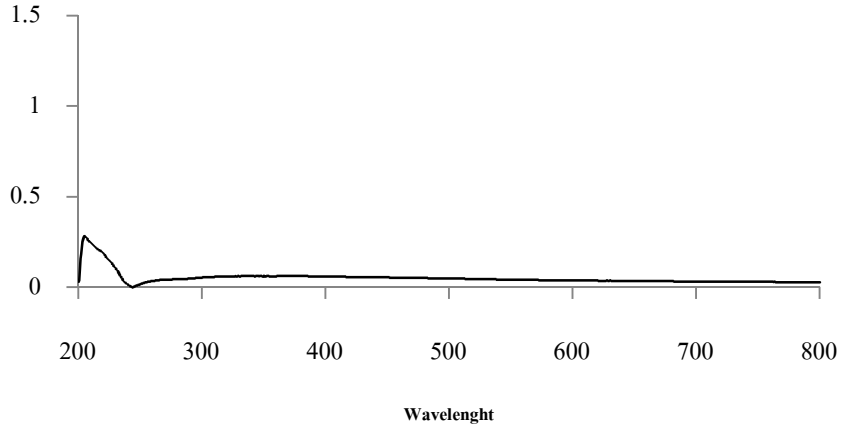

Figure A9 Absorption spectrum of Cremophor RH® 40 in methanol

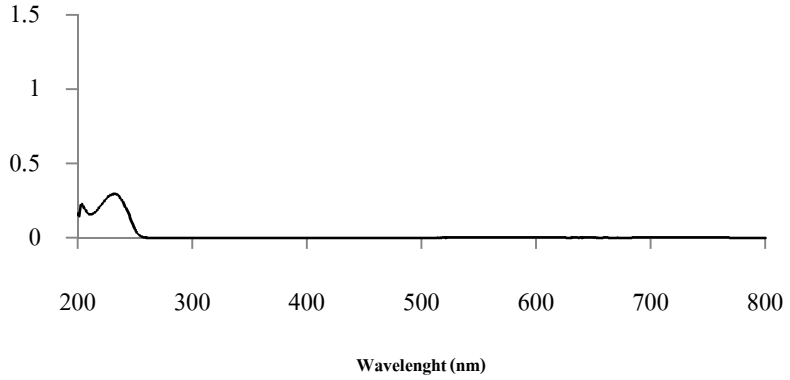

Figure A10 Absorption spectrum of Brij® 97 in methanol

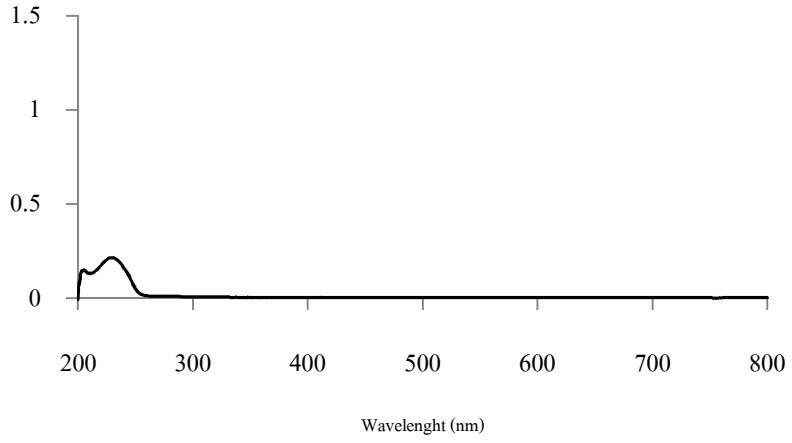

Figure A11 Absorption spectrum of Tween® 80 in methanol

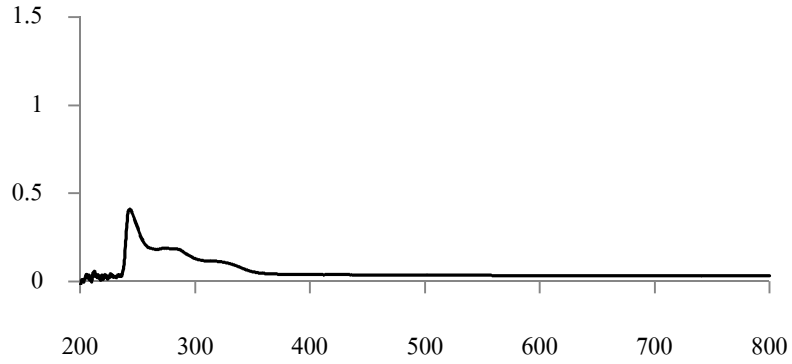

Figure A12 Absorption spectrum of rice bran oil in chloroform

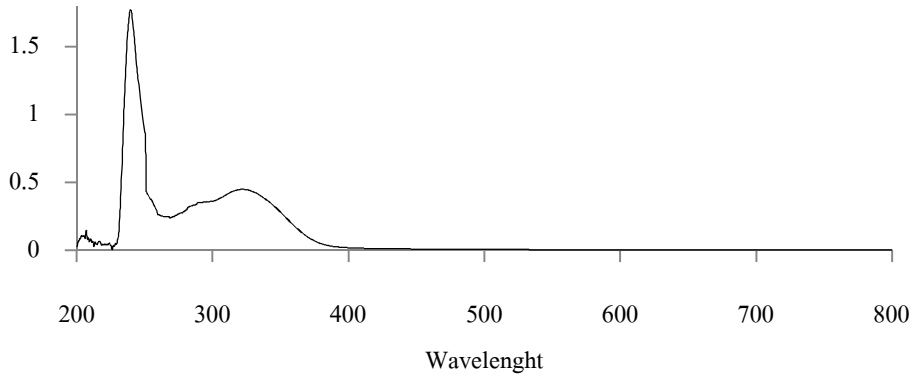

Figure A13 Absorption spectrum of sweet orange oil in chloroform

APPENDIX B

Validation of HPLC method

(The United States Pharmacopieal Convention, 2010)

Validation for the quantitative determination of ellagic acid in methanol by HPLC method (For extraction method)

1. Specificity

Under the HPLC method used, the peak chromatogram of ellagic acid must not be interfered by the peak chromatogram of other components in the sample.

2. Linearity

Six standard solutions of ellagic acid ranging from 0.8 to 3.3 µg/mL for methanol system were prepared and analyzed. Linear regression analysis of the absorbance versus their concentration was performed. The linearity was determined from the coefficient of determination.

3. Accuracy

Ellagic acid at 1, 2, and 3 µg/mL in methanol were prepared. Three sets of each concentration were prepared. Each individual was analyzed by HPLC method.

4. Precision

4.1 Within run precision

Three sets of the three standard solutions of ellagic acid in three interval of time in the same day were analyzed. The mean, standard deviation (SD), and coefficient of variation (%CV) of each standard solution were evaluated.

4.2 Between run precision

Three sets of the three standard solutions of ellagic acid were analyzed in three interval of time in the different days. The mean, standard deviation (SD), and coefficient of variation (%CV) of each standard solution were evaluated.

Validation for the quantitative determination of ellagic acid in methanol by HPLC method (For extraction method)

The validation of analytical method is the process by which performance characteristics of the method are established to meet the requirements for the intended analytical parameters. The analytical parameters used for the assay validation were specificity, linearity, accuracy, and precision.

1. Specificity

The specificity of an analytical method is its ability to measure the given analyte accurately and specificity in the presence of other components in the sample. The chromatograms (Figure B2-B4) indicated that there is no interference of solvent or mobile phase. Standard solution and internal standard solution were separated completely. It is indicated that this conditions is optimized.

2. Linearity

The linearity of an analytical method is its ability to elicit test results that are directly proportional to the concentration of the analyte in samples within a given range. The standard curve of ellagic acid solution with methanol was shown in Figure B 1. The standard curve was found to be linear with coefficient of determination 0.9990.

Table B1 Data for calibration curve of ellagic acid in methanol by HPLC

Concentration	Peak area ratio			Mean	SD	%CV
(µg/mL)	Set 1	Set 2	Set 3			
0.8	0.600709	0.614208	0.593133	0.602683	0.010675	1.771251
1.3	1.052316	1.076141	1.091541	1.073333	0.019763	1.841254
1.8	1.670425	1.641866	1.663544	1.658612	0.014905	0.898632
2.3	2.125325	2.13262	2.147621	2.135189	0.011368	0.532396
2.8	2.598753	2.68863	2.630056	2.639146	0.045623	1.7287
3.3	3.144898	3.259714	3.18765	3.19742	0.058028	1.814847

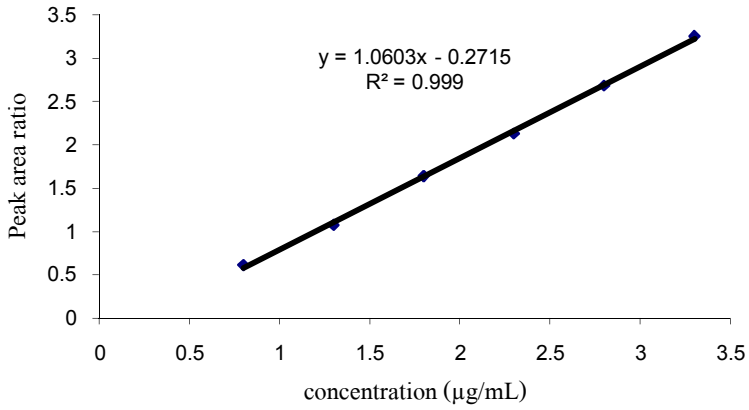

Figure B1 Calibration curve of ellagic acid in methanol by HPLC

3. Accuracy

The accuracy of an analytical method is the closeness of test results obtained by intended method to the true value. Accuracy may often be expressed as percent recovery by the assay of known, added amount of analyte. The percentage of analytical recovery of each ellagic acid in methanol is shown in Table B 2. All percentage recovery of ellagic acid solution was in the range of 98-102. Thus, it could be used for analysis of ellagic acid in all concentration used.

Table B2 The percentage of analytical recovery of ellagic acid in methanol by HPLC

Concentration (µg/mL)	**%Analytical recovery**			**Mean**	**SD**
	Set 1	**Set 2**	**Set 3**		
1	99.28017	98.01501	98.00719	98.43412	0.732706
2	98.93912	98.70992	101.4509	99.69999	1.520675
3	98.12405	99.96377	98.33183	98.80655	1.007554

4. Precision

The precision of an analytical method is the degree of agreement among individual test results when the procedure is applied repeatedly to multiple samplings of a homogeneous sample. The

precision of an analytical method is usually expressed as the standard deviation or relative standard deviation (coefficient of variation).

The precision of the analysis of ellagic acid in methanol was determined both within run precision and between run precision as illustrated in Table B3-B4. All percentage coefficient of variation values were lower than 2.00%, indicating that of the HPLC method used were precise for quantitative analysis of ellagic acid in the range studied.

Table B3 Data of within run precision of ellagic acid in methanol by HPLC

Concentration	**Calculated Conc. (µg/mL)**					
(µg/mL)	**Set 1**	**Set 2**	**Set 3**	**Mean**	**SD**	**%CV**
1	0.992802	0.98015	0.980072	0.984341	0.007327	0.744362
2	1.978782	1.974198	2.029018	1.994	0.030414	1.525251
3	2.943721	2.998913	2.949955	2.964197	0.030227	1.019724

Table B4 Data of between run precision of ellagic acid in methanol by HPLC

Concentration	**Calculated Conc. (µg/mL)**					
(µg/mL)	**Set 1**	**Set 2**	**Set 3**	**Mean**	**SD**	**%CV**
1	1.019256	1.018771	0.996632	1.011553	0.012924	1.277674
2	2.160906	2.200333	2.228816	2.196685	0.034102	1.552416
3	3.070493	3.134613	3.192935	3.13268	0.061244	1.954996

In conclusion, the analysis of ellagic acid in methanol by HPLC developed in this study showed good specificity, linearity, accuracy, and precision.

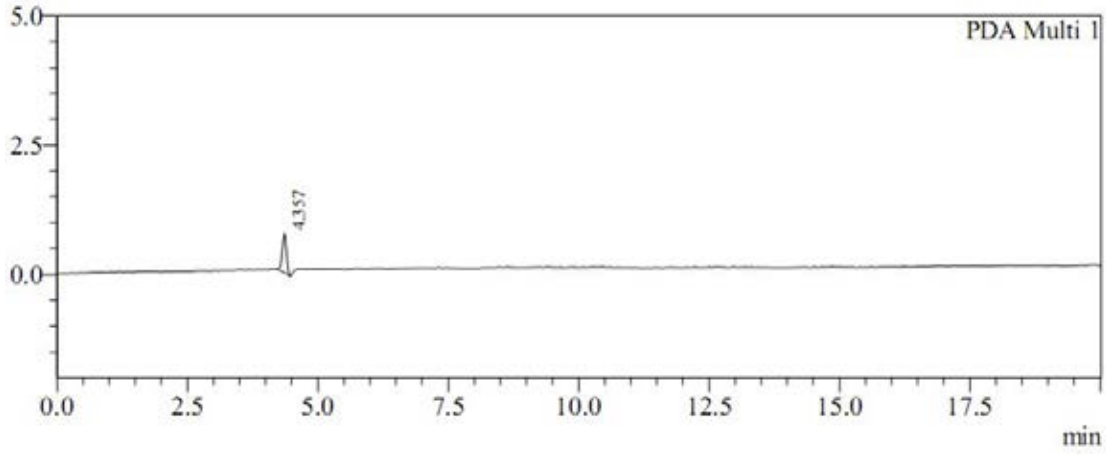

Figure B2 HPLC chromatogram of methanol

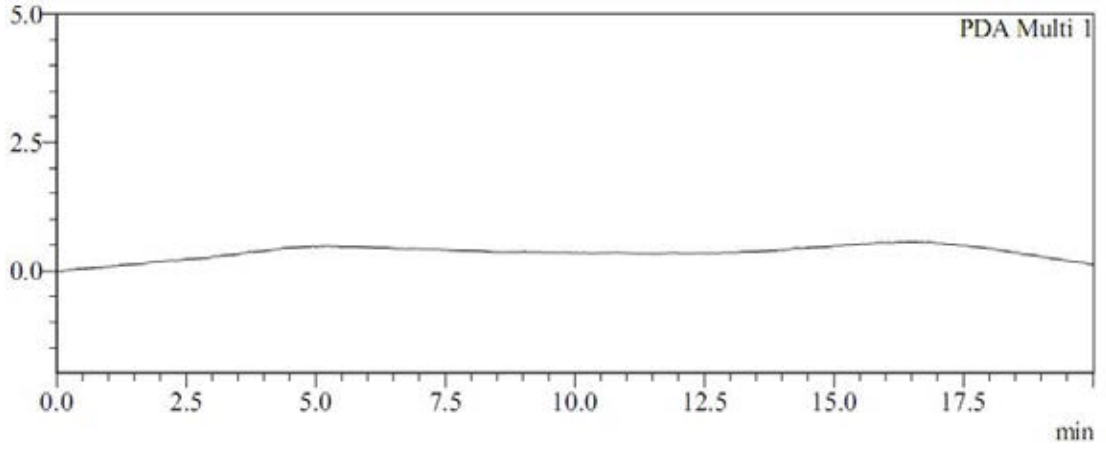

Figure B3 HPLC chromatogram of mobile phase

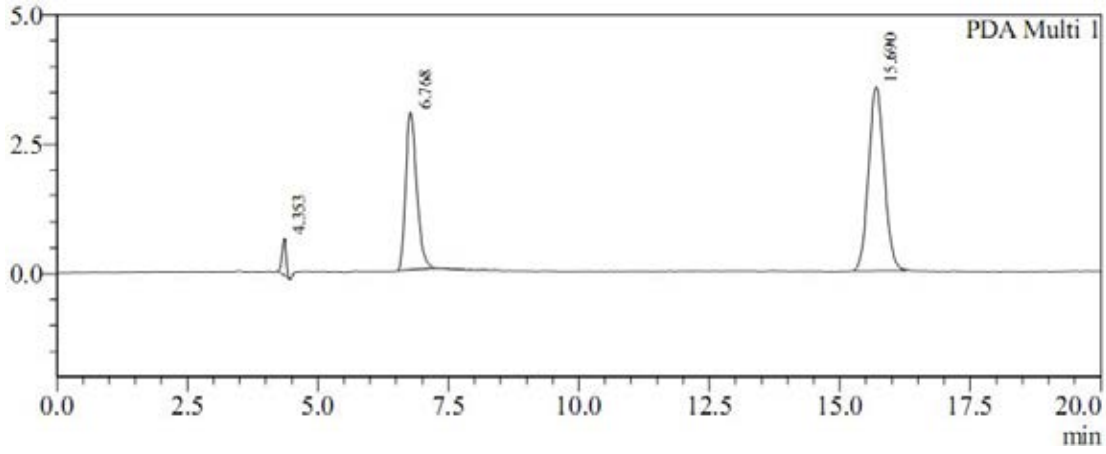

Figure B4 HPLC chromatogram of ellagic acid and propyl paraben in methanol

Validation for the quantitative determination of ellagic acid in methanol by HPLC method (For ellagic solubility in formulation, release study)

1. Specificity

Under the HPLC method used, the peak chromatogram of ellagic acid must not be interfered by the peak chromatogram of other components in the sample.

2. Linearity

Six standard solutions of ellagic acid ranging from 0.2 to 8 μg/mL for methanol system were prepared and analyzed. Linear regression analysis of the absorbance versus their concentration was performed. The linearity was determined from the coefficient of determination.

3. Accuracy

Ellagic acid at 1, 3, and 5 μg/mL in methanol were prepared. Three sets of each concentration were prepared. Each individual was analyzed by HPLC method.

4. Precision

4.1 Within run precision

Three sets of the three standard solutions of ellagic acid in three interval of time in the same day were analyzed. The mean, standard deviation (SD), and coefficient of variation (%CV) of each standard solution were evaluated.

4.2 Between run precision

Three sets of the three standard solutions of ellagic acid were analyzed in three interval of time in the different days. The mean, standard deviation (SD), and coefficient of variation (%CV) of each standard solution were evaluated.

Validation for the quantitative determination of ellagic acid in methanol by HPLC method (For ellagic solubility in formulation, release study, permeation study)

The validation of analytical method is the process by which performance characteristics of the method are established to meet the requirements for the intended analytical parameters. The analytical parameters used for the assay validation were specificity, linearity, accuracy, and precision.

1. Specificity

The specificity of an analytical method is its ability to measure the given analyte accurately and specificity in the presence of other components in the sample. The chromatograms (Figure B5-B11) indicated that there is no interference of solvent or mobile phase. Standard solution and internal standard solution were separated completely. It is indicated that this conditions is optimized.

2. Linearity

The linearity of an analytical method is its ability to elicit test results that are directly proportional to the concentration of the analyte in samples within a given range. The standard curve of ellagic acid solution with methanol was shown in Figure B 1. The standard curve was found to be linear with coefficient of determination 0.9995.

Table B5 Data for calibration curve of ellagic acid in methanol by HPLC

Concentration	**Peak area ratio**					
(µg/mL)	**Set 1**	**Set 2**	**Set 3**	**Mean**	**SD**	**%CV**
0.2	0.629293	0.626501	0.615508	0.623767	0.007288	1.168324
0.5	2.007032	2.078894	2.073618	2.053181	0.040054	1.950802
2	20.70316	20.54883	20.97877	20.74358	0.217801	1.049967
4	37.57917	38.36425	38.78026	38.24122	0.609921	1.59493
6	60.23223	61.58608	60.32156	60.71329	0.757175	1.247131
8	80.98902	81.71472	80.09916	80.9343	0.80917	0.999787

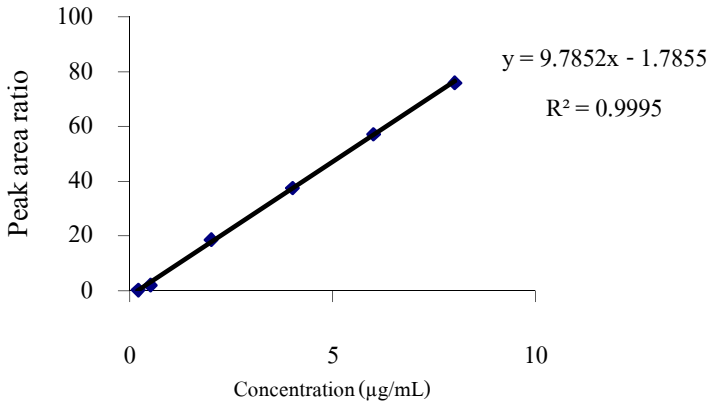

Figure B5 Calibration curve of ellagic acid in methanol by HPLC

3. Accuracy

The accuracy of an analytical method is the closeness of test results obtained by intended method to the true value. Accuracy may often be expressed as percent recovery by the assay of known, added amount of analyte. The percentage of analytical recovery of each ellagic acid in methanol is shown in Table B 1. All percentage recovery of ellagic acid solution was in the range of 98-102. Thus, it could be used for analysis of ellagic acid in all concentration used.

Table B6 The percentage of analytical recovery of ellagic acid in methanol by HPLC

Concentration (µg/mL)	**%Analytical recovery**			**Mean**	**SD**
	Set 1	**Set 2**	**Set 3**		
1	98.46259	101.5282	101.1092	100.3666	1.662215
3	98.50499	102.3837	100.5184	100.469	1.939839
5	101.9008	102.1821	98.8639	100.9822	1.839933

4. Precision

The precision of an analytical method is the degree of agreement among individual test results when the procedure is applied repeatedly to multiple samplings of a homogeneous sample. The precision of an analytical method is usually expressed as the standard deviation or relative standard deviation (coefficient of variation).

The precision of the analysis of ellagic acid in methanol was determined both within run precision and between run precision as illustrated in Table B7-B8. All percentage coefficient of variation values were lower than 2.00%, indicating that of the HPLC method used were precise for quantitative analysis of ellagic acid in the range studied.

Table B7 Data of within run precision of ellagic acid in methanol by HPLC

Concentration	**Calculated Conc. (µg/mL)**					
(µg/mL)	**Set 1**	**Set 2**	**Set 3**	**Mean**	**SD**	**%CV**
1	0.984626	1.015282	1.011092	1.003666	0.016622	1.656143
3	2.95515	3.071512	3.015552	3.014071	0.058195	1.930783
5	5.095038	5.109105	4.943195	5.049112	0.091997	1.822036

Table B8 Data of between run precision of ellagic acid in methanol by HPLC

Concentration	**Calculated Conc. (µg/mL)**					
(µg/mL)	**Set 1**	**Set 2**	**Set 3**	**Mean**	**SD**	**%CV**
1	0.981574	0.992133	1.007912	0.993873	0.013255	1.333674
3	2.952666	3.000964	2.983821	2.979151	0.024485	0.821891
5	4.943782	5.094654	5.103168	5.047201	0.089665	1.77652

In conclusion, the analysis of ellagic acid in methanol by HPLC developed in this study showed good specificity, linearity, accuracy, and precision.

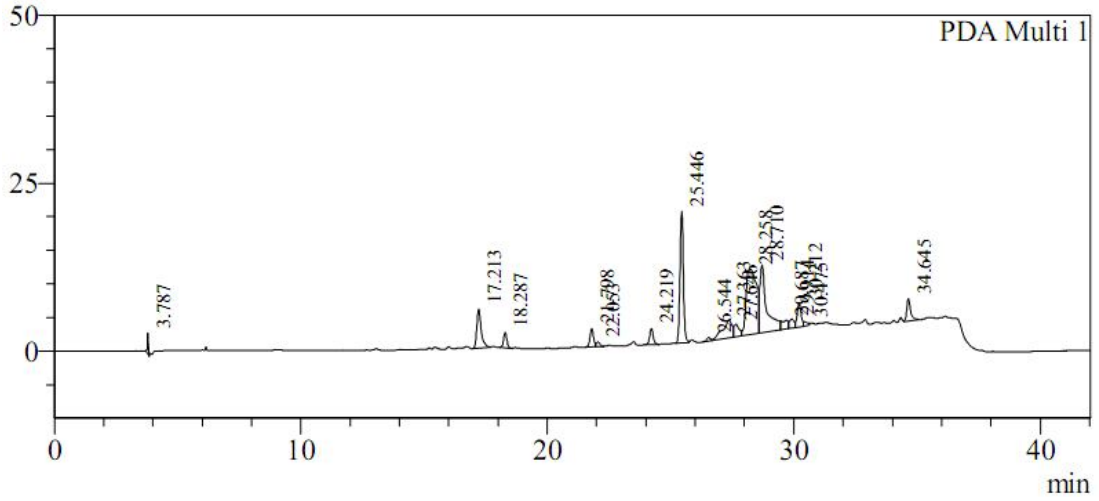

Figure B6 HPLC chromatogram of ellagic acid in S10T2B9310X, ellagic acid (retention time 17.213), propyl paraben (retention time 24.219)

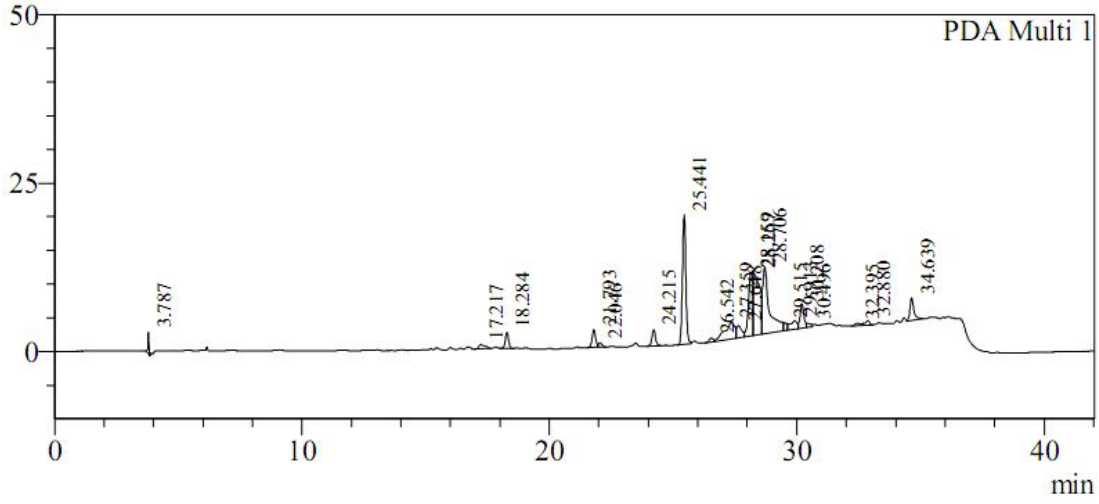

Figure B7 HPLC chromatogram of ellagic acid in S10T2B9710, ellagic acid (retention time 17.217), propyl paraben (retention time 24.215)

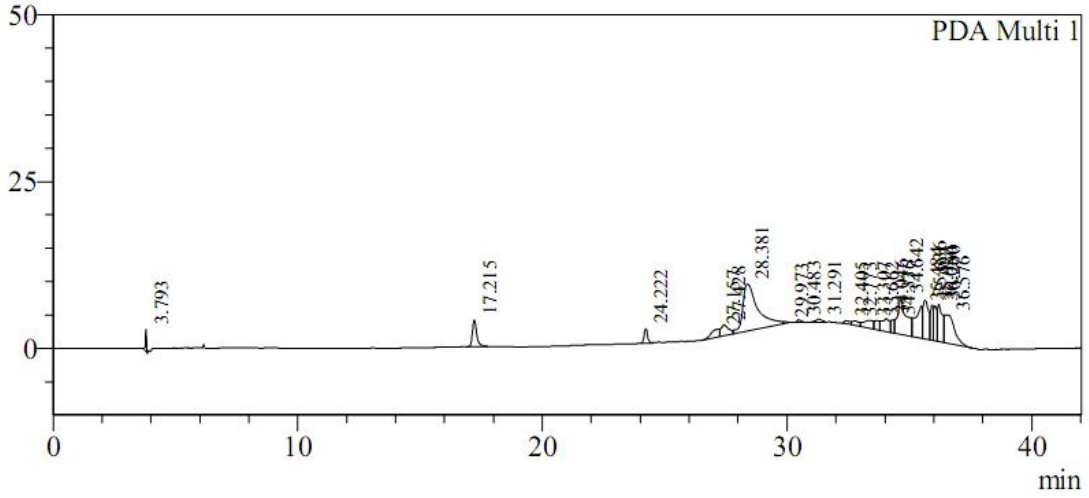

Figure B8 HPLC chromatogram of ellagic acid in O20T2C4010, ellagic acid (retention time 17.215), propyl paraben (retention time 24.222)

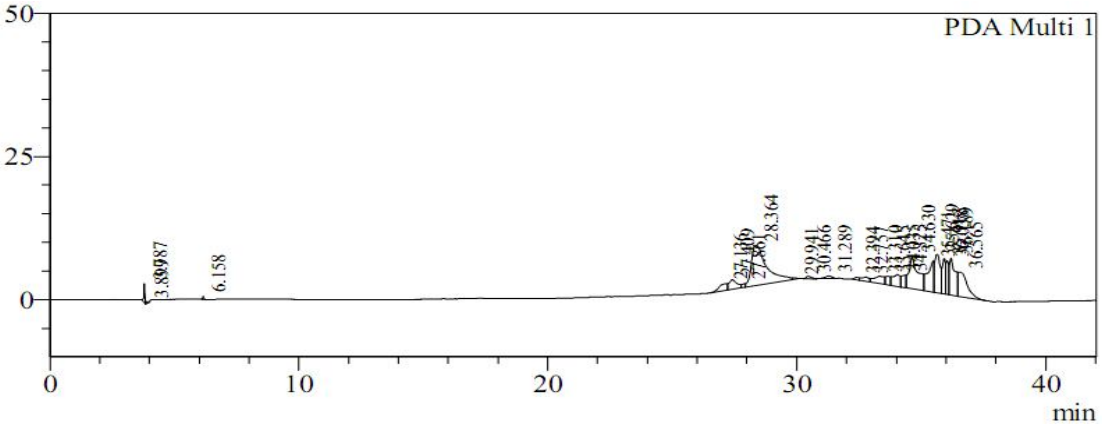

Figure B9 HPLC chromatogram of blank O20T2C4010

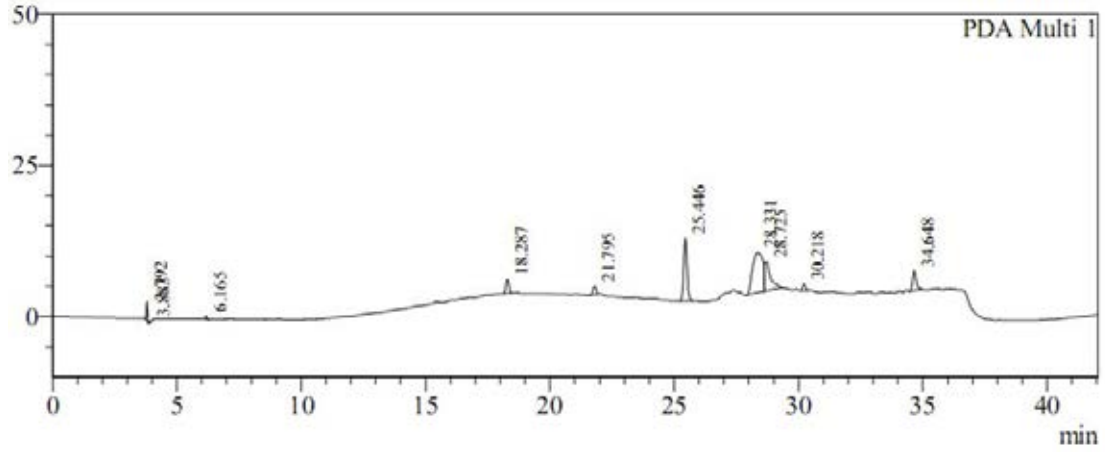

Figure B10 HPLC chromatogram of blank S10T2B9710

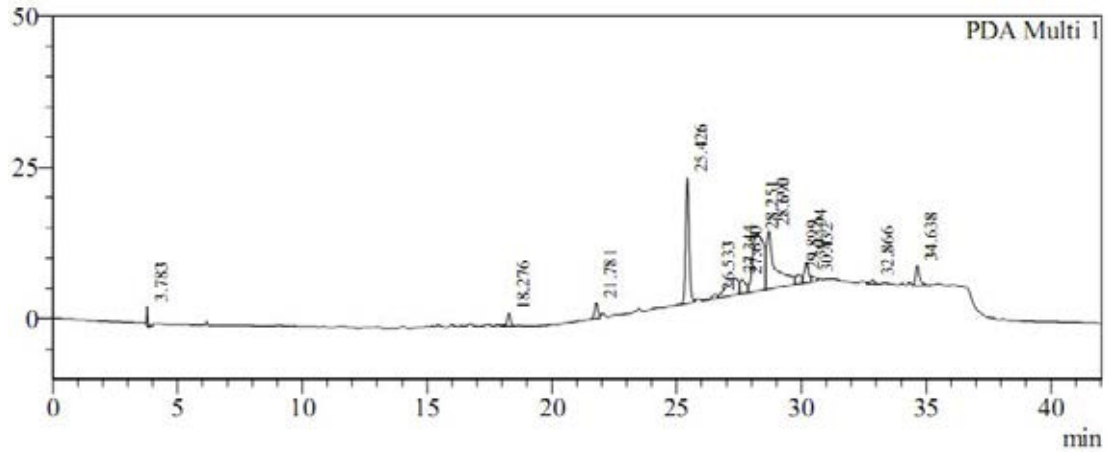

Figure B11 HPLC chromatogram of blank S10T2B9310X

APPENDIX C

Molecular structure and physical properties of some materials

Properties of some selected material

1. Polyoxyethylene 20 sorbitan monooleate (Tween®80)

Structural formula

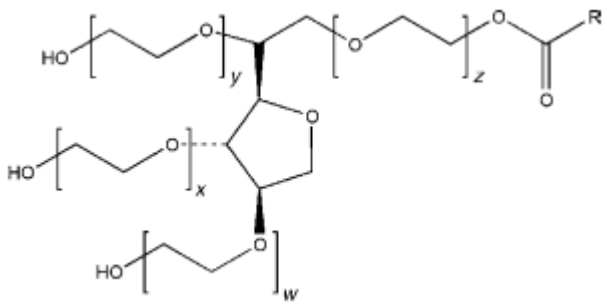

w+x+y+z = 20, R = oleic acid

Molecular weight 1,310

Viscosity 375-480 mPas (25 °C)

HLB 15

2. Polyoxyethylene 20 sorbitan monolaurate (Tween®20)

Structural formula

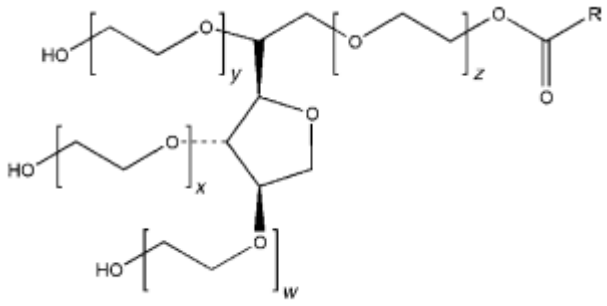

w+x+y+z = 20, R = lauric acid

Molecular weight 1227.54

Viscosity 250-450 mPas (25 °C)

HLB 16.7

3. Sorbitan monooleate ester

Structural formula

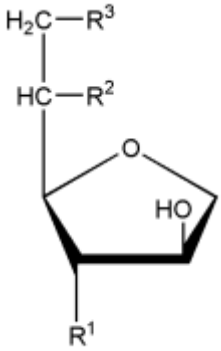

$R^1 = R^2 = OH$, R^3 = oleic acid

Molecular weight 429

Viscosity 970-1,080 mPas (25 ^{o}C)

HLB 4.3

4. Sorbitan monolaurate

Structural formula

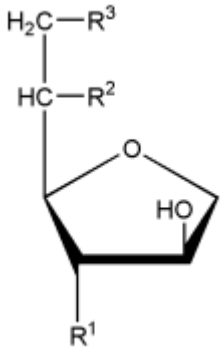

$R^1 = R^2 = OH$, R^3 = lauric acid

Molecular weight 346

Viscosity 3,900-4,900 mPas (25 °C)

HLB 8.6

5. Polyoxyethylene 10 oleyl ether (Brij®97)

Structural formula

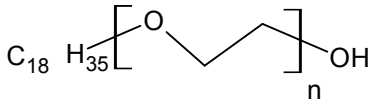

n = 10

Molecular weight 1,150

Viscosity 100 mPas (25 °C)

HLB 12.7

6. Polyoxyethylene 2 oleyle ether (Brij®93)

Structural formula

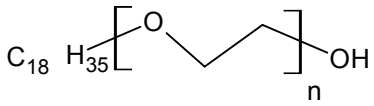

n = 2

Molecular weight 356.58

Viscosity 30 mPas (25 °C)

HLB 4.9

7. Polyoxyethylene 4 lauryl ether (Brij® 30)

Structural formula

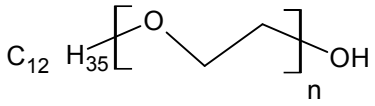

n = 4

Molecular weight 362.56

Viscosity 30 mPas (25 °C)

HLB 9.7

8. Polyoxyethylene 40 castor oil derivatives (Cremophor RH® 40)

Cremophor RH 40 consist of

Hydrophobilc part: glycerol polyethylene glycol hydroxystearate, together with fatty acid glycerol polyglycol esters;

Hydrophilic part: polyethylene glycols and glycerol ethoxylate

Viscosity 20-40 mPas (30% w/v) solution (25 °C)

HLB 14-16

9. Oleic acid

Structural formula

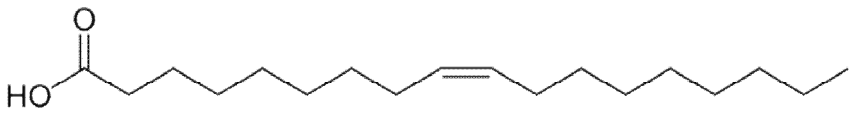

Molecular weight 282.47

Viscosity 26 mPas (25 °C)

10. Rice bran oil

Compositions of rice bran oil are as follows.

Fatty acidPalmitic acid 18-23% w/w of total

Oleic acid 21-42% w/w of total

Linoleic 28-38% w/w of total

Neutral lipids Triglyceride 58-79% w/w of total lipids

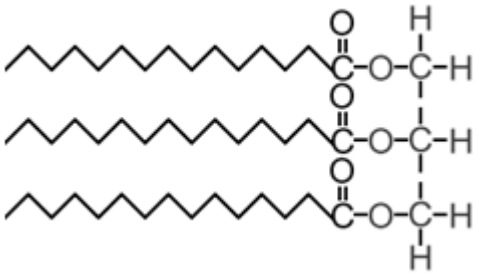

Glycolipid 2-25% w/w of total lipids

Phospholipid 7-11% w/w of total lipids

Viscosity 58 mPas (29 ^{o}C)

11. Sweet orange oil

Compositions of rice bran oil are as follows.

d-limonene 94-95% w/w

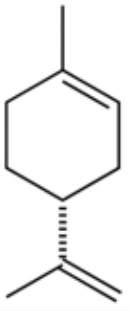

Myrcene 1.78-2.18% w/w

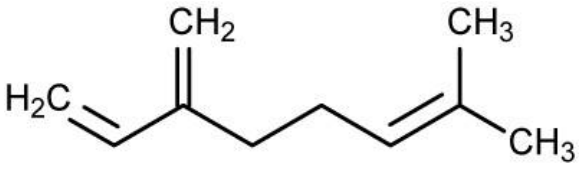

Linalool 0.25-0.62% w/w

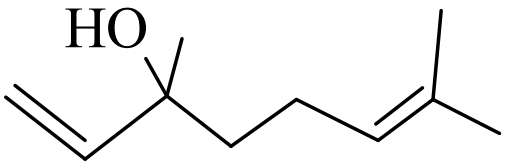

Decanal 0.24-0.46% w/w

Viscosity 0.89 mPas (21 ^{o}C)

VITA

Nattawee Intanai was born in Ubonratchathani, Thailand, on October 8, 1984. She received the bachelor's degree of science in pharmacy from Ubonratchathani University in 2008. Since graduation, she entered the master's degree program in pharmacy at Chulalongkorn University in 2008.